การเปลี่ยนแปลงของไมโครอาร์เอ็นเอในมีแซงเจียลเซลล์ที่ถูกกระตุ้นด้วยแอนติบอดี้แอนตี้ดับเบิ้ลสแตนดีเอ็นเอ

นางสาวภัทริน ตั้งธนตระกูล

วิทยานิพนธ์นี้เป็นส่วนหนึ่งของการศึกษาตามหลักสูตรปริญญาวิทยาศาสตรดุษฎีบัณฑิต
สาขาวิชาจุลชีววิทยาทางการแพทย์ (สหสาขาวิชา)
บัณฑิตวิทยาลัย จุฬาลงกรณ์มหาวิทยาลัย
ปีการศึกษา 2559

EFFECT OF AUTO ANTI-
DOUBLE STRANDED DNA ON MESANGIAL CELLS MICRORNA PROFILES

Miss Pattarin Tangtanatakul

A Dissertation Submitted in Partial Fulfillment of the Requirements
for the Degree of Doctor of Philosophy Program in Medical Microbiology
(Interdisciplinary Program)
Graduate School
Chulalongkorn University
Academic Year 2016

Thesis Title	EFFECT OF AUTO ANTI-DOUBLE STRANDED DNA ON MESANGIAL CELLS MICRORNA PROFILES
By	Miss Pattarin Tangtanatakul
Field of Study	Medical Microbiology
Thesis Advisor	Professor Nattiya Hirankarn, M.D.
Thesis Co-Advisor	Assistant Professor Asada Leelahavanichkul, M.D., Ph.D.

Accepted by the Graduate School, Chulalongkorn University in Partial Fulfillment of the Requirements for the Doctoral Degree

.....Dean of the Graduate School
(Associate Professor Sunait Chutintaranond, Ph.D.)

THESIS COMMITTEE

.....Chairman
(Associate Professor Ariya Chindamporn, Ph.D.)
.....Thesis Advisor
(Professor Nattiya Hirankarn, M.D.)
.....Thesis Co-Advisor
(Assistant Professor Asada Leelahavanichkul, M.D., Ph.D.)
.....Examiner
(Assistant Professor Kanitha Patarakul, M.D.)
.....Examiner
(Sita Virakul, Ph.D.)
.....External Examiner
(Associate Professor Thawornchai Limjindaporn, M.D.)

ภัทริน ตั้งธนตระกูล : การเปลี่ยนแปลงของไมโครอาร์เอ็นเอในมีแซงเจียลเซลล์ที่ถูกกระตุ้นด้วยแอนติบอดี้แอนตี้ดับเบิ้ลสแตนดีเอ็นเอ (EFFECT OF AUTO ANTI-DOUBLE STRANDED DNA ON MESANGIAL CELLS MICRORNA PROFILES) อ.ที่ปรึกษาวิทยานิพนธ์หลัก: ศ. ดร. พญ. ณัฏฐิยา หิรัญกาญจน์, อ.ที่ปรึกษาวิทยานิพนธ์ร่วม: ผศ. ดร. นพ. อัษฎาศ์ ลีฬหวนิชกุล, 110 หน้า.

วัตถุประสงค์ของการศึกษาวิจัยนี้คือ การศึกษาการตอบสนองของเซลล์ไตเมื่อถูกกระตุ้นด้วยแอนติดับเบิลสแตนดีเอ็นเอ โดยศึกษาระดับการแสดงออกของยีนและไมโครอาร์เอนเอ การศึกษาเริ่มจากการนำมีแซงเจียลเซลล์ ซึ่งพบจำเพาะในไต กระตุ้นด้วยแอนติบอดี จากนั้นใช้เทคโนโลยีเอ็นจีเอสและไมโครอะเรเพื่อวิเคราะห์การแสดงออกของไมโครอาร์เอนเอและยีน จากผลการทดลองพบว่า แอนติบอดีกระตุ้นในเกิดการเปลี่ยนแปลงของระดับไมโครอาร์เอนเอ และ ยีน ซึ่งเกี่ยวข้องในกระบวนการแบ่งตัว และการเจริญเติบโตของเซลล์ รวมทั้งการหลั่งคีโมไคน์ต่างๆ และยังพบว่า ไมโครอาร์เอนเอ 10a (miR-10a) ลดการแสดงออกในเซลล์ที่ถูกกระตุ้น สอดคล้องกับผลการแสดงออกของไมโครอาร์เอนเอในไตของคนไข้ ผลดังกล่าวมีความสัมพันธ์กับค่าโปรตีนรั่วในปัสสาวะของคนไข้ เมื่อศึกษาบทบาทของ miR-10a พบว่าทำหน้าที่ในการควบคุมการแบ่งตัวของเซลล์ ยิ่งไปกว่านั้นยังทำหน้าที่ควบคุมการสร้างคีโมไคน์ที่สำคัญในการดึงดูดเม็ดเลือดขาว (IL-8) จากผลการทดลองจะเห็นได้ว่า แอนติบอดีมีผลโดยตรงต่อการแสดงออกของไมโครอาร์เอนเอและยีนในมีแซงเจียลเซลล์ การรักษาเพื่อปรับระดับการแสดงออกของไมโครอาร์เอนเอหรือใช้ในการติดตามโรค อาจเป็นแนวทางใหม่เพื่อพัฒนาคุณภาพชีวิตของคนไข้ ต่อไป

สาขาวิชา จุลชีววิทยาทางการแพทย์ ลายมือชื่อนิสิต .....

ปีการศึกษา 2559 ลายมือชื่อ อ.ที่ปรึกษาหลัก .....

ลายมือชื่อ อ.ที่ปรึกษาร่วม .....

5387798220 : MAJOR MEDICAL MICROBIOLOGY
KEYWORDS: LUPUS NEPHRITIS / ANTI-DOUBLE STRANDED DNA ANTIBODY / MIR-10A / MESANGIAL CELLS

PATTARIN TANGTANATAKUL: EFFECT OF AUTO ANTI-DOUBLE STRANDED DNA ON MESANGIAL CELLS MICRORNA PROFILES. ADVISOR: PROF. NATTIYA HIRANKARN, M.D., CO-ADVISOR: ASST. PROF. ASADA LEELAHAVANICHKUL, M.D., Ph.D., 110 pp.

Autoantibodies-mediated inflammation at the resident kidney cells is crucial in the lupus nephritis (LN) pathogenesis. The objective of this study is to investigate the role of miRNA in human mesangial cells (HMCs) stimulated with auto anti-dsDNA IgG antibodies. The cells were treated with antibodies purified from active LN patients or non-specific IgG controls in the present of normal serum. The aberrant miRNA was screened using high throughput sequencing. Results showed that anti-dsDNA IgG upregulated 103 miRNAs and down-regulated 20 miRNAs which regulate genes in the cell cycle, catabolic process, regulation of transcription and apoptosis signaling. The miR-10a, which was listed in the top ten high abundance miRNA in HMCs, was specifically downregulated upon anti-dsDNA IgG induction. Interestingly, the expressions of miR-10a in kidney biopsy from LN patients (n=29) were downregulated compared to cadaveric donor kidney (n=6). The downregulation was correlated with proteinuria, which is the earliest sign of renal defect (r^2 = 0.5266, p-value = 0.0115). Functional studies highlight the downstream regulator of miR-10a in the chemokine signaling and cell proliferation or apoptosis pathway. The luciferase assay confirmed for the first time that IL-8 was a direct target of miR-10a in HMCs. In conclusion, anti-dsDNA IgG Ab down-regulated miR-10a expression in HMC resulting in the induction of various target genes involved in HMCs proliferation and chemokine expression. Manipulation of miR-10a might be a new option for targeted therapy for LN.

Field of Study: Medical Microbiology Student's Signature .....
Academic Year: 2016 Advisor's Signature .....
Co-Advisor's Signature .....

ACKNOWLEDGEMENTS

First, I would like to thank you my thesis adviser, Prof. Dr. Nattiya Hirankarn for giving a chance to join the Center of Excellent in Immunology and Immune-Mediated Disease Center under a funding support from Thailand Research Fund (TRF) under the Royal Golden Jubilee (RGJ) PhD program. I have to thank you my thesis co-adviser, Asst. Prof. Dr. Asada Leelahavanichkul for a valuable suggestion and he always teach me how to improve a research skills. I also would like to thanks Dr. Supranee Buranapraditkun for teaching me cell culture technique. I won't be able to complete this study without their support. I am also sincerely thanks RGJ for the support as well. It is very nice to work with lupus team especially Dr. Pattadon Sukapan, Dr. Thitima Benjachart, Dr. Pimpayao Sodsai, Dr. Wipasiri Soonthornchai and Dr. Poorichaya Somparn who always give me a valuable resources and precise advice to improve my work.

I would like to special thanks to Mr. Preecha Ruangvejvorachai, Department of Pathology, Chulalongkorn Memorial Hospital for helping me conducting immunohistochemistry.

I would like to thanks everyone in the Center of Excellent in Immunology and Immune-Mediated Disease that I didn't mention here who encouraged and supported me to complete this dissertation as well.

I would like to express my great appreciation to the funding from the Royal Golden Jubilee Ph.D. scholarship Grant (RGJ-Ph.D. Ph.D. program 2014 PHD/0321/2551) of Thailand Research Fund (TRF), Thailand. The financial support provided by Government Budget (Fiscal year 2014) Chulalongkorn University and the research grant for Graduate Studies from National Research Council of Thailand (Fiscal year 2014) are greatly appreciated. The 90th Anniversary of Chulalongkorn university fund (Ratchadaphiseksomphot Endowment Fund).

Finally, I would to thank you my family for their unconditional support during my entire study life and help me to be the person I am today.

CONTENTS

Page

CONTENTS OF FIGURES

CONTENTS OF TABLES

LIST OF ABBREVIATIONS

Anti-dsDNA	Anti-double stranded DNA
CREB1	CAMP responsive element binding protein 1
DAVID	Database for Annotation, Visualization and Integrated Discovery
DNA	Deoxyribonucleic Acid
DGCR8	DiGeorge syndrome critical region gene 8
GEO	Gene Expression Omnibus database
GO	Gene Ontology
HER2	Human epidermal growth factor receptor 2
HMCs	Human mesangial cells
HOXA1	Homeobox A1
IFN	Interferon
IgG	Immunoglobulin G
IL-6	Interleukin-6
IL-8	Interleukin-8
LN	Lupus nephritis
MAP3K7	Mitogen-activated protein kinase kinase kinase 7
MAP4K4	Mitogen-Activated Protein kinase kinase kinase kinase 4
mRNA	Messenger Ribonucleic Acid
miR-10a	microRNA-10a
NFAT5	Nuclear Factor of Activated T-Cells 5
NF-κB	Nuclear factor kappa-light-chain-enhancer of activated B cells
NGS	Next Generation Sequencing
PIK3CA	Phosphatidylinositol-4,5-Bisphosphate 3-Kinase Catalytic Subunit Alpha
SLE	Systemic Lupus Erythematosus
RefSeq	Reference Sequences Database
RNA	Ribonucleic Acid
RNA-Seq	RNA Sequencing
RISC	RNA-induced silencing complex
TRBP	Trans-activating response RNA-binding protein

Chapter I

Introduction

Lupus nephritis (LN) is an autoimmune mediated kidney inflammation affecting systemic lupus erythematosus (SLE) patients, and is highlighted as a poor prognosis for SLE survival (1). Due to lack of insight in disease pathogenesis, heavily immunosuppressant usages without satisfactory treatment are often met during the therapeutic process (2). Although kidney biopsy, a gold standard for LN diagnosis, could provide a lot of valuable information, LN patients might risk from several complications particularly in bleeding or infection etc. Thus, it is necessary to understand the cause of disease to create a novel potential medication as well as biomarker for disease stage prediction.

Regarding to the association between the development of LN disease and a specific antibodies detection (3-5), anti-double stranded DNA antibody, was considered as a major leading cause of LN disease (6, 7). Either the presence of anti-dsDNA-immune complexes within the glomerular site or a certain binding of anti-dsDNA antibodies to implanted chromatin structure on residential kidney cells and glomerular basement membrane was described as a key contributor to driving inflammation in the kidney (8, 9). However, the assumptions were not completely clear as some patients who bear anti-dsDNA antibodies do not develop LN. Therefore, several observations reported an emerging mechanism for anti-dsDNA antibodies induced kidney injury (10-12). The cross-reactive anti-dsDNA IgG antibodies to several resident cells antigens and glomerular basement membrane in glomerular and tubular region is more likely to represent the development of LN rather than antibodies activity determination (6).

Mesangial cells are macrophages-derived cells located specifically in the kidney. Interestingly, the cells obtain smooth muscle cell-like phenotype which support glomerular structure and dialysis mechanism (13). Moreover, the cells play several important roles to promote inflammation in the kidney including cytokine and chemokine production and being as antigen presenting cells etc. (14, 15). Aberrant function of mesangial cells due to a specific stimulation was led to drastically accumulate mesangial matrix within glomerular resulting in kidney fibrosis and massive foreign antigens entrap within dense mesangial matrixes (16). In LN,

mesangial cells proliferation is a typical histology features in class I – IV which represents a crucial role of mesangial cells in both downstream and upstream during glomerulonephritis processes. However, a few studies were paid attention in mesangial cells. Recently, an evidence showed that anti-dsDNA IgG antibodies cross-reacted to annexin II expressed on human mesangial cells (HMCs) inducing IL-6 expression and was correlated with disease activity (17). In addition, purified anti-dsDNA IgG antibodies mediated myofibroblast like phenotype and endoplasmic reticulum stress proteins signalling induced inflammation in mesangial cells (12, 18). Transcriptome analysis in anti-dsDNA antibodies treated mouse mesangial cells (MMSs) revealed changing of various genes in several pathways including NF-kB signalling, nitric oxide production, chemokine and cytokine production and cell proliferation or apoptosis (19). The mesangiolysis by specific antibodies induced acute nephritis with drastic proteinuria and mesangial cells proliferation *in vivo* (13). This indicated that antibodies mediated mesangial cells injury might be an early inflammation sign in kidney which also found in LN histology.

As describe above, it is suggested that anti-dsDNA antibodies mediated mesangial cells function might be crucial for LN pathogenesis. Precisely design drug target to inhibit mesangial cells response might reduce side effect from board spectrum immunosuppressant, and might be a good biomarker to determine the recurrence of active glomerulonephritis among LN and SLE patients.

The microRNA (miRNA) is a novel regulator which becomes a trending topic in term of therapeutic targets and biomarker. The miRNA is small non-coding RNA that regulate protein translation and gene expression at post-transcriptional level (20). It plays an important role in many cellular processes including differentiation, transformation, replication and regeneration (21). As secreted miRNAs could be detected in some various bodily fluids and its expression was restricted to certain specific tissues and biological stages, the miRNAs were considered as a potential candidate biomarker in many diseases. In hepatitis C virus infection, inhibition of miR-122 by anti-miR-122 drug (anti-miravirsen), were successfully decreased viral replication and it is currently in the clinical trial phase II (22).

Exploring the role of miRNA in kidney might help to understand LN pathogenesis. In SLE, a number of miRNA expressions were disturbed compared to

healthy controls (23). For example, down-regulated miR-146a and up-regulated miR-155 in PBMCs were examined as a potential regulator for type I interferon production (24). For LN, study of the miRNA from kidney biopsy revealed a hundred of miRNAs were disrupted compared to healthy control (25). Study the role of the miRNA in spontaneous develop LN prone mice showed that an up-regulation of let-7a which supported IL-6 expression during disease course (26). In addition, using molecular probe technique identified miR-26a and miR-30a were identified as mediator in the mesangial cells proliferation through HER-2 (27). Since LN pathogenesis is due to anti-dsDNA antibodies, study the role of miRNA in antibody mediated inflammation model might useful to explain the actual pathogenic process occurred in LN patients.

Objective

1) To investigate role of miRNA in mesangial cells which responded to anti-dsDNA IgG antibodies

2) To examine miRNA expression in mesangial cells which stimulated with antibodies

Conceptual framework

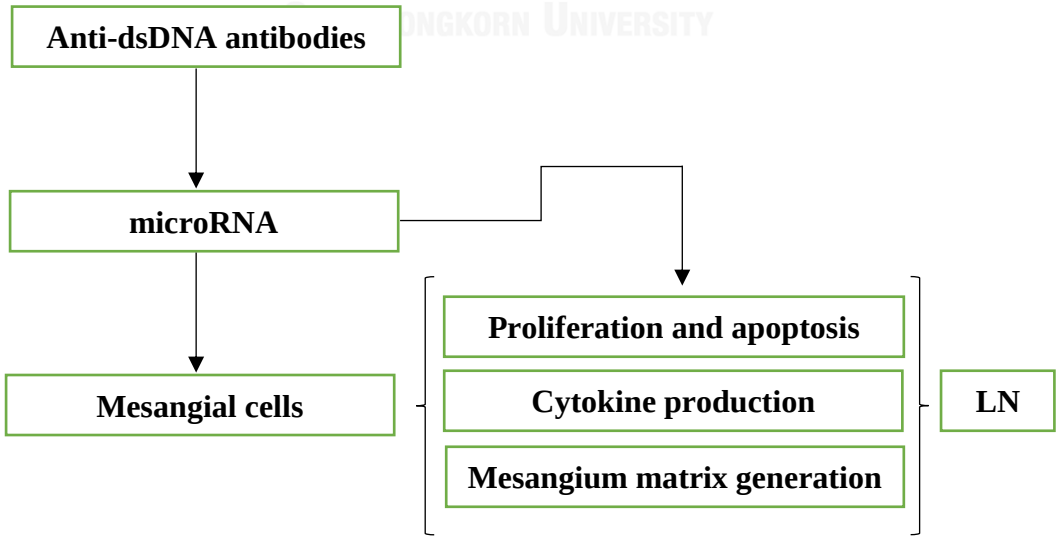

Chapter II

Literature review

The microRNA

miRNA is an endogenous non-translated small RNA that controls gene expression at post-transcriptional level (20, 28). The size is about 19-25 base-pairs in mature form. It was discovered in the *Caenorhabditis elegans* during developmental stage from larva stage L2 to L3 known as small temporal RNA (29). Surprisingly, the sequences from small temporal RNA was similar across several species including human. The consensus sequences were identified in human genome with related function resembling small temporal RNA. In consequent, the small temporal RNA was named as miRNA.

For miRNA biogenesis and regulatory function, the miRNA gene were normally encoded within intron and co-expressed with mRNA under specific stimulation. The microRNAs were transcribed by RNA polymerase II generating microRNA precursor called "pri-miRNA". In the following, the pri-miRNA was processed by Dorsha/DGCR8 enzymes into "pre-miRNA". Next, the pre-miRNA was transferred to cytoplasm by a specific protein called "Expotin5". Finally, the pre-miRNA was cleaved by ribonuclease enzymes (Dicer) producing mature miRNA. The mature miRNA was short RNA duplex with one strand preferentially select to be incorporated with RISC complexes. The miRNA-RISC complexes are complementary binding to 3'UTR region of mRNA resulting in mRNA degradation and translational blocking (30) (figure 1). A complementary or partially binding between "seed region" (2^{nd} base to 8^{th} from 5'-miRNA) to 3'untranslated region (UTR) of target mRNA is critical for its inhibitory effects (figure 2). Complete recognition of the miRNA to 3'UTR might drive mRNA degradation while partially binding cause translation inhibition (figure 3). However, accumulative evidences showed a complexity of miRNAs regulatory function (31). The observation showed the miRNAs repress protein translation through multiple pathways including (1) co-translation protein degradation, (2) inhibition of translational elongation (3) premature termination of translation and (4) inhibition of translation inhibition. Moreover, the miRNAs can

exclude the translational machinery known as P bodies resulting in translational inhibition (figure 4). Although it is hardly to conclude that which mechanism is the main mechanism for miRNA to silence gene expression, studies comparing natural full-length 3'UTR suggested that the final outcome of miRNA regulation depends on the features and sequence of the target's 3'UTR (31). Additional reports showed that several factors might influence miRNA regulatory function such as the presence and cooperation between miRNA-recognition elements (MREs), the spacing between MREs, proximity to stop codon, position within the 3'UTR, AU composition and target mRNA secondary structure (32).

According to short seed region and the ability to regulated gene expression by incomplete binding, it is known that one miRNA might control several mRNAs and transcription factor expression in certain pathways simultaneously. In addition, difference miRNA containing similar seed region might influence the same gene expression. Because of the redundancies function of the miRNA, this mechanism could "fine-tune" gene expression which is essential for balancing and maintain suitable cell response to a variety of stimuli.

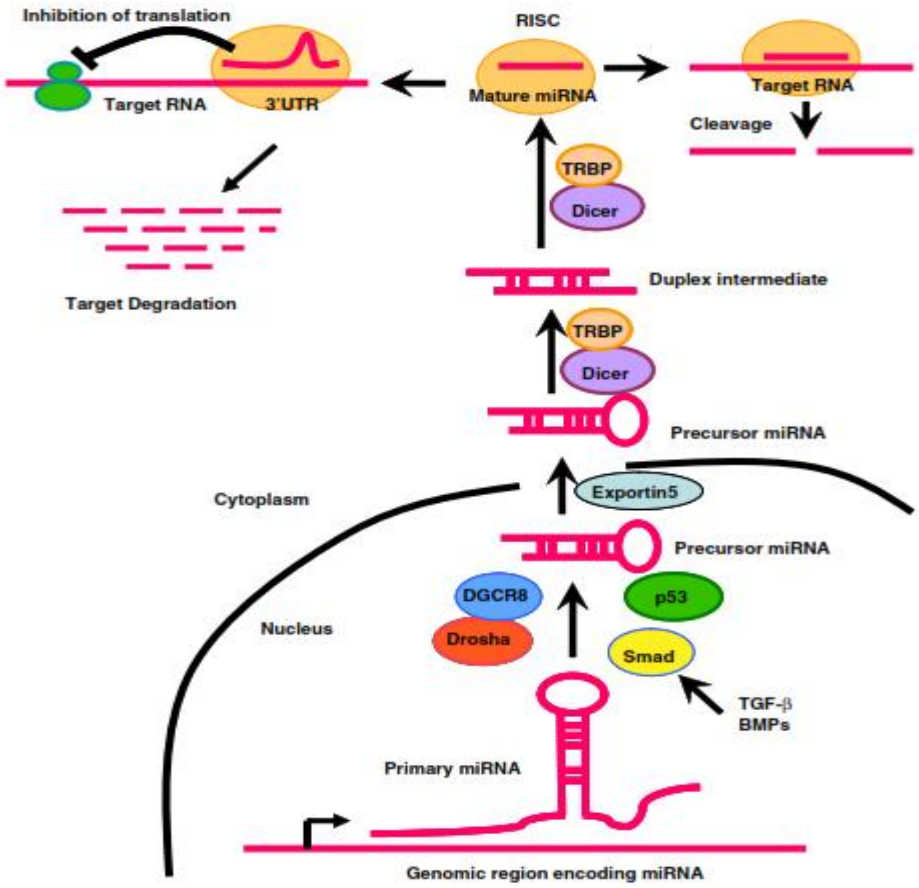

Figure 1 The microRNA biogenesis

The miRNAs transcripts were originated from long length pri-miRNA which encoded in human genome. The pri-miRNA was then processed by RNase III enzymes (DGCR8 and Drosha) generated intermediate transcripts known as pre-miRNA. In the following, a ribonuclease enzyme called Dicer, cleaves pre-miRNA to duplex-small RNA. The mature guide strand miRNAs were load into RISC complexes and function to down-regulate gene expression depending on binding capacity, while another strand was degraded. RISC, RNA-induced silencing complex; DGCR8, DiGeorge syndrome critical region gene 8, an essential cofactor for Drosha; TRBP, transactivating response RNA-binding protein, a cofactor for Dicer.(33)

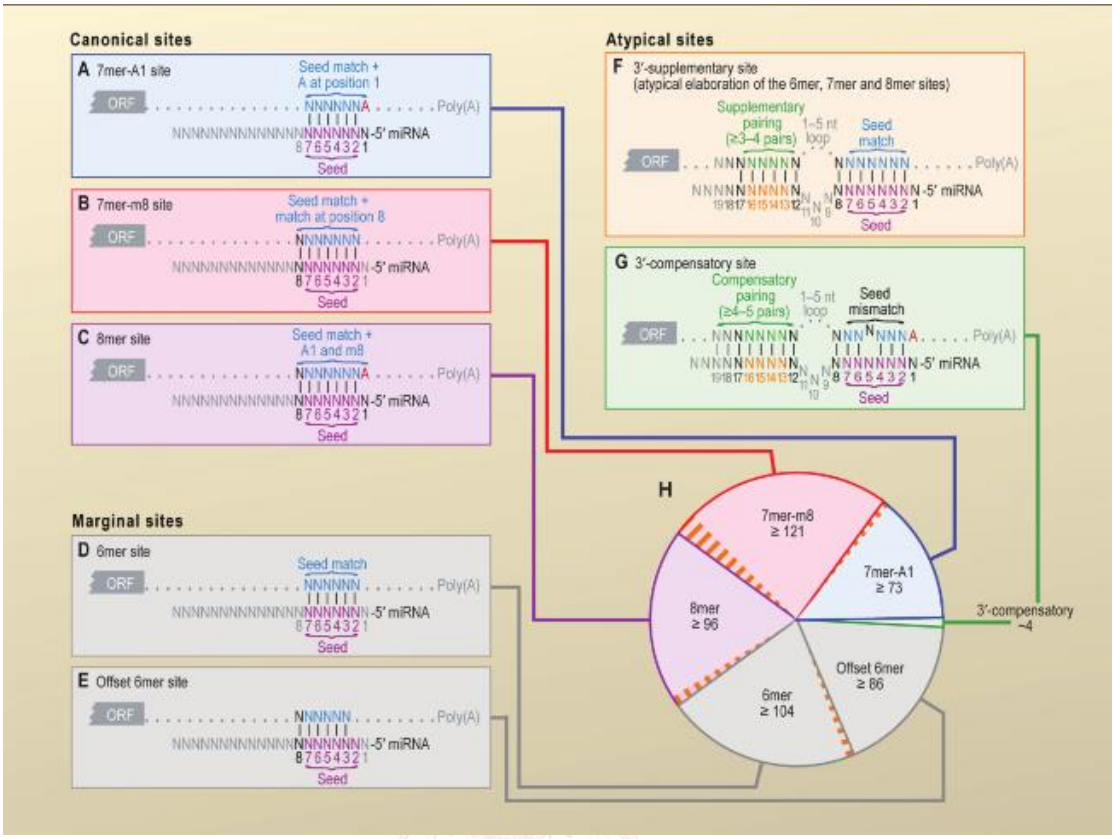

Figure 2 Types of microRNA target site based on Watson-Crick pairing at seed region.

(A-C) Canonical, complementary binding between miRNA and target mRNA at seed region (7-8 nt seed matched sites). Vertical dashes indicate contiguous Watson–Crick pairing.

(D-E) Marginal, imperfect binding at seed region (6 nt sites matching the seed region). These 6mer sites typically have reduced efficacy and are conserved by chance more frequently than the larger sites.

(F–G) Sites with productive 3' pairing. There are two types including 3'-supplementary sites and 3'-compensatory sites.

For 3'-supplementary sites **(F),** Watson–Crick pairing usually centring miRNA nucleotides 13–16 (orange) supplements a 6–8 nt site **(A–E).** At least 3–4 well-positioned contiguous pairs are typically required for increased efficacy.

For 3'-compensatory sites **(G),** Watson–Crick pairing usually centering on miRNA nucleotides 13–16 (orange) can compensate for a seed mismatch and thereby create a functional site.

(H) Number of preferentially conserved mammalian sites matching a typical highly conserved miRNA. For each site matching the seed region, orange-hatched subsectors indicate the fraction of conserved sites with preferentially conserved 3'-supplementary pairing. Analysis was performed with the 87 miRNA families highly conserved in vertebrates. A 7mer site is counted only if it is not part of 8mer site, and a 6mer site is counted only if it is not part of a larger site. Values plotted are the number of preferentially conserved sites confidently detected above background, calculated as the average number of conserved sites minus the upper 95% confidence limit on the sites estimated to be conserved by chance. Thus, for each site type of panels **(A)–(E),** there is 95% confidence that the actual average of preferentially conserved sites is higher than that plotted (34).

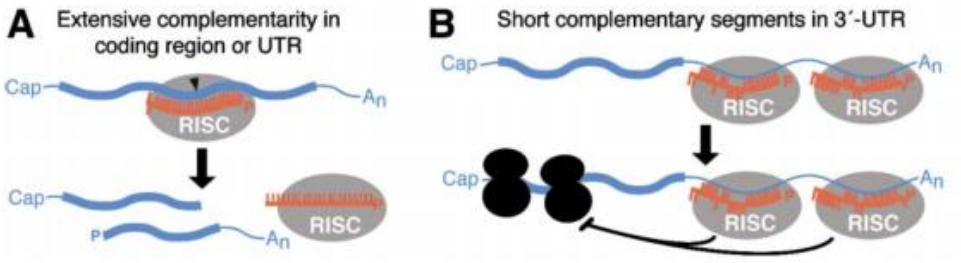

Figure 3 The Actions of miRNA (20)

(A) An Extensive complementarity between miRNA and its target at coding region or UTR could result in messenger RNA cleavage.

(B) Translational repression by miRNAs which short complementarity segments in 3’UTR.

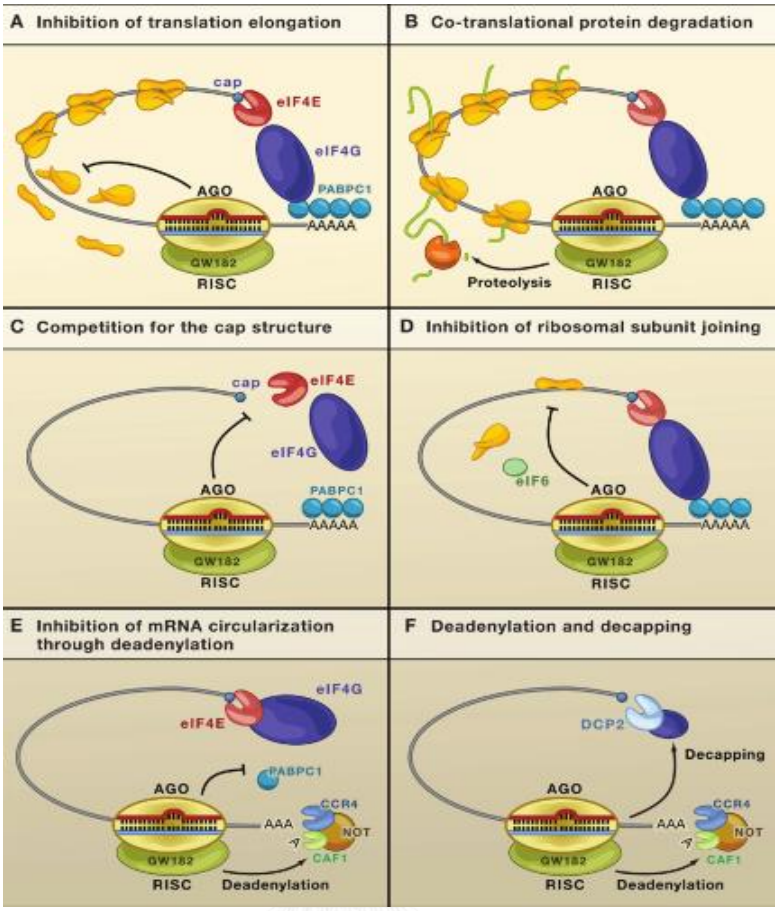

Figure 4 Mechanism of miRNA mediated gene silencing (31)

(A) Post-translation initiation mechanisms. The miRNAs (red) block translation elongation or by promoting premature dissociation of ribosomes (ribosome drop-off).

(B) Co-translational protein degradation. This model proposes that translation is not inhibited, but rather the nascent polypeptide chain is degraded co-translationally. The putative protease is unknown.

(C–E) Translation initiation mechanisms. The miRNAs interfere with a very early step of translation, prior to elongation.

(C) Argonaut proteins compete with eIF4E for binding to the cap structure (cyan dot).

(D) Argonaut proteins recruit eIF6, which prevents the large ribosomal subunit from joining the small subunit.

(E) Argonaut proteins prevent the formation of the closed loop mRNA configuration by an ill-defined mechanism that includes deadenylation.

(F) MicroRNA-mediated mRNA decay. The miRNA trigger deadenylation and subsequent decapping of the mRNA target. Proteins required for this process are shown including components of the major deadenylase complex (CAF1, CCR4, and the NOT complex), the decapping enzyme DCP2, and several decapping activators (dark blue circles). RISC is shown as a minimal complex including an Argonaut protein (yellow) and GW182 (green). The mRNA is represented in a closed loop configuration achieved through interactions between the cytoplasmic poly-A binding protein (PABPC1; bound to the 3' poly-A tail) and eIF4G (bound to the cytoplasmic cap-binding protein eIF4E).

The microRNA and immune response

Obviously, the miRNA regulation is crucial for many immunological aspects such as development of immune cells and differentiation (figure 5) (32). For example, miR-17~92 cluster was identified as a ubiquitous regulator of B-cells, T-cell and monocyte development. Studies showed that miR-17~92 were drastically up-regulated at pre-B cell stage which prolong pre-B cell life by targeting pro-apoptotic proteins Bim (35). Meanwhile miR-181a is reported as regulation of B-cell differentiation and CD4+T-cell selection, activation and sensitivity (36). The miR-155 and miR-146a are examined as innate immune response upon Toll-like-receptors (TLRs) stimulation and type I interferon secretion (37). For myeloid precursor differentiation, the miR-223 is involved in granulocyte development (38). In adaptive immunity, such as antibodies production and inflammatory mediator release, the miRNA regulation is currently based on an impact of its controlling of immune cells differentiation and development. Interestingly, by using bioinformatics prediction tools, the miRNA seed regions were found to regulate more than 45% of immune genes (25). Many miRNAs were characterized during immune response summarized in table 1. It is suggested that fine-tune expression might benefit immune responses in term of appropriate activation and inhibition. As the miRNA is transiently expressed under specific conditions and tissue,

it becomes a new candidate for disease stage biomarker and therapeutic targets in immune dysregulation disease.

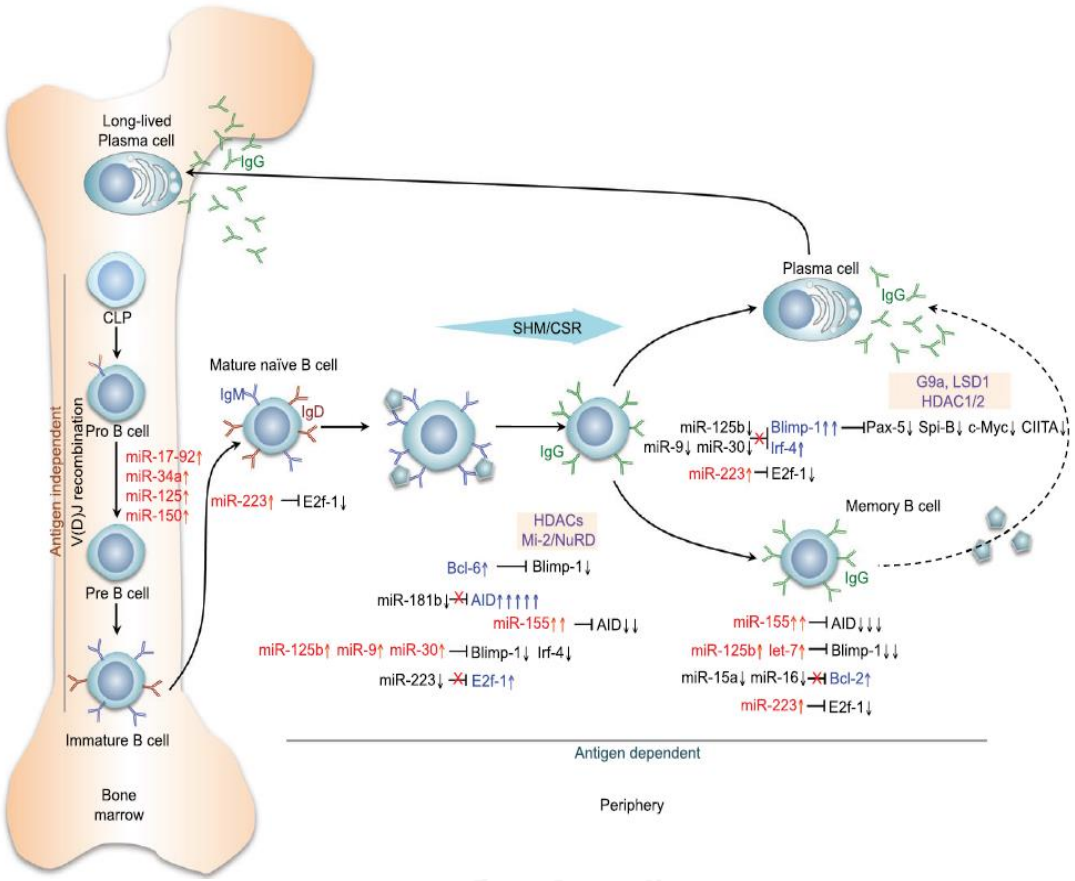

Figure 5 The miRNA in immune and autoimmune responses (39)

The selected miRNAs regulation is critical at different stages of peripheral B cell differentiation. Several miRNAs (miR-17-92, miR-34a, miR-125 and miR-150) are involved in the pro-B to pre-B cell transition and regulate the generation of B cells in the bone marrow during the early stages of development. The miR-181b and miR-155, target AID, whereas miR-125b, miR-9 and miR-30 target Blimp-1 and Irf4, which mediate plasma cell differentiation. Upregulation (red arrow) or downregulation (black arrow) of miRNAs results in alterations in the expression of these key genes. AID, activation-induced cytidine deaminase; Blimp-1, B-lymphocyte-induced maturation protein-1; Irf4, interferon regulatory factor-4.

Table 1 The list of previous characterized miRNAs and its function with putative known target in immune cells and immunological response (32).

miRNA	Function	Transcriptional regulation	Targets
miR-15a	Decreased expression in chronic lymphocytic leukaemia		Bcl-2
miR-16	Binds to UA rich elements in the 3' UTR and induces TNFα mRNA degradation		TNFα
miR-21	Increased expression in B-cell lymphoma and chronic lymphocytic leukaemia		
miR-17~5p	In combination with miR-20a and miR-106a inhibits monocyte proliferation, differentiation and maturation	AML-1	AML-1
miR-17~92 cluster	Regulates pro- to pre- transition during B- and T-cell development		Bim, PTEN
miR-20a	In combination with miR-17~5p and miR-106a inhibits monocyte proliferation, differentiation and maturation	AML-1	AML-1
miR-24	Inhibits replication of vesicular stomatitis virus		
miR-29a	Down-regulated in B-cell chronic lymphocytic leukemia		Tcl-1
miR-32	Inhibits replication of primate foamy virus type 1		
miR-93	Inhibits replication of vesicular stomatitis virus		
miR-106a	In combination with miR-17~5p and miR-20a inhibits monocyte proliferation, differentiation and maturation	AML-1	AML-1
miR-122	Required for hepatitis C proliferation in liver		
miR-125b	Expression downregulated by LPS and oscillations in expression after exposure to TNFα	NFκB	TNFα
miR-146a	Expression induced in macrophages and alveolar/bronchial epithelial following activation of TLR-2, -4 and -5 or exposure to TNFα and IL-1β.	NFκB	IRAK1, TRAF6
miR-146b	LPS induced expression induced in macrophages		IRAK1, TRAF6
miR-150	Increased expression leads to suppression of B-cell formation by blocking in pro- to pre-B cell transition. Decreased expression in chronic lymphocytic leukaemia (CLL)		
miR-155	Increased expression in Hodgkin and non-Hodgkin lymphomas and chronic lymphocytic leukaemia (CLL)		
miR-155	Required for normal production of isotype-switched, high-affinity IgG1 antibodies in B-cells, determines Th1 and Th2 differentiation and positive regulator of antigen induced responses in T-cells	AP-1	PU.1, c-Maf
miR-155	Increased expression following activation of the innate immune response. Inhibits inflammatory mediator release and stimulates granulocyte and monocyte proliferation	AP-1	
miR-181a	Positive regulator of B-cell development and $CD4^+$ T-cell selection, activation and sensitivity.		SHP-2, PTPN22, DUSP5, DUSP6
miR-196	Induced by IFNβ and inhibits replication of hepatitis C virus		
miR-223	Negative regulator of neutrophil proliferation and activation	PU.1, C/EBPα, NFI-A,	Mef2c, IGFR
miR-296	Induced by IFNβ and inhibits replication of hepatitis C virus		
miR-351	Induced by IFNβ and inhibits replication of hepatitis C virus		
miR-431	Induced by IFNβ and inhibits replication of hepatitis C virus		
miR-448	Induced by IFNβ and inhibits replication of hepatitis C virus		

Lupus Nephritis and current issues in disease monitoring and treatment

Lupus nephritis (LN) is a severe autoimmune attack kidney injury causing acute glomerulonephritis or chronic nephrotic syndrome. It is the most common complication among SLE patients (40). Usually, patients got sudden and unexplained swelling at extremity part of body with high blood pressure. Proteinuria is found in 100% of LN patients, while microscopic haematuria can be detected in 80% of LN patients. Macroscopic haematuria is relatively rare in LN patients. The reports showed that some of the patients might have low glomerular filtration rate (GFR). In some cases, symptoms are likely to acute renal injury. The Tamm-Horse fall proteins, β2-microglobulin, light chain antibodies were secreted in urine since the renal tubular cells were defected according to immunological offensive (41).

The epidemiology study showed that cumulative incidence and prevalence of LN are highly in Asian and Afro-Caribbean races compared with Caucasians(42). In addition, up to 25% of these patients developed end-stage renal disease (ESRD) within 10 years after onset of renal compromise(43). Most patients with LN had a renal flare within five years after first diagnosis of nephritis. Heavily immunosuppressive therapy was applied to maintain disease activity to quiescent stage (44). This greatly increases risk of systemic infection which is a major leading cause of death in SLE patients (45). Balancing between immune response and immune suppression is an issue for LN treatments. Specific treatment against reactive immune cells or direct target to kidney might help to reduce side effects from board immune suppressants usages.

The causes of the LN are multi-factors such as genetic mutations, environmental inducers and hormonal factors (46, 47). In case of genetic factors, most of LN patients were found multiple genetics aberrant incorporated with predisposing environmental factors (smoking, exposing to ultraviolet light, Epstein-Barr Virus (EBV) infection and some medication); however, single mutation in significant genes also can result in SLE too (figure 6). For example, mutation in C3 complement pathways or HLA genes cause lupus-like disease. The Genome Wide Association Study (GWAS) in Asian populations identified variants in *ETS1* and *WDFY4* which associated with LN (47). Not only the genetic variation, epigenetics dysfunction also can drive LN. Previously, the study of DNA methylation or histone modification contributed to the over-expression of auto-immune related genes in SLE patients (48).

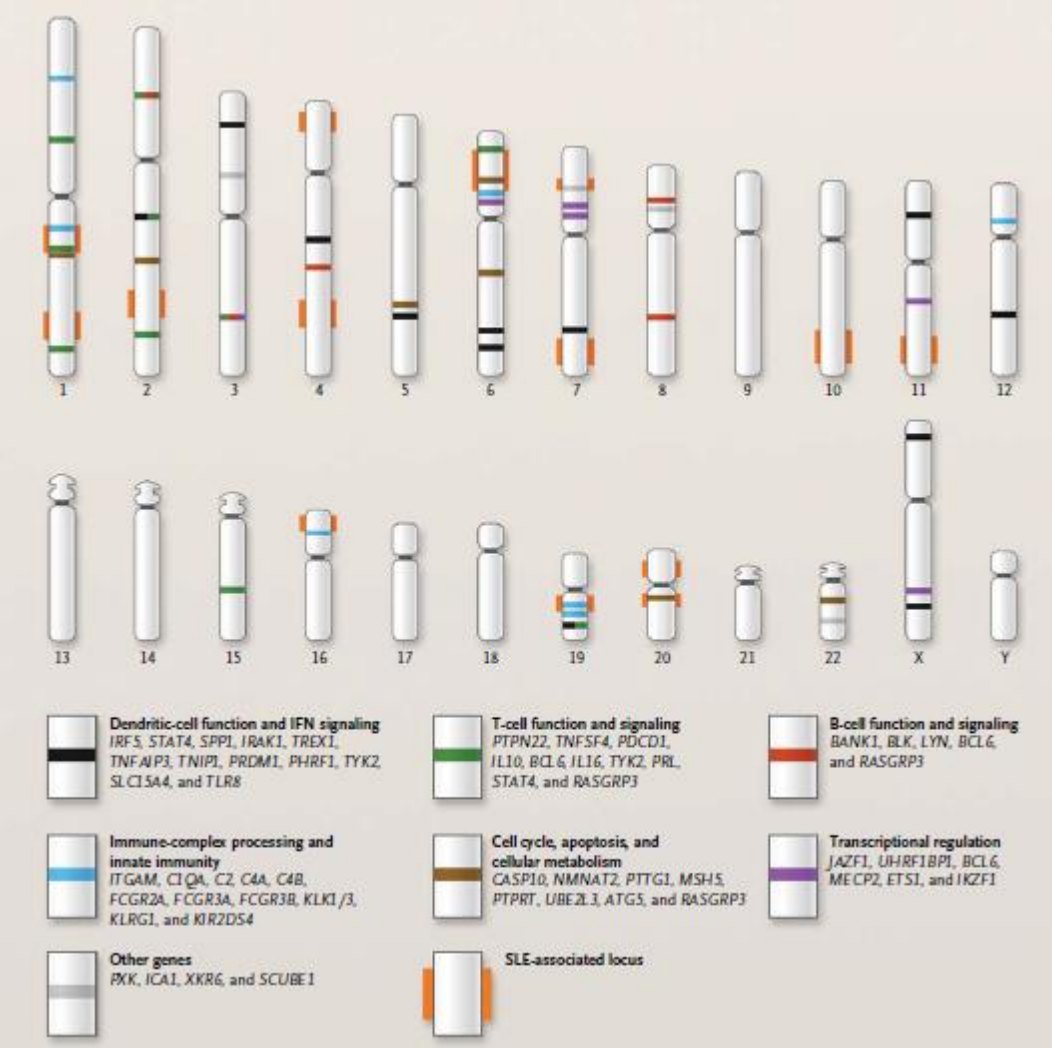

Figure 6 The chromosome loci and gene associated with SLE or LN (46)

The approximate chromosome location of gene associated with SLE or LN. The genes were classified by their known functions and represented with difference colour. The grey colour is a set of genes which is not belong to those groups. The chromosome with orange bar in both sides represents genes which are large associated with SLE disease.

Combination between genetic factors and environmental factor could result in the defect in immunological tolerance and negative selection of auto-reactive T and B cells clone. In addition, increasing in many apoptotic cells were often found in LN patients as well as reduction of apoptotic body clearance. Simultaneously, detection of nuclear antigens by professional antigens presenting cells (APCs) which present auto-antigens to auto-reactive T-cells could be a key major pathogenesis of LN disease. This led to have a persistence of auto-reactive B cells and T cells in patients' circulation and over-production of various nephritogenic auto antibodies, chemokine and pro-inflammatory cytokine inducing an inflammation.(49).

For LN diagnosis and disease monitoring, presence of protein, white blood cells and red blood cells leakage in urine with retention of waste products (creatinine, UREA) in sera might represent disease activity. Basically, these biomarkers are correlated with severity and stage of patients. However, in some cases called "silencing LN", patients usually get a large damage in kidney without showing any symptoms. In addition, serological and urinary examination might not be able to tell the early sign of kidney injuries (50). Thus, the gold standard of LN detection and disease monitoring is to evaluate their kidney biopsy histology. It provides a useful information leading to plan a treatment strategy for patients. Based on histological features, the LN patients can be classified into 6 classes depending on cell and affected area. The International Society of Nephrology/Renal Pathology Society (ISN/RPS) were revised and provided standard criteria for LN classification listed here below (figure 7).

1. **Class I** : Minimal Mesangial cell proliferation
2. **Class II** : Mesangial proliferative nephritis
3. **Class III** : Focal lupus nephritis
4. **Class IV** : Diffuse segmental (IV-S) or global (IV-G) lupus nephritis
5. **Class V** : Membranous lupus nephritis
6. **Class VI** : Advanced sclerosing lupus nephritis

In general, percutaneous kidney biopsy is safe. However, it is an invasive technique which can carried a lot of potential risks such as infection, bleeding and internal damage to the target organs. Therefore, the non-invasive tool to monitor relapse as well as to guide the treatment decision are still needed.

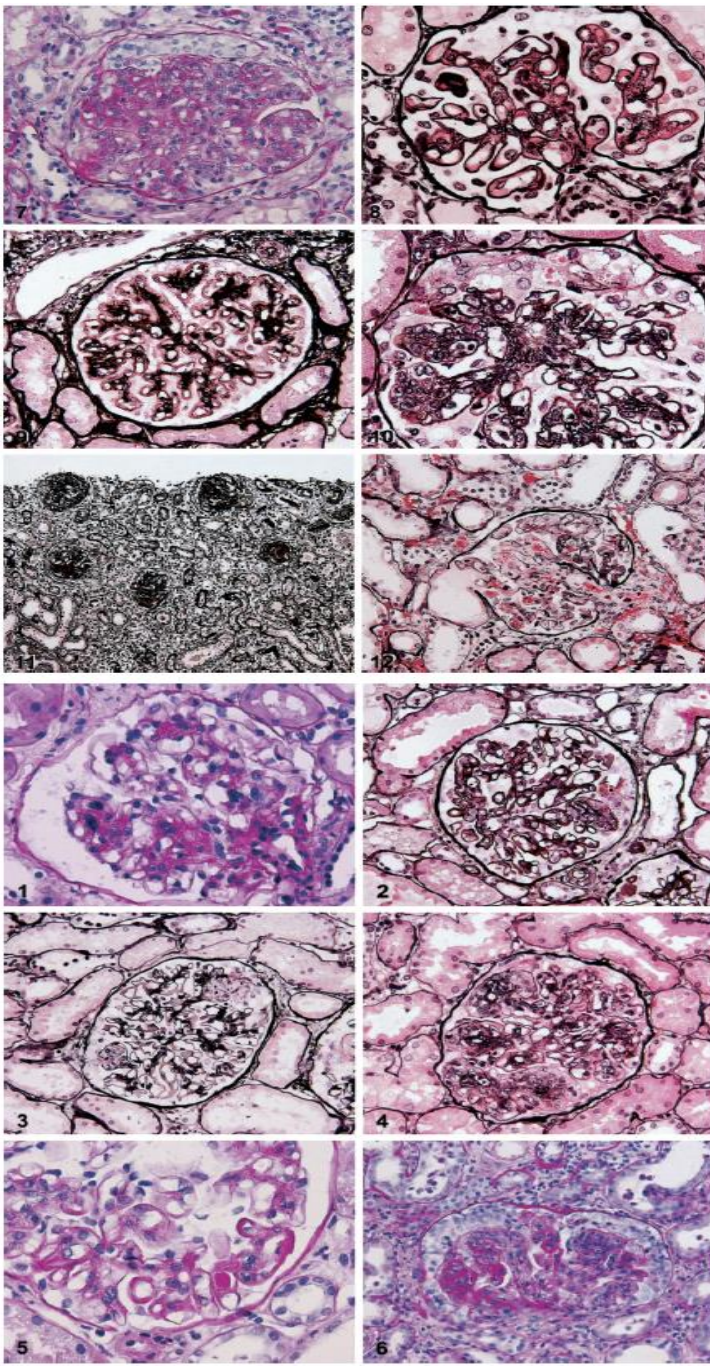

Figure 7 Histological features of LN kidney biopsy class I – VI (1)

(1) LN class II. The histology of a glomerulus with periodic acid-Schiff staining under light microscope shows mild mesangial hyper cellularity.

(2) LN class III (A). The histology of a glomerulus with methenamine silver staining under light micrograph shows segmental of glomerulus with endocapillary hyper cellularity, mesangial hyper cellularity, capillary wall thickening, and early segmental capillary necrosis.

(3) LN class III (A). The histology of a glomerulus with methenamine silver staining under micrograph shows segmental capillary necrosis with sparing of the remainder of the capillary tuft called vasculitis-like lesion.

(4) LN class IV-G (A). The histology of a glomerulus staining with methenamine under light micrograph shows global involvement of endocapillary and mesangial hyper cellularity and matrix expansion, influx of leukocytes, and occasional double contours.

(5) LN class IV-S (A). The histology of a glomerulus staining with periodic acid-Schiff staining under light microscope shows segmental of a glomerulus and endocapillary hyper cellularity, capillary wall double contours, wire loop lesions, and hyaline thrombi.

(6) LN class IV-G (A/C). The histology of a glomerulus with periodic acid-Schiff staining under light microscope shows global severe endo- and extra capillary proliferation, wire loop lesions, leukocyte influx, apoptotic bodies, capillary necrosis, and mesangial expansion with hyper cellularity and matrix expansion; marked interstitial inflammatory infiltration.

(7) LN class IV-G (A/C). The histology of a glomerulus with periodic acid-Schiff staining shows global endocapillary proliferation, leukocyte influx and apoptotic bodies, double contours, crescent formation with tubular transformation, early sclerosis, and disruption of Bowman's capsule.

(8) LN class IV-G (A). The histology of a glomerulus in methenamine silver staining with widespread sub endothelial immune deposits (wire loop lesions) associates with basement membrane new formation along the inner

side of the capillaries but without endocapillary leukocyte infiltration or hyper cellularity.

(9) LN class V. The histology of a glomerulus staining with methenamine silver from advanced-stage lupus membranous nephropathy characterized by massive sub epithelial accumulation of immune deposits (immunofluorescence: full house) and interdigitating spike formation.

(10) LN mix-class (class IV and V (A/C)). The histology of a glomerulus staining with methenamine silver shows lupus membranous nephropathy with sub epithelial spike formation combined with global endocapillary and mesangial hyper cellularity, early crescent formation, and beginning mesangial and capillary sclerosis.

(11) LN class VI. The histology of a glomerulus with methenamine silver staining shows renal cortex that almost diffuse, global glomerular sclerosis accompanied by interstitial fibrosis, mononuclear inflammatory infiltrates, and vascular sclerosis

(12) Thrombotic microangiopathy in a patient with SLE and circulating anticoagulants. A glomerulus with methenamine silver staining shows severe capillary and arteriolar thrombosis, endothelial cell swelling and necrosis, neutrophil influx, and stasis of erythrocytes. No signs of immune deposits.

For LN treatment, standard treatment for LN is the combination of immunosuppressive drug including corticosteroids and cyclophosphamide. The clinical outcome of LN patients is considerably improved (51). However, patients might get several complications including nausea, cardiovascular disorder, gonadal abnormality and thrombotic syndrome. Among several side effects from immunosuppressive treatment, infection is the most frequent and most dangerous adverse events associated with standard induction immunosuppressive treatment. The previous reports showed that severe infections were very common after the introduction of cyclophosphamide into treatment of AAV with 46% of patients experiencing severe

infection within 8 years of follow-up (52). Therefore, new modes of treatment are needed especially in patient's refractory, intolerant to, or frequently relapsing on the standard immunosuppressive treatment. Treatment considerations aim to avoid or at least lessen the still unacceptably high short- and long-term toxicity of the treatment. Organ damage (e.g. advanced chronic kidney disease), either due to late diagnosis and referral (in AAV), or due to relatively slow response to treatment (in LN) further increases the adverse events of the treatment.

Anti-double stranded DNA antibodies and mesangial cells

The difficulty in the development of suitable treatment and diagnostic biomarker is the complexity of disease pathogenesis. At present, it is known that auto anti-dsDNA antibodies level is significantly associated with LN development (53). Auto anti-dsDNA antibodies specific to several DNA structures including right handed double helix dsDNA (B-DNA), zig-zag shape dsDNA (Z-DNA), cruciform DNA and *Critidia luciliae* kinetoplast DNA. The origin of anti-dsDNA antibodies was described therefore from excessive apoptosis cells without proper clearance. This leads to massive presence of nucleosome in the circulation induced auto antibodies production (54). The chromatin fragment containing histone proteins and wrapped DNA showed immunogenicity which recognized by auto-reactive B cells specific to B-DNA or Z-DNA (figure 8).

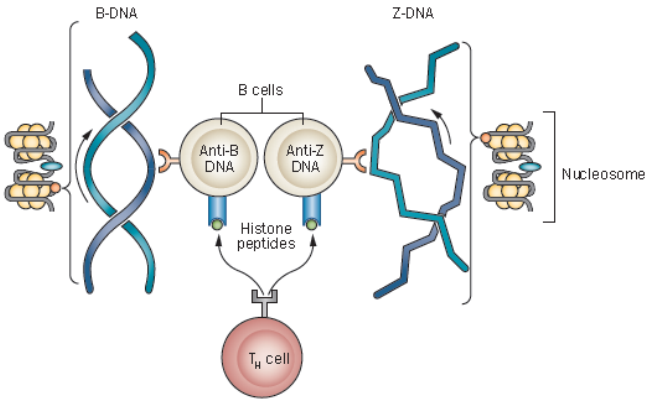

Figure 8 Origin of anti-dsDNA antibody (54)

Auto reactive B-cells recognized DNA structure on histone proteins. The double stranded DNA structure is hapten, while histone proteins were known as carrier protein. In consequent, the auto reactive T-cells recognize antigens present by B-cells and promote antibodies class switching.

The clinical implication of anti-dsDNA antibodies was started by 4 groups. The reports were independently detected anti-dsDNA antibodies in the LN patients' sera. In the following, the anti-dsDNA antibodies administration could induce severe proteinuria and nephritis *in vivo* (55). This suggested that anti-dsDNA antibodies might be a key factor drive LN in SLE patients. The antibodies activity and concentration was commonly used as a specific marker for LN and SLE (56). Nevertheless, anti-dsDNA antibodies could be found in SLE patients' circulation without present of LN. This raises the question of whether anti-dsDNA antibodies were an actual cause of LN pathogenesis. New theory with clear evidences expanded LN-pathogenesis knowledge. The studies showed two categories of anti-dsDNA antibodies including pathogenic anti-dsDNA antibodies and non-pathogenic anti-dsDNA antibodies (table 2) (54). In general, antibodies could trigger an inflammation within the kidney by two pathways including pre-existing immune complexes deposition and chromatin structure recognition on glomerular basement membrane or heparan sulphate via ionic force (57). Recently, increasing evidences highlighted the contribution of cross-reactive antibodies and kidney resident cells in LN pathogenesis (figure 9) (11, 58). The cross-reactive capacity was considered as pathogenicity of antibodies. Several antigens on renal cells

were confirmed to recognized by anti-dsDNA antibodies including ribosomal P protein (59), alpha-actinin (10), annexin II (17). After binding, the antibodies contain repeated arginine at variable region were capable to penetrate into the cells and nuclease activated ERK and increased cellular protein level of Bcl-2 (60).

Table 2 Characteristic of pathogenic and non-pathogenic anti-dsDNA antibodies (61)

	Non-nephritogenic anti-dsDNA Ab	Nephritogenic anti-dsDNA Ab	Cross-reactive anti-dsDNA Ab
Class	IgG, M and A	IgG mainly	IgG mainly
Somatic mutations	No	Yes	Yes
Affinity	Low	High	High
Cross-reactivity	No	Yes	Yes
Living cell internalization	No	Yes	suspected
Glomerular direct binding	No	Yes	Yes
Proteinuria	No	Yes	mainly

Anti-dsDNA antibodies could cross-react to several antigens expressed on various cell types in kidney. Particularly in glomerulus, there are composed of four major cell types (endothelial cells, epithelial cells, glomerular basement membrane, mesangial cells). One of the most interesting cells which uniquely found in kidney and involved in inflammatory process is “mesangial cells” (15). Mesangial cells are an immune cell resided within glomerulus connected to glomerular basement membrane and endothelial cells (14). The cells are responsible for both structural support and immunological feedback. For structural support, mesangial cells are behaved like a smooth muscle cells which express receptor for vasodilation and vasoconstriction agents assisting ultrafiltration mechanism (62). In addition, the cells generated mesangial matrixes which help to maintain glomerular structure. On the other hand, the cells are act as phagocytic cells. The mesangial cells can engulf foreign antigens (immune complexes) and promote inflammation by presenting antigens to T-cells. Moreover, the cells can produce pro-inflammatory cytokine and chemokine recruited leukocytes that might amplify inflammation. It is believed that mesangial cells were delivered from macrophages (63, 64). Nonetheless, when co-culture mesenchymal stem cells with injured mesangial cells, the cell were unexpectedly differentiated into mesangial cells like phenotype (65). *In vivo* experiment also found that mesenchymal stem cells, a multipotent stromal cell which normally differentiate to osteoblast (bone

cells), chondrocytes (cartilage cells), myocytes (muscle cells) and adipocytes (fat cells), could derive into mesangial cells during glomerulonephritis course (66). Eventually, there is a controversy about the origin of mesangial cells. Further analysis is still needed to identify certain origin of mesangial cells.

Interestingly, mesangial cells proliferation is distinct feature of LN class I-IV histology (figure10). This indicated that mesangial cells might play a role in LN pathophysiology. However, there were a few studies determine the role of mesangial cells in LN development.

Analysis of anti-dsDNA antibodies cross reaction on mesangial cells provided several interesting issues (67). For example, the cells exerted cytotoxicity after poly-clonal anti-dsDNA antibodies stimulation (68). The anti-dsDNA antibodies increased IL-6, IL-1β, and TNF-α expression in both mouse (MMCs) and human mesangial cells (HMCs) (69). The anti-dsDNA antibodies induction could stimulate fibronectin production and protein kinase C phosphorylation which inhibit by mycophenolatemofetil (immunosuppressant which commonly used for LN treatment) (70). Furthermore, anti-dsDNA antibodies cause excessive hyaluronan generation that led to kidney fibrosis in chronic renal disease (71). The anti-dsDNA antibodies stimulation transformed mesangial cells into myofibroblast like phenotype (18). Transcriptomic analysis displayed a whole picture of mesangial cells response against anti-dsDNA antibodies stimulation showing NF-κB signalling, nitric oxide synthesis, proliferation and apoptosis were upregulated (19). Beside the anti-dsDNA antibodies could induce endoplasmic reticulum (ER) stress via pERK-eIF2α-ATF4 promoting inflammation (12).

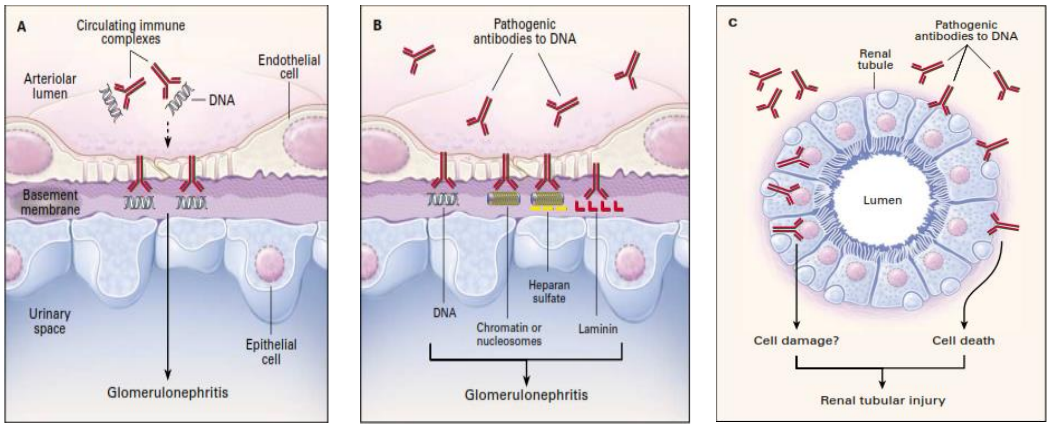

Figure 9 The proposed mechanisms by which anti-dsDNA antibodies caused tissue damages (3)

(A) represents anti-dsDNA antibodies immune-complexes induced inflammation.

(B) represents pathogenic anti-dsDNA antibodies which attached to DNA structure, heparan sulphate and laminin triggering complement activation.

(C) represents anti-dsDNA antibodies cross-reacted with renal antigens inducing cell death and damage.

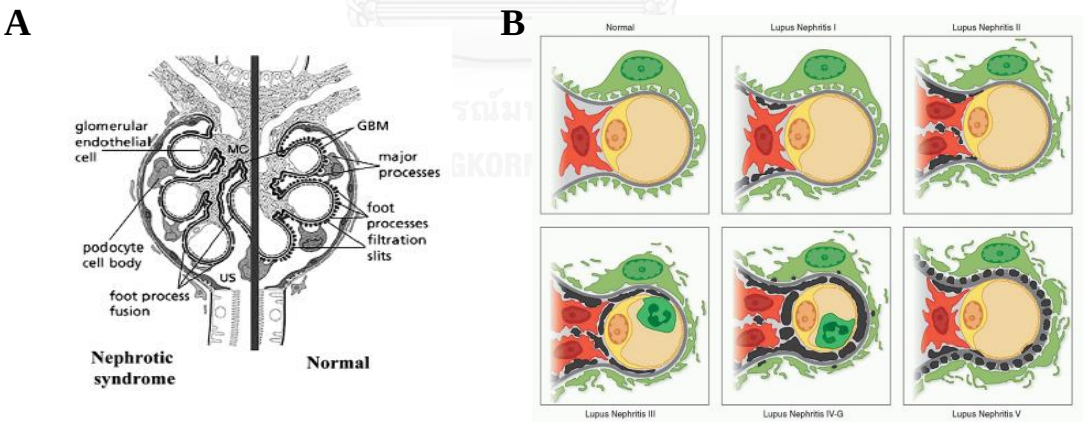

Figure 10 The contribution of mesangial cells in the glomerulus within the different types of LN

(A) represents mesangial cell proliferation in nephrotic syndrome.

(B) represents histology in one glomerulus from different class of LN (class I-VI).

The study of microRNA in Lupus nephritis

Recently, a comparison of miRNA profiling studies in kidney biopsies from LN and healthy control raise up an interesting question about the role of miRNA in LN pathogenesis (72-74). Several miRNAs were studies to characterize the role miRNA in both immune-related cells and kidney residential cells in LN pathogenesis (table 3) (75-79). For example, in PBMC, the miR-146a were reported to target IRAK1 and TRAP6, a signalling protein in the type I interferon (IFN) pathways which known as signature cytokine in SLE pathophysiology (37) as well as miR-155 which target negative regulator, SOCS1 and SHIP1 resulting in AKT and type I IFN over-production. The miR-21 was found to control PDCD4, tumour suppressor proteins, related to NF-kB signalling pathways. Studies of miRNA in mesangial cells isolated from spontaneous develop LN mouse model demonstrated that up-regulation of let-7 during active stages could enhance IL-6 expression (26). The miR-26a and miR-30a in human mesangial cells were important in mesangial cells proliferation (27).

As described above, miRNA was specifically expressed at each time point and stimulation, the miRNA expression in anti-dsDNA IgG antibodies stimulated mesangial cells which considered as initial stage for inflammation induction in LN patients was necessary to investigate. The aim of this study is to identify role of miRNA in HMCs upon anti-dsDNA antibodies activation compared to IgG control. This might expand our understanding about antibodies mediated resident kidney cells induced inflammation with the miRNA regulatory mechanism which could be a novel therapeutic target or disease stage biomarker in the future.

Table 3 Summarized miRNA in lupus nephritis in difference cell or tissue types (80)

Cell or tissue type	miR ID(s)	Origin	Strain	Expression	Results	Mechanism(s)
Dendritic cells	155	H	—	↑	Induced by TLR stimulation after miR-155*; overexpression of miR-155 in normal pDCs significantly decreased *IFN-α*, *IFN-β*, and *TNF-α* expression	The 3′ UTR of the type I IFN regulator *TAB2* is a target of miR-155, indirectly decreasing IFN-α and IFN-β
	155*	H	—	↑	Induced by TLR stimulation before miR-155; overexpression of miR-155* in normal pDCs significantly increased *IFN-α*, *IFN-β*, and *TNF-α* expression	The 3′ UTR of the negative IFN regulator *IRAKM* is a target of miR-155*, indirectly increasing IFN-α and IFN-β
Splenocytes	15a	M	NZB/W	↑	Increased expression after disease was accelerated by IFN administration; differentially expressed in B cell subsets	Unknown
	21	M	B6.Sle123	↑	Inhibition increased *PDCD4* expression in T cells and reversed splenomegaly, improving overall disease outcome	The 3′ UTR of *PDCD4* is a target of miR-21
		M and H	MRL-*lpr*	↑	Downregulated *DNMT1* expression in T cells	The 3′ UTR of the *DNMT1* upstream regulator *RASGRP1* is a target of miR-21, indirectly downregulating *DNMT1*
	126	H	—	↑	Overexpression contributes to T cell autoreactivity by decreasing *DNMT1* expression	The 3′ UTR of *DNMT1* is a target of miR-126
					Overexpression in healthy donors was sufficient for T cell autoreactivity and B cell hyperstimulation, while inhibition in SLE patients resulted in T and B cell inactivation	Unknown
	142-3p and 142-5p	H	—	↓	Underexpressed in SLE $CD4^+$ T cells	Dysregulated DNA and histone methylation of the miR-142 promoter
					Underexpression in $CD4^+$ T cells increased production of CD84, IL-10, and SAP	The 3′ UTR of *CD84* and *IL-10* are targets of miR-142-3p; the 3′ UTR of *SAP* is a target of miR-142-5p
					Inhibition in healthy donor $CD4^+$ T cells caused T cell overactivation and B cell hyperstimulation, while overexpression in SLE $CD4^+$ T cells had the opposite effect	Although CD84 and SAP stimulate T-B cell interactions, the exact mechanism of miR-142 is unknown
	146a	M	MRL/*lpr*	↑	Increased expression associated with disease development	Unknown
	148a	M and H	MRL/*lpr*	↑	Downregulated *DNMT1* expression in T cells	The protein coding region of the *DNMT1* transcript is a target of miR-148a
					Induced overexpression of autoimmune-associated, methylation-sensitive genes in $CD4^+$ T cells including *CD70* and *LFA-1*	Inhibition of *DNMT1* results in DNA hypomethylation and the overexpression of methylation-sensitive genes
	155	M	MRL/*lpr*, NZB/W	↑	Increased expression associated with disease development	Unknown
Renal	21 and 214	R	WKY (anti-Thy1.1)	↑	Expression is induced by TGF-*β* in tubular epithelial cells *in vitro* and in renal tissue *in vivo*	Unknown
					Overexpression in tubular epithelial cells *in vitro* decreased *E-cadherin* expression and increased *collagen type I* and *α-SMA* expression	Unknown
	146a	M	B6.MRLc1	↑	Increased expression positively correlated with *IL-1β*, *IL-10*, and *CXCL* expression, severe glomerular and interstitial lesions, and T cell and macrophage infiltration	Unknown
		H	—	↑	Glomerular expression positively correlated with estimated GFR and histological activity index	Unknown
	638	H	—	↑	Tubulointerstitial expression positively correlated with proteinuria and disease activity score	Unknown
PBMCs	21	H	—	↑	Strongly correlated with disease activity and activated T cells	Unknown
					Inhibition *in vitro* reversed the activated T cell phenotype by increasing *PDCD4* expression	The 3′ UTR of *PDCD4* is a target of miR-21
	125a	H	—	↓	Underexpression contributes to the elevated expression of *RANTES* (*CCL5*) in SLE, increasing T cell recruitment to inflammatory tissues	The 3′ UTR of the *RANTES* upstream regulator *KFLI3* is a target of miR-125a, indirectly increasing *RANTES* expression
	145	H	—	↓	Decreased expression increased *STAT1* expression in SLE patients	The 3′ UTR of *STAT1* is a target of miR-145
	146a	H	—	↓	Inversely correlated with disease activity and IFN-α/β scores	Unknown
					Overexpression reduced the induction and downstream effects of type I IFN	The 3′ UTR of *IRF5* and *STAT1* are targets of miR-146a, reducing the induction of type I IFN
					Promoter variant associated with SLE disease risk	SLE-associated SNP (rs57095329) decreases miR-146a expression levels
					Positively correlated with GFR, CRP, and other renal function parameters; inversely correlated with proteinuria and SLEDAI	Unknown
	155	H	—	↓	Positively correlated with GFR, CRP, and other renal function parameters	Unknown
	224	H	—	↑	Increased expression accelerated T cell activation-induced cell death by suppressing *API5* expression in SLE patients	The 3′ UTR of *API5* is a target of miR-224
Mesangial cells	Let-7a	M	NZB/W	↑	Increased expression throughout the lifetime of NZB/W lupus mice; overexpression increased *IL-6* expression and IL-6 production *in vitro*	The 3′ UTR of *IL-6* is a target of let-7a; the exact mechanism of let-7a is unknown

Chapter III

Material and Methods

Sample Collection

Sera (3 mL) were collected from active LN patients (N=20). All participant must be fulfilled at least 4 of 11 criteria in the American College of Rheumatology diagnosis criteria for SLE patients. LN patients who undergoes active stage were defined by routine urine examination. The urine protein and creatinine index (UPCI) which is higher than 1.0, and the presence of microscopic RBCs or WBCs in urine more than 5 cells/HPF without an infection or the presence of RBC/WBC cast, granular cast, hyaline cast and renal tubular cells cast are generally considered as renal flare. All sera from healthy controls were collected from donor at blood donation centre, Thai Red Cross, Thailand. All the protocols were approved by ethic committee from Faculty of Medicine, Chulalongkorn University, EC. No. 268/56.

Polyclonal anti-dsDNA antibodies Preparation

To purify anti-dsDNA antibodies, each serum sample was diluted five times with PBS pH 7.4 and applied onto a protein G sepharose column (2 x 16mm, GE Healthcare life science, Thailand) equilibrated with PBS. The matrix was subsequently washed with the equilibrating buffer to remove unbound proteins. The bound antibodies were eluted with 0.1 M Glycine buffer pH 2.6 and the collected fractions were immediately neutralized with 1M Tris-HCl buffer pH 9. The purified antibodies, previously dialyzed against 25 mM Tris-HCl buffer pH 7.4 containing 1 mM EDTA, 50 mM NaCl, 1 mM β-mercaptoethanol, 10% glycerol, were loaded onto a DNA-cellulose column (3 x 16mm, GE Healthcare life science, Thailand) equilibrated with the same buffer to isolate the anti-dsDNA IgG After an extensive washing step to remove any unbound antibodies, the anti-dsDNA IgG were eluted by addition of 2M NaCl in the buffer. The purified fractions were dialyzed against PBS pH 7.4 and stored at -80 ^{o}C until further analysis.

Antibodies activity and concentration

Antibody activity and purity were examined by Direct ELISA (cat no. EA 1572-9601G, Euroimmun, Hausen Bernstein, Thailand) and SDS-PAGE, respectively. Antibodies specificity was also confirmed by immunofluorescent against HEp-2 cells. Briefly, HEp-2 cells were pre-coated to the slide. The purified anti-dsDNA antibodies were added following with anti-IgG antibodies labelled FITC. The staining pattern were determined as indicated in the previous study (81). Purified anti-dsDNA IgG antibodies showed homogenous pattern. Total IgG concentration were determined by nephelometry technique (BN prospec System, Siemens, Berlin, Germany).

Primary HMCs culture and antibodies stimulation

HMCs (Sciencell, Meditop, Thailand), passage 4-7, were seeded in 75mm^2 culture flask with Mesangial Culture Medium (Sciencell, Cat. No. 4201) at 37 ^{o}C, 5% CO_2. The cells ($2x10^5$ cells/well in 24 well plate) were cultured in serum deprivation medium for 24 hours before incubated with serum (1:10, 1:100, 1:1000) for 0, 3, 6, 12, 24 hours. For antibodies stimulation, the cells were incubated with anti-dsDNA IgG antibodies or non-specific IgG (10 µg/mL) with or without serum 1:100 for 3 hours. For transfection experiment, the cells were prepared in serum and antibiotic deprivation medium for 24 hours to get high transfection efficiency.

Flow-cytometry

To determine anti-dsDNA IgG antibodies interaction on HMCs membrane antigens, flow cytometry were conducted as describe previously (17). In brief, confluent HMC ($1x10^6$ cells) were trypsinized and cultured in suspension overnight (EBSS + 2% FBS, no agitation). The cells were pelleted and washed with FACs buffer (DPBS+2%FBS) for 3 times. Next anti-dsDNA IgG antibodies or non-specific IgG (10, 20, 50, 100 µg/ml) were incubated for 1 hour on ice, then stained with anti-human IgG Fc region conjugated with FITC or isotype control (Biolegend, Advance Medical Sciences, Thailand). To confirm its direct binding activity, the FcγR blocking reagent (Miltenyi Biotec, ITS, Thailand) were pre-incubated with HMCs (1:5 reagent volume per cells)

for 10 minutes at 4^{o} C in the dark chamber. The cells were subsequently washed and stained with anti-dsDNA IgG antibodies as described above. HMCs were also stained with anti-HLA class I (clone W6/32) and anti-platelet derived growth factor β antibodies conjugated with FITC (Biolegend, Advance Medical Sciences, Thailand) as a positive control. Flow cytometric results were analysed by Flowjo.

RNA preparation

Both Total RNA and small RNA were extracted using mirVana® small RNA extraction kit (Invitrogen Life Technologies, ABI, Thailand). The principle for small RNA extraction is to increase ethanol concentration in order to precipitate small RNA, the small RNA eventually struck above the silicone column and be eluted with RNase-free water. All the steps were followed the small RNA enrichment manufacturers' procedures. Purified RNA samples, processed with DNase treatment at 37^{o}C, were stored at -80°C until use. The RNA purity and concentration were evaluated by nanodrop 1000 (Thermo-scientific). The OD 260/280 ratio which is larger than 1.8 are considered as a good quality RNA and subsequently used for RT and real-time PCR. For transcriptomic study and small RNA study, the RNA were analysed for RNA integrity and concentration on Agilent 2100 Bioanalyzer (Agilent Technologies, Palo Alto, USA) using small RNA chip assay. The RNA must contain RNA integrity number (RIN) larger than 8 and the ratio between 28s rRNA and 18s rRNA larger than 1.6.

Reverse transcription PCR and Real-Time PCR

The isolated total RNA fraction (250 ng) was retro-transcribed using the Applied Biosystems^{TM} High Capacity cDNA Reverse Transcription kit (Thermo Fisher Scientific, ABI, Thailand). Reaction preparation were carried out according to manufacturers' instruction. Real-Time PCR was carried out by using Applied Biosystems® 7500 Real-Time PCR System. List of primers were shown in table 4.

Table 4 List of Primers used throughout the study

Official gene name	*Sequence primer*	*Amplicon Size*
GADPH	Forward 5'-GCACCGTCAAGGCTGAGAAC-3' Reverse 5'- ATGGTGGTGAAGACGCCAGT-3'	142 bp
IL-6	Forward 5'-GGCACTGGCAGAAAACAACC-3' Reverse 5'-GCAAGTCTCCTCATTGAATCC-3'	85 bp
IL-8	Forward 5'-ACACTGCGCCAACACAGAAATTA-3' Reverse 5'-TTTGCTTGAAGTTTCACTGGCATC-3'	185 bp
IL-1β	Forward 5'- ACAGATGAAGTGCTCCTTCCA -3' Reverse 5'- GTCGGAGATTCGTAGCTGGAT-3'	73 bp
TNF-α	Forward 5'-CTTCTCCTTCCTGATCGTGG -3' Reverse 5'-GCTGGTTATCTCTCAGCTCCA-3'	266 bp
MMP-10	Forward 5'-GGCTCTTTCACTCAGCCAAC-3' Reverse 5'-TCCCGAAGGAACAGATTTTG-3'	176 bp
CREB1	Forward 5'-ACGAAAGCAGTGACGGAGG-3' Reverse 5'-CGGTGGGAGCAGATGATGTT-3'	198 bp
NFAT5	Forward 5'-CAACAACATGACACTGGCGG-3' Reverse 5'-TCGAAAAACCAATCTGGCACG-3'	124 bp
PIK3CA	Forward 5'-TCCAGACGCATTTCCACAGC-3' Reverse 5'- GTCACATAAGGGTTCTCCTCCA-3'	186 bp
SMAD2	Forward 5'- CACAGCCCTCACTCACTGTA-3' Reverse 5'- GCACTCAGCAAAAACTTCCCC-3'	170 bp
MAP4K4	Forward 5'-TGTTAAAACGGGTCAGTTGGC-3' Reverse 5'-TGTCCTGGAGGGCTCTTTTTG-3'	159 bp
MAP3K7	Forward 5'-ACTTGATGCGGTACTTTC-3' Reverse 5'-GGTTGCGGCGATCCTA-3'	350 bp
KLF4	Forward 5'-GGGCTGCGGCAAAACCTACACA-3' Reverse 5'-CCATCCACAGCCGTCCCAGTCA-3'	103 bp
HOXA1	Forward 5'-CCAGGAGCTCAGGAAGAAGAGAT-3' Reverse 5'-CCCTCTGAGGCATCTGATTGGGTTT-3'	247 bp

Stem-loop RT and qPCR

Since miRNA are short RNA sequences, its hold a similar sequence with little different between group of miRNAs. The stem-loop primers were designed to increase more specificity and melting temperature which help amplification reactions. The stem-loop primers were used in RT-PCR step. In the following, a specific probe was used to increase uniquify during quantitative Real-time PCR. The miRNA stem-loop primers were purchased from available company (Invitrogen Life Technologies, ABI, Thailand).

In this study miR-10a (ID479241_mir), miR-143 (ID478713_mir), miR-411 (ID 478086_mir), miR-181a (ID 477857_mir), miR-125b (ID 478666_mir), miR-127(ID 477891_mir) were selected for small RNASeq validation. All the expression data were normalized with U44 (ID 001094) expression as reference genes. The cDNA samples were subsequently detected by specific TaqMan probe from same assay. The expression were determined by cycle threshold and expression fold change were calculated as previous reports (82).

cDNA Microarray

Total RNA from anti-dsDNA IgG antibodies stimulated HMC and transient miR-10a knockdown HMC were amplified and purified using the Ambion Illumina RNA amplification kit (Ambion, Austin, USA) to yield biotinylated cRNA according to the manufacturer's instructions. Briefly, 550 ng of total RNA was retrotranscribed to cDNA using a T7 oligo(dT) primer. Second-strand cDNA was synthesized and labelled with biotin-NTP. After purification, the cRNA was quantified using the ND-1000 Spectrophotometer (NanoDrop, Wilmington, USA). 750 ng of labelled cRNA samples were hybridized to human HT-12 expression v.4 bead array for 16-18 h at 58°C, according to the manufacturer's instructions (Illumina, Inc., San Diego, USA). Detection of array signal was carried out using Amersham fluorolink streptavidin-Cy3 (GE Healthcare Bio-Sciences, Little Chalfont, UK) following the bead array manual. Arrays were scanned with an Illumina bead array Reader confocal scanner according to the manufacturer's instructions. The quality of hybridization and overall chip performance were monitored by visual inspection of both internal quality control checks and the raw scanned data. Raw data were extracted using the software provided by the manufacturer (Illumina GenomeStudio v2011.1 (Gene Expression Module v1.9.0)). Array probes transformed by logarithm and normalized by quantile method. Statistical significance of all expression data was determined using un-pair *t*-test and fold change in which the null hypothesis was that no difference exists among groups. False discovery rate (FDR) was controlled by adjusting p-value using FDR algorithm (p-value < 0.05). For a DEG set, Hierarchical cluster analysis was performed using complete linkage and Euclidean distance as a measure of similarity. Gene Set

Enrichment (GSE), Gene Ontology (GO) and Functional Annotation analysis for significant probe list were performed using DAVID (http://david.abcc.ncifcrf.gov/home.jsp). All data analysis and visualization of differentially expressed genes were conducted using R 3.0.2 (www.r-project.org). The microarray data from anti-dsDNA IgG antibodies stimulated HMC and transient knockdown miR-10a in HMC were deposited in GEO database as repository number GSE80364 and GSE79574, respectively.

Small RNA library preparation and next generation sequencing with sequence annotation

Small RNA libraries were prepared by using TruSeq Small RNA library preparation kits (Illumina®, Bioactive Ltd, Thailand). Regarding manufacturer's protocol, small RNA (1 µg) were pooled and ligated with the adapter using T4 RNA ligase. The processed RNAs were retro-transcribed and amplified with PCR primer. The cDNA libraries were selectively purified by 6% polyacrylamide gel electrophoresis using custom RNA ladder and high-resolution ladder as molecular weight references. The libraries were extracted by gel breaker tube and eluted from the gel by ultrapure water. Finally, the cDNA was denatured with NaOH before loading into MiSeq Reagent cartridge (Illumina®, Bioactive Ltd, Thailand). The sequencing was run by MiSeq Sequencing System (Illumina®, Bioactive Ltd, Thailand) and all the data were imported by Illumina® GenomeStudio Software. Sequencing files (.fastq) were analyzed by using two independent bioinformatics tool including miRDeep 2.0 (83) and sRNAbench (84). Sequencing quality was evaluated by FastQC program. The sequences were aligned to miRbase 20 database. The number of amplicons was normalized to reads per million reads (RPM).

miRNA transfection

The HMC (passage 4-7) ($1x10^5$ cells) were transfected with miR-10a inhibitor, miR-10a mimic and scramble controls using Lipofectamine RNAiMax (RNA 5 pmol: RNAiMax 1.5 µL/well) (Thermo Fisher Scientific, Gibthai, Thailand) for 24, 48, 72 hours. Then, miR-10a expression were determined by using stem-loop RT and Real-

Time PCR as described above. For anti-dsDNA antibodies stimulation, cells were transfected with miR-10a inhibitor for 24 hours, subsequently, the cells were stimulated with anti-dsDNA IgG antibodies (10 µg/mL) for 0, 3, 6, 12 and 24 hours.

Cell Viability assay

The miR-10a knock-down HMC were cultured overnight. In the following, cell proliferation assay (MTS, Cell Aqueous One Solution Cell Proliferation Assay, Promega, USA) were added into culture medium and incubated for 4 hours. Cell density was detected by absorbance (OD490) by Verioskan (Thermo Fisher Scientific, Gibthai, Thailand). The standard curve was conducted by using a various number of cells from 5,000 to 60,000 cells. Three biological replicates with three independent experiments were required.

Luciferase assay

The pmirGLO dual luciferase miRNA Target expression vector (Promega, DKSH, Thailand) was used as reporter plasmid. The miR-10a binding sites and binding capacity presence in the 3'UTR of IL-8 and NFAT5 were predicted using three independent programs including TargetScan (85), miRanda and RNAhybrid (86). These sequences were inserted into the pmirGLO plasmid. In consequent, the plasmid was transformed into complete cells (*Escherichia coli* species TOP10). As plasmid carried ampicillin resistant gene, bacteria that are holding plasmid were selected by growing in ampicillin-medium. The plasmids were extracted by Fast and Easy Plasmid Prep kit (JenaBioscience, Zcell, Thailand) with low-endotoxin contamination. Inserted plasmids were confirmed by sanger sequencing and aligned to plasmid sequences in the database. The pmirGlo containing 3'UTR IL-8 or 3'UTR NFAT5 were co-transfected into HMCs with miR-10a inhibitor, miR-10a mimic and scramble control for 48 hours using Lipofectamine 2000 (DNA 500 ng: 15 pmol RNA: Lipofectamine 1 µL/ 24 wells) (Thermo Fisher Scientific, Life Technology, Thailand). Luciferase activity were determined by Dual-Glo® Luciferase assay systems (Promega, DKSH, Thailand). Transfection efficacy were examined by Renilla-luciferase. The luciferase-renilla luciferase ratio were reported.

Interleukin-8 ELISA

The HMCs were transfected with miR-10a inhibitor, miR-10a mimic and scramble control for 24, 48 and 72 hours. Culture supernatant were collected according to these conditions. The IL-8 secretion was studied using hIL-8 ELISA duo kit (R&D).

Statistical analysis

Expression data were compared using un-pair student's *t*-test. The non-parametric Mann-Whitney U-test was used to draw comparisons between groups, with the exception that an un-pair *t*-test was used to compared reporter gene activity. To compare the different between the group, two-way ANOVA were applied. For correlation study, Pearson-Spearman method was used. *P*-values less than 0.05 were considered as statistically significant.

Chapter IV

Results

Anti-dsDNA antibodies cross reacted to membrane antigen of HMCs and stimulated IL-6 expression which marked as an early activation marker

Anti-dsDNA antibodies were purified from the serum of LN patients (N = 20) while non-specific IgG controls were isolated from healthy serum (N = 20) using affinity chromatography (sample demographic data are in table 5). The antibodies activity against DNA was confirmed by ELISA and immunofluorescent with HEp-2 cells. Percent antibodies recovery were calculated using total IgG concentration after purified divided by total IgG in starting material. The results showed that 10-20% of antibodies were recovered as anti-dsDNA IgG antibodies.

Table 5 Lupus nephritis patients' demographic data and clinical scores

Characteristic	Active Ln	Healthy	P-value
Number	20	20	n/a
Sex (F/M)	19/1	19/1	n/a
Age (years)	33.75 ± 8.52	38.3 ± 8.93	0.1518
Clinical parameter			
Serum Creatinine (mg/dL)	1.002 ± 0.1065	n/a	n/a
Proteinuria (g/day)	3.081 ± 0.3996	n/a	n/a
Urinary Erythrocyte Count (/HPF)	10.55 ± 4.863	n/a	n/a
MDRD[a] GFR (mL/min)	82.08 ± 7.259	n/a	n/a
LN Renal Histology			
Class III	1/20	n/a	n/a
Class IV	11/20	n/a	n/a
Class V	2/20	n/a	n/a
Class III + V	1/20	n/a	n/a
Class IV + V	5/20	n/a	n/a
Activity Index[b]	5.9 ± 3.63	n/a	n/a
Chronicity Index[c]	5.2 ± 3.85	n/a	n/a
Steroid Dose (mg/day)	19.63 ± 2.829	n/a	n/a

[(a)] The MDRD equation for Thais is as follows: 175 × Cr(Enz) ((-1.154)) × Age ((-0.203)) × 0.742 (if female) × 1.129 (if Thai).
[(b)] Activity index is number of containing lesions such as cellular crescents,
[(c)] Chronicity index is number of composed of glomerulosclerosis s and interstitial fibrosis

As previous report demonstrated that anti-dsDNA IgG antibodies drove IL-6 expression in HMC related to the inflammation in LN (10), we therefore selected to detect the IL-6 expression as a response of HMC to anti-dsDNA antibodies in this study. Preliminary study using serum stimulation, the cells were stimulated with crude serum from healthy control and LN patients in various conditions (serum final concentration 1:1000, 1:100 and 1:10 at different time-point 0, 3, 6, 12, 24 hours). The results showed that patients serum (1:100 and 1:10) could upregulate IL-6 expression compared to healthy controls (p-value < 0.01) (figure 11A). The high serum titer (1:10) were obviously induced cell apoptosis more than low serum titer (1:100). We therefore use serum titer at 1:100 in this study. The expression of IL-6 were also detected in time-dependent manner. We found a remarkable increase of the IL-6 expression after serum treatment (1:100) for 3 hours (figure 11B).

With the same condition, the HMCs were treated with purified anti-dsDNA IgG antibodies (10 µg/mL) in the presence of normal serum (1:100) for 3 hours. Similarly, the anti-dsDNA IgG antibodies could up-regulated IL-6 expression significantly compared to non-specific IgG controls (p-value < 0.01) (figure 12A). This suggested that rapid activation of HMC using anti-dsDNA IgG antibodies could trigger a pro-inflammatory cytokine expression. In this case, the IL-6 expression was represented as responding marker of HMCs.

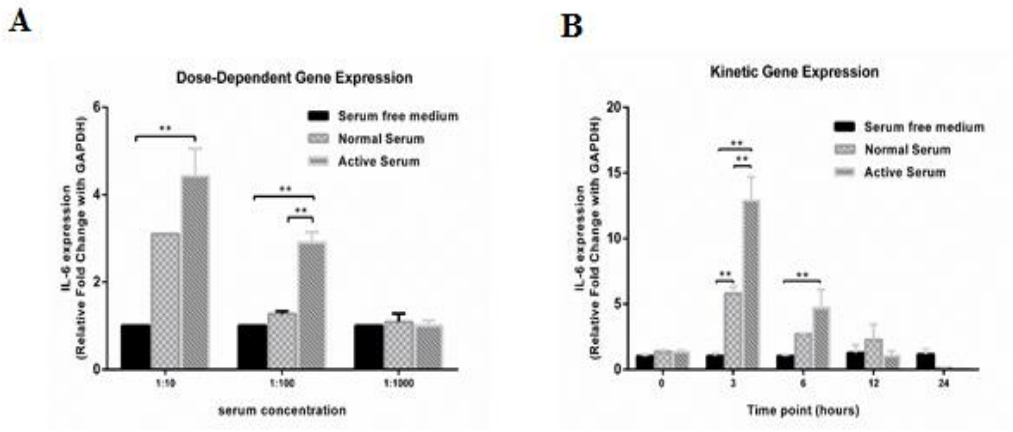

Figure 11 Preliminary study using serum from healthy control and active LN patients.

The HMCs were cultured in serum free medium over night before serum stimulaton. **A.** The serum were diluted with culture medium into three titer including 1:10, 1:100 and 1:1000. The HMCs were treated with various concentration of serum at 6 hours. **B.** The HMCs were stimulated with serum (1:100). The IL-6 expression was determined at different time point (0, 3, 6, 12, 24 hours) after serum stimulation. The (*), (**), (***) denote the significant *p*-value from less than 0.05, 0.01 and 0.001, respectively.

In order to investigate the mechanism which promoted IL-6 expression in HMC, previous studies demonstrated that cross-reactive binding of anti-dsDNA IgG antibodies onto HMC membrane antigens could markedly upregulated IL-6 expression. To test whether anti-dsDNA IgG antibodies could cross react with HMCs membrane antigens, the HMCs were cultured in suspension over-night. Subsequently, the HMCs were incubated with anti-dsDNA IgG antibodies following with secondary antibodies against IgG conjugated with FITC. An increasing number of FITC positive cells represents number of cross reacted antibodies compared to non-specific IgG control. Using flow-cytometry detection, the FITC positive cells were increasing in anti-dsDNA IgG antibodies stimulation in dose-dependent manner (10, 50, 100 µg/mL) (figure 12B).

This suggested that anti-dsDNA IgG antibodies could bind directly to HMCs. To exclude the possibility that anti-dsDNA IgG antibodies were recognized by Fc gamma receptor expressed on HMCs, the cells were pre-treated with Fc gamma receptor blocking reagents before anti-dsDNA IgG antibodies activation. The results showed that blocking Fc gamma receptor did not reduce any binding activity of anti-dsDNA IgG antibodies to HMCs (anti-dsDNA Ab 20.5% VS. IgG 2.22% and anti-dsDNA Ab 20.5% VS 2nd Ab 2.19%, *p*-value < 0.05) (figures 12C and 12D). This indicated that anti-dsDNA IgG antibodies cross reacted to the antigens on HMCs and it might drive IL-6 expression in HMCs.

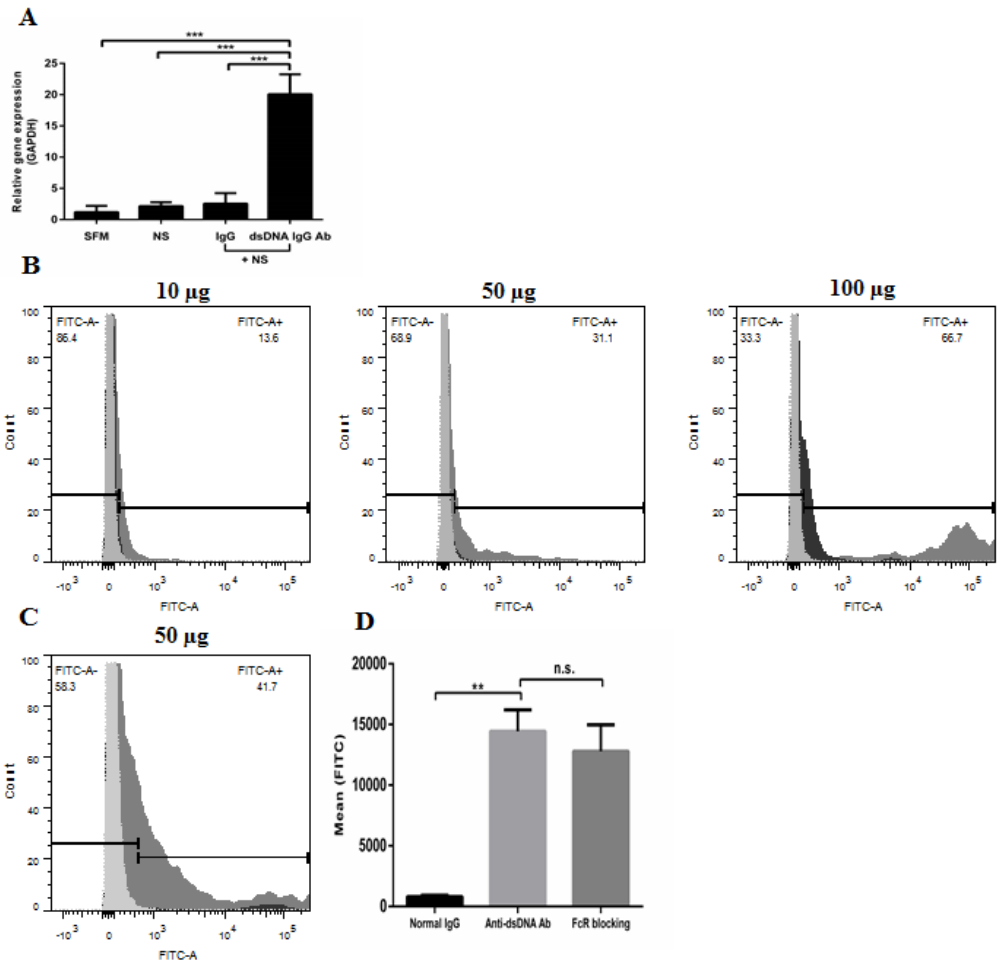

Figure 12 The interleukin-6 expression in HMCs stimulated with anti-dsDNA IgG antibodies and antibodies cross-reactivity onto HMCs cells membrane.

A. The HMCs (2 x 10^5 cells) were cultured in serum-free medium over-night. The antibodies (10 µg/mL) were added into cultured medium for 3 hours with normal serum (1:100). The IL-6 expression was detected using Real-Time PCR. Bar graph represents mean ± SEM from three independent experiments with three biological replicates. Data were expressed as mean ± SEM. The (*), (**), (***) denotes $P < 0.05$, $P < 0.01$, $P < 0.001$ versus serum free medium, respectively. **B.** Flow-cytometry results showed anti-dsDNA IgG antibodies binding to suspended HMCs in dose-dependent manner (10, 50 and 100 µg/mL). The HMCs ($1x10^6$ cells) were cultured in the EBSS-containing 10% FBS overnight. Antibodies staining were carried out under 4^o C for 1 hour following with either secondary antibodies conjugated FITC or isotype controls. **C.** The cells were pre-incubated with Fc-gamma receptor blocking reagents for 30 minutes in dark chamber. The anti-dsDNA IgG antibodies (50 µg/mL) were stained as described above. The histogram represent number of FITC positive cells. The light grey represents isotype control, black represents IgG control and dark grey represent anti-dsDNA antibodies. **D.** According to flow cytometry data, the mean fluorescent intensity was calculated. Data shown represent a minimum of 3 biological replicates in three independent experiments. The un-pair students' *t*-test were used to compare the mean fluorescent intensity. The (**) denotes P-value < 0.01.

The miRNA expression profiling in HMC stimulated with anti-dsDNA IgG antibodies

To investigate miRNA profiling in HMC treated with anti-dsDNA IgG antibodies, small RNA sequencing was conducted. The small RNA quality was performed period to library preparation using small RNA bioanalyzer chip assay (Agilent). The data were analysed using two bioinformatics tools called miRDeep2 (https://www.mdc-berlin.de/8551903/en/) (83) and sRNAbench 1.0 or sRNAtoolbox software (http://bioinfo5.ugr.es/sRNAbench/sRNAbench.php) (87). As the rule of thumb, it is known that a gene need to have a count of 5-10 in a library to be considered expressed in that library. The low expression transcripts were filtered out in order to normalize small RNA sequencing data. Top ten microRNA expression in each condition were reported in table 6. Among these, the miR-10b is the highest abundance miRNA in HMCs in IgG stimulation while miR-22 is the highest in anti-dsDNA IgG antibodies stimulation. Fold change difference between anti-dsDNA IgG antibodies and non-specific IgG control was calculated by ratio of read per million (RPM). Next, the miRNA which up-regulated or down-regulated more than 1.5-fold were considered as responded to anti-dsDNA IgG antibodies. However, it should be noted that there was no statistical analysis data since only one pooled samples in each group was used. The advantages of using pooled samples are reducing variations between samples and could be represented overall changing of microRNA expressions upon stimulation. Regarding to sequencing results, 61 miRNAs were up-regulation and 14 miRNAs were down-regulation (listed in table 7 and table 8). The miRNAs were then compared to previous reports which showed miRNA expression in kidney biopsy from LN patients. The miR-320, miR-134, miR-130b, miR-200 which involve in the apoptotic induction or prolong cell proliferation and epithelial-mesenchymal transformation (EMT) inhibition were consistently up-regulated as found in biopsy. However, several miRNAs which reported in the kidney biopsy did not find any elevation in this model. This might be due to a mixture of cells in the kidney biopsy. Additionally, the miRNA which expressed in this model are mostly represented a prompt response of HMCs to antibodies, while miRNA in kidney biopsy might be a result from chronic inflammation and infiltrated lymphocytes.

In the following, the potential miRNAs were selected for further validation regarding to the inclusion criteria such as an amount of each miRNA in the library, fold change and its previous known functions which associated with kidney inflammation and cell proliferation or apoptosis. These are including miR-181a, miR-127, miR-411, miR-125b and miR-10a (data were summarized in table 9). Although the miR-146a were relatively low expressed and did not change after anti-dsDNA IgG antibodies stimulation, we picked miR-146a for validation according to previous reports in the LN kidney biopsy which found miR-146a upregulation in LN kidney especially in glomerular part (88).

From validation result, experiment showed that miR-146a and miR-411 were unexpectedly down-regulated in both IgG and anti-dsDNA IgG antibodies stimulation. This was different from sequencing results which found up-regulation of miR-411 and no-change in miR-146a expression. The discrepancies between validation results and screening results might be because of the technique sensitivity and specificity. However, the validation technique is more reliable procedure to detect miRNA expression. While miR-10a were down-regulated only in anti-dsDNA IgG antibodies stimulation similarly to sequencing results, other miRNAs were shown no alteration (figure 13A). Hence, this suggested that the down-regulation of miR-10a in HMCs were specifically responded to anti-dsDNA IgG antibodies whereas the down-regulation of miR-146a and miR-411 were reacted to non-specific antibodies stimulation.

The miR-10a expression were also detected in kidney biopsy from LN patients compared to cadaveric donor kidney nephrectomy. In consistent, the miR-10a expression were significantly down-regulation in kidney biopsy collected from LN patients class IV (severe type of LN with large mesangial cells expansion) (figure 13B). Despite we did not find the down-regulation of miR-10a in kidney biopsy from LN patients class III + V, a few samples showed down-regulated of miR-10a expression. The correlation of miR-10a expression and clinical data were plotted. We found that the miR-10a expression were correlated with urine protein creatinine index (UPCI) in LN patients ($r^2 = 0.5266$, p-value = 0.0115) but it was not correlated with creatinine clearance ($r^2 = 0.0247$, p-value = 0.547) (figure 13B). Regarding to the result, this suggested miR-10a might be associated with LN pathogenesis in term of anti-dsDNA

IgG antibodies induced-inflammation to HMCs. Moreover, the perturbance of miR-10a expression in HMCs might be involved in a protein leakages in LN patients which is an early marker of active LN patients.

Table 6 Top ten microRNA expression in HMC stimulated with anti-dsDNA IgG antibodies and non-specific IgG controls with fold change difference.

miRNA	Ranking No.	IgG (RPM*)	Ranking No.	Anti-dsDNA Ab (RPM*)	Ratio (dsDNA Ab/IgG)
hsa-miR-10b-5p	#1	147909.4151	#4	65422.86937	0.442317139
hsa-miR-22-3p	#2	100507.5979	#1	132886.7562	1.322156325
hsa-miR-100-5p	#3	84597.5886	#2	77032.93499	0.910580742
hsa-miR-21-5p	#4	83722.62559	#3	75054.69997	0.896468541
hsa-miR-10a-5p	#5	76251.63459	#7	38997.60429	0.511433027
hsa-miR-191-5p	#6	38078.98689	#8	39596.09153	1.039840993
hsa-let-7a-5p	#7	37228.5825	#9	37605.53472	1.010125344
hsa-miR-143-3p	#8	23724.82095	#5	40051.41123	1.688164952
hsa-miR-26a-5p	#9	30015.30788	#10	33761.72111	1.124816752
hsa-miR-127-3p	#10	23762.20573	#6	38517.34762	1.62095001

Table 7 List of miRNAs which up-regulated in HMC stimulated with anti-dsDNA IgG antibodies compared to non-specific IgG controls.

Gene	FC
hsa-miR-215-5p	27.27223435
hsa-miR-665	3.444939845
hsa-miR-1260b	3.138414604
hsa-miR-130b-5p	3.064417801
hsa-miR-33b-5p	2.576904033
hsa-miR-92a-2-5p	2.501403055
hsa-miR-212-5p	2.343857619
hsa-miR-194-5p	2.208774886
hsa-miR-320b	2.126469588
hsa-miR-654-5p	2.112805442
hsa-miR-3152-5p	2.066891777
hsa-miR-128-2-5p	2.065792951
hsa-miR-1307-5p	2.044881651
hsa-miR-24-2-5p	1.966259641
hsa-miR-24-3p	1.966259641
hsa-miR-24-1-5p	1.965891746
hsa-miR-431-5p	1.96065317
hsa-miR-27a-5p	1.94468231
hsa-miR-584-5p	1.941964166
hsa-miR-940	1.867604691
hsa-miR-652-5p	1.851391504
hsa-miR-107	1.847019928
hsa-miR-210-5p	1.82666615
hsa-miR-766-5p	1.814666654
hsa-miR-200b-5p	1.803832823
hsa-miR-410-5p	1.788796434
hsa-miR-323a-5p	1.782310582

Gene	FC
hsa-miR-151b	1.772254056
hsa-miR-345-5p	1.751595461
hsa-miR-143-5p	1.720790203
hsa-miR-1322	1.717936022
hsa-miR-134-5p	1.716779769
hsa-miR-33a-5p	1.712942022
hsa-miR-889-5p	1.689349567
hsa-miR-199b-5p	1.688961015
hsa-miR-199a-5p	1.688425961
hsa-miR-181b-5p	1.675043962
hsa-miR-126-5p	1.669171692
hsa-miR-615-5p	1.659657655
hsa-miR-532-5p	1.659652949
hsa-miR-483-5p	1.655773863
hsa-miR-127-5p	1.653583482
hsa-miR-3661	1.644118459
hsa-miR-708-5p	1.635985011
hsa-miR-25-5p	1.621898532
hsa-miR-181a-5p	1.621608753
hsa-miR-589-5p	1.619763267
hsa-miR-1185-5p	1.614880786
hsa-miR-92a-1-5p	1.614278826
hsa-miR-106b-5p	1.613123574
hsa-miR-484	1.609798085
hsa-miR-487b-5p	1.609506498
hsa-miR-411-5p	1.603115545
hsa-miR-27b-5p	1.577707495
hsa-miR-192-5p	1.570935414
hsa-miR-132-5p	1.560567837
hsa-miR-140-5p	1.507966064

Gene	FC
hsa-miR-218-5p	1.503554584
hsa-miR-1303	1.503194019
hsa-miR-487a-5p	1.503194019
hsa-miR-5094	1.503194019

Table 8 List of miRNAs which down-regulated in HMC stimulated with anti-dsDNA IgG antibodies compared to non-specific IgG controls.

Gene	FC
hsa-miR-1254	0.590541
hsa-miR-548au-5p	0.544687
hsa-miR-10a-5p	0.520564
hsa-miR-664a-5p	0.507102
hsa-miR-502-5p	0.484901
hsa-miR-497-5p	0.457494
hsa-miR-10b-5p	0.450269
hsa-miR-5690	0.409962
hsa-miR-362-5p	0.397396
hsa-miR-145-5p	0.33849
hsa-miR-190a-5p	0.273308
hsa-miR-19b-1-5p	0.26473
hsa-miR-19b-2-5p	0.226492
hsa-miR-7974	0.200967

Table 9 List of microRNAs for validation from miRNA expression profiles with their known functions.

miRNA	*FC*	*Known Function*	*References*
miR-181a	1.62	- Up-regulated in serum from SLE patients	(89)
		- Up-regulated in human hepatocyte cell line in response to TGF-beta inducing epithelial-mesenchymal transition (EMT)	(90)
miR-127	1.62	- Up-regulated in purified splenocytes from MRL/lpr, B6-lpr and NZB/W F_1 lupus nephritis mice	(91)
miR-146a	1.26	- Down-regulated in THP-1 cells and WBC from SLE patients as a result of IFN type I stimulation	(92)
		- Up-regulated in kidney biopsy from lupus nephritis patients especially in the glomerular part	(88)
		- Down-regulated in serum from SLE patients but up-regulated in urine from SLE patients	(75)
miR-411	1.55	- Up-regulated in lung cancer cells promoting cell proliferation by target FOXO genes	(93)
		- Up-regulated in hepatocellular carcinoma enhanced cell proliferation by target ITCG genes	(94)
miR-125b	0.09	- Down-regulated in T-lymphocytes from Lupus nephritis patients and involved in IFN-signaling pathways by regulating STAT3 and ETS1	(78)
miR-10a/b	0.51	- Down-regulated in kidney biopsy from ischemic-reperfusion and streptozotocin (STZ)-induced renal injury mouse model	(95)
		- Up-regulated in CD19+ cells from asymptomatic SLE patients compared to healthy controls	(96)

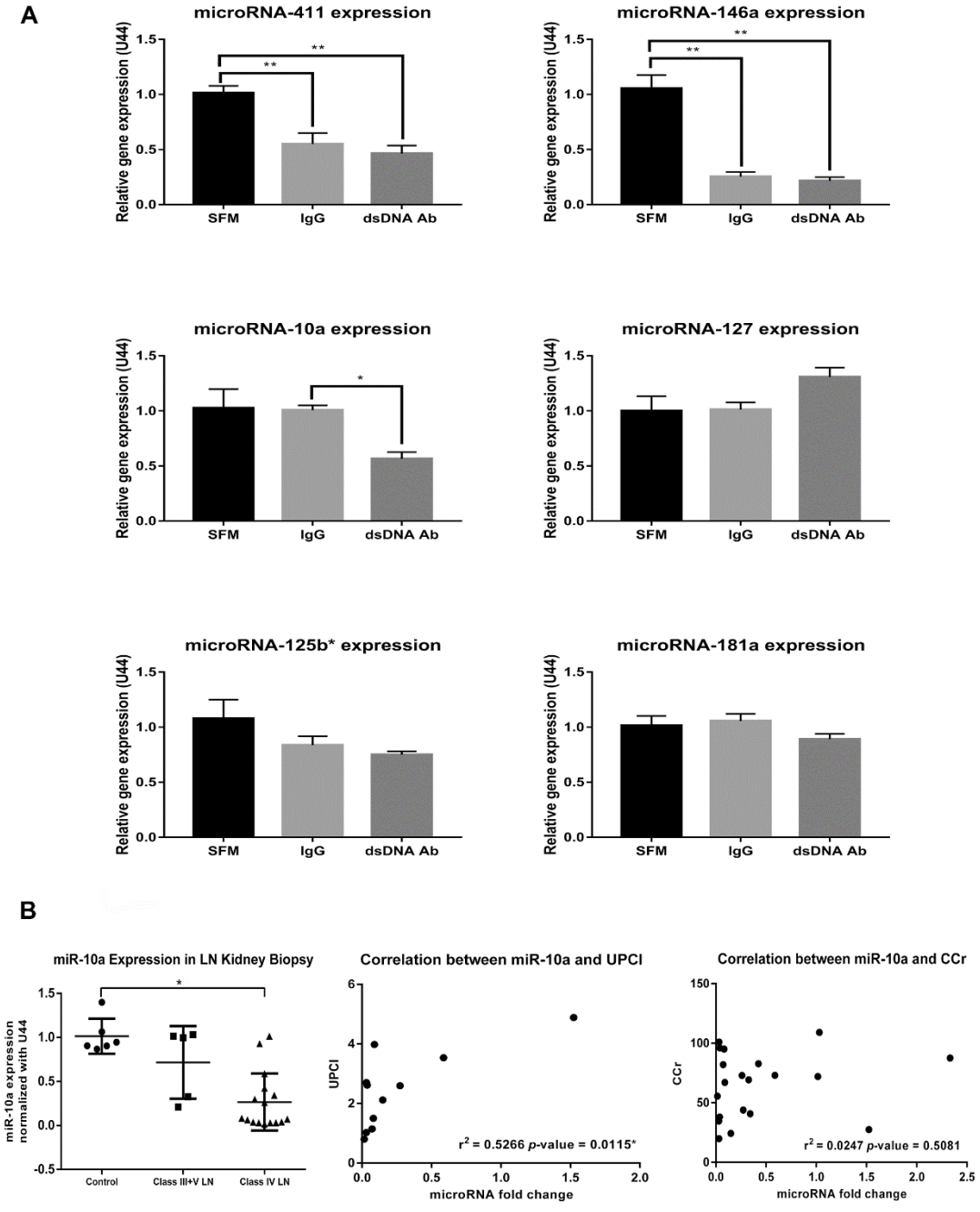

Figure 13 The qPCR validation of candidate miRNA from sequencing result, miR-10a expression in kidney biopsy from LN patients and correlation test between miR-10a expression and clinical data

A. Graphs show miRNA expression in HMC-treated with anti-dsDNA IgG antibodies (10 μg/mL) for 3 hours using stem-loop RT-PCR and qPCR. Data shown were normalized with U44 expression and compared to untreated condition (SFM). **B.** (Upper) Graphs represent miR-10a expression in kidney biopsy from LN patients grouping by histology class including III+V (n=6) and class VI (n=23) compared to cadaveric donor kidney biopsy (n=6). The expressions were normalized with U44 expression. Data were expressed as mean ± SEM. (*) or (**) indicate significantly different from normal healthy IgG controls or cadaveric donor kidney (*p*-value < 0.05) or ($p < 0.001$). (Lower) Graphs show the correlation between miR-10a expression and disease severity which composed of creatinine clearance (CCr) or urine protein creatinine index (UPCI). Pearson's correlation was applied to obtain r-square and *p*-value.

The miRNA and its target genes with their regulatory network

To identify the role of microRNA in HMCs responded to antibodies, mRNA profiling was carried out. Total RNA from previous experiments were used as starting material for cDNA microarray study. Differential gene expression (DEG) were processed and analysed using Lumi R Bioconductor statistic packages. The results showed that 342 genes were up-regulate whereas 496 genes were down-regulated (figure 14A) (Genes were listed in Table 10). The gene ontology study revealed cellular functions of these particular genes which are mostly about cell cycle regulation, macro-molecules catabolic processing and transcription or apoptosis (figure 14A). This defined that early respond to anti-dsDNA IgG antibodies could be linked to HMC proliferation or intracellular signalling as a major phenotype. To be more concise, the functional gene annotation using KEGG pathway analysis pointed that anti-dsDNA IgG antibodies stimulation induced the upregulation of gene in cancer pathways, WNT-signalling, JAK-STAT signalling, mTOR signalling, p53 signalling and SLE-signalling pathway (FC > 1.2, FDR adj. p-value < 0.05). Among this, we observed several genes involved in cellular recruitment were upregulated such as IL-6, IL-1, IL-8 etc. In concurrent, the anti-dsDNA IgG antibodies decreased gene expression in the apoptosis pathway, NOD-like receptor signalling and cytokine-cytokine receptor interaction

pathways (FC < -1.2, FDR adj. p-value < 0.05) (figure 14B). In order to validate microarray results, we selected various transcripts for quantitative Real-time PCR. The results were found that anti-dsDNA IgG antibody were enhanced several cytokines and cell proliferation molecules (figure 14C)

To characterize miRNAs which are responsible to control genes in the above pathways, the miRNA expression data were integrated and analysed with its mRNA expression. The mRNAs were predictively bind to certain microRNAs *in silico* using TargetScan. High prediction scores and experimental approve mRNA targets were selected for further analysis. The miRNA target prediction tools use information about number of binding site in 3'UTR, pattern of binding to seed region, and conserved microRNA among species. Inverse correlation between miRNAs were sorted. The validated miRNA which is not significantly different from previous experiments were excluded. Interestingly, the high abundance and upregulated miRNA after anti-dsDNA IgG antibodies stimulation (miR-1260b, miR-130a, miR-151b, miR-199b, miR-411 and miR-654) have common predicted target genes. They predicted to regulate genes which function as enhancer of enzymes binding, phosphotransferase activity, protein kinase activity, protein serine/threonine kinase activity and kinase activity (figure 14D). Pathway analysis showed that the early responses of HMCs to anti-dsDNA IgG antibodies markedly alter signalling proteins especially in the PI3K/AKT pathways. Gene ontology (GO) using biological processes classification were categorized genes in several groups including cell differentiation, regulation of transcription or cellular component biosynthesis (table 11). On the other hand, the miR-145 which down-regulated after anti-dsDNA IgG antibodies stimulation were predicted to control gene with another function such as cytoskeleton protein binding, enzyme binding, transcriptional activator activity and transcription factor activity. The GO term analysis by biological processes were characterized genes in a regulation of transcription from RNA polymerase II promoter and regulation of gene expression (table 12). From network analysis result, it is clearly showed that miRNA play an important role in gene expression in HMCs during anti-dsDNA IgG antibodies stimulation. However, it should be reminded that those target genes were using bioinformatics tools to generate. Further experiment to identify miRNA target genes is necessary to discover miRNA functional role in HMCs.

Table 10 The list of upregulated transcripts after anti-dsDNA IgG antibodies stimulation

GeneSymbol	Accession No.	GeneName	logFC	adj.P.Val
PPA2	NM_176866.2	pyrophosphatase (inorganic) 2	1.20	0.03
RDH10	NM_172037.2	retinol dehydrogenase 10 (all-trans)	1.20	0.02
STK4	NM_006282.2	serine/threonine kinase 4	1.20	0.02
COL8A1	NM_020351.2	collagen, type VIII, alpha 1	1.21	0.00
COL8A1	NM_020351.2	collagen, type VIII, alpha 1	1.21	0.00
SPTLC1	NM_178324.1	serine palmitoyltransferase, long chain base subunit 1	1.21	0.02
ATXN2	NM_002973.2	ataxin 2	1.21	0.00
TOR3A	NM_022371.3	torsin family 3, member A	1.22	0.00
ZNF674	NM_001039891.1	zinc finger protein 674	1.22	0.00
MBNL1	NM_207293.1	muscleblind-like splicing regulator 1	1.22	0.00
PTBP3	#N/A	polypyrimidine tract binding protein 3	1.22	0.01
TP53INP2	NM_021202.1	tumor protein p53 inducible nuclear protein 2	1.22	0.00
EPAS1	NM_001430.3	endothelial PAS domain protein 1	1.22	0.00
LILRB1	NM_006669.2	leukocyte immunoglobulin-like receptor, subfamily B (with TM and ITIM domains), member 1	1.22	0.01
NLRP8	NM_176811.2	NLR family, pyrin domain containing 8	1.22	0.04
GGA1	NM_013365.3	golgi-associated, gamma adaptin ear containing, ARF binding protein 1	1.22	0.02
COL15A1	NM_001855.3	collagen, type XV, alpha 1	1.22	0.00
RAP1GAP	NM_002885.1	RAP1 GTPase activating protein	1.22	0.01
KIAA0101	NM_001029989.1	KIAA0101	1.23	0.01
IL6	NM_000600.1	interleukin 6	1.23	0.00
LAMA1	XM_001130075.1	laminin, alpha 1	1.23	0.00
C1QBP	NM_001212.3	complement component 1, q subcomponent binding protein	1.23	0.00
AFF4	NM_014423.3	AF4/FMR2 family, member 4	1.23	0.00
ATP1B1	NM_001677.3	ATPase, Na+/K+ transporting, beta 1 polypeptide	1.23	0.01
CRCP	NM_014478.4	CGRP receptor component	1.23	0.03
ROR2	NM_004560.2	receptor tyrosine kinase-like orphan receptor 2	1.23	0.00
LOC100128288	NR_024447.1	uncharacterized LOC100128288	1.23	0.04
TTC3	NM_003316.3	tetratricopeptide repeat domain 3	1.24	0.00

COL11A1	NM_001854.2	collagen, type XI, alpha 1	1.24	0.00
EPDR1	NM_017549.3	ependymin related 1	1.24	0.00
MX1	NM_002462.2	MX dynamin-like GTPase 1	1.24	0.03
KCNJ16	NM_170742.1	potassium channel, inwardly rectifying subfamily J, member 16	1.24	0.00
XPNPEP3	NM_022098.2	X-prolyl aminopeptidase 3, mitochondrial	1.24	0.04
SNORA25	NR_003028.1	small nucleolar RNA, H/ACA box 25	1.25	0.01
DVL3	NM_004423.3	dishevelled segment polarity protein 3	1.25	0.01
FLNC	NM_001458.3	filamin C, gamma	1.25	0.02
MTSS1	NM_014751.4	metastasis suppressor 1	1.25	0.00
PLXDC2	NM_032812.7	plexin domain containing 2	1.25	0.00
LINC00114	#N/A	long intergenic non-protein coding RNA 114	1.25	0.03
LITAF	NM_004862.2	lipopolysaccharide-induced TNF factor	1.25	0.01
TPP1	NM_000391.3	tripeptidyl peptidase I	1.25	0.00
METTL21A	#N/A	methyltransferase like 21A	1.26	0.04
SORT1	NM_002959.4	sortilin 1	1.26	0.00
TULP4	NM_001007466.1	tubby like protein 4	1.26	0.00
PDGFRA	NM_006206.3	platelet-derived growth factor receptor, alpha polypeptide	1.26	0.00
FBN1	NM_000138.3	fibrillin 1	1.27	0.00
EPHA2	NM_004431.2	EPH receptor A2	1.27	0.00
SEC16A	NM_014866.1	SEC16 homolog A, endoplasmic reticulum export factor	1.27	0.00
SCARB2	NM_005506.2	scavenger receptor class B, member 2	1.27	0.01
GPC6	NM_005708.2	glypican 6	1.27	0.02
PTPRD	NM_130393.2	protein tyrosine phosphatase, receptor type, D	1.27	0.01
ZNF106	#N/A	zinc finger protein 106	1.27	0.00
FOXO1	NM_002015.3	forkhead box O1	1.27	0.00
TRRAP	NM_003496.1	transformation/transcription domain-associated protein	1.27	0.00
PLTP	NM_006227.2	phospholipid transfer protein	1.28	0.00
CAMK2D	NM_001221.2	calcium/calmodulin-dependent protein kinase II delta	1.28	0.00
ZFC3H1	NM_144982.4	zinc finger, C3H1-type containing	1.28	0.00
ITGA11	NM_001004439.1	integrin, alpha 11	1.28	0.00
NBPF10	XM_930715.1	neuroblastoma breakpoint family, member 10	1.28	0.02
SON	NM_032195.1	SON DNA binding protein	1.28	0.00
NCOA3	NM_181659.1	nuclear receptor coactivator 3	1.28	0.00
TNS1	NM_022648.3	tensin 1	1.28	0.00
SLC4A7	NM_003615.3	solute carrier family 4, sodium bicarbonate cotransporter, member 7	1.28	0.01
PODXL	NM_001018111.2	podocalyxin-like	1.28	0.00

ORC6	#N/A	origin recognition complex, subunit 6	1.28	0.01
INO80D	NM_017759.4	INO80 complex subunit D	1.29	0.00
ZNF69	NM_021915.1	zinc finger protein 69	1.29	0.03
NONO	NM_007363.3	non-POU domain containing, octamer-binding	1.29	0.00
SEL1L3	NM_015187.3	sel-1 suppressor of lin-12-like 3 (C. elegans)	1.29	0.03
TNFSF14	NM_003807.2	tumor necrosis factor (ligand) superfamily, member 14	1.29	0.00
NBPF9	XM_933971.1	neuroblastoma breakpoint family, member 9	1.29	0.02
LINC00957	#N/A	long intergenic non-protein coding RNA 957	1.30	0.03
STAT2	NM_005419.2	signal transducer and activator of transcription 2, 113kDa	1.30	0.00
KRT18P55	#N/A	keratin 18 pseudogene 55	1.30	0.01
MACF1	NM_033044.2	microtubule-actin crosslinking factor 1	1.30	0.04
IRF7	NM_004031.2	interferon regulatory factor 7	1.30	0.00
LOC727808	XR_041978.1	uncharacterized LOC727808	1.31	0.00
CMIP	NM_030629.1	c-Maf inducing protein	1.31	0.00
LOC100190986	NR_024456.1	uncharacterized LOC100190986	1.32	0.00
POFUT1	NM_015352.1	protein O-fucosyltransferase 1	1.32	0.02
BCL6	NM_001706.2	B-cell CLL/lymphoma 6	1.32	0.00
RN7SL1	NR_002715.1	RNA, 7SL, cytoplasmic 1	1.32	0.01
IGF2R	NM_000876.2	insulin-like growth factor 2 receptor	1.32	0.00
COL3A1	NM_000090.3	collagen, type III, alpha 1	1.32	0.00
CCND2	NM_001759.2	cyclin D2	1.32	0.05
DTWD2	NM_173666.1	DTW domain containing 2	1.32	0.01
DAPP1	NM_014395.1	dual adaptor of phosphotyrosine and 3-phosphoinositides	1.33	0.03
CLIP3	NM_015526.1	CAP-GLY domain containing linker protein 3	1.33	0.00
BTAF1	NM_003972.2	BTAF1 RNA polymerase II, B-TFIID transcription factor-associated, 170kDa	1.33	0.00
MYADM	NM_001020821.1	myeloid-associated differentiation marker	1.33	0.01
ROCK2	NM_004850.3	Rho-associated, coiled-coil containing protein kinase 2	1.33	0.01
APOPT1	#N/A	apoptogenic 1, mitochondrial	1.34	0.04
AHR	NM_001621.2	aryl hydrocarbon receptor	1.34	0.01
SERPINE1	NM_000602.1	serpin peptidase inhibitor, clade E (nexin, plasminogen activator inhibitor type 1), member 1	1.34	0.00
ADM2	NM_024866.4	adrenomedullin 2	1.34	0.00
MSH3	NM_002439.2	mutS homolog 3	1.34	0.01
NPC1	NM_000271.3	Niemann-Pick disease, type C1	1.34	0.00
CEP19	#N/A	centrosomal protein 19kDa	1.34	0.04
FBLN5	NM_006329.2	fibulin 5	1.35	0.02
EFHC1	NM_018100.2	EF-hand domain (C-terminal) containing 1	1.35	0.00

SULT1A1	NM_177536.1	sulfotransferase family, cytosolic, 1A, phenol-preferring, member 1	1.36	0.02
DDX51	NM_175066.3	DEAD (Asp-Glu-Ala-Asp) box polypeptide 51	1.36	0.04
PTBP3	#N/A	polypyrimidine tract binding protein 3	1.36	0.00
MMP23B	NM_006983.1	matrix metallopeptidase 23B	1.36	0.02
AEBP1	NM_001129.3	AE binding protein 1	1.36	0.00
CDK6	NM_001259.5	cyclin-dependent kinase 6	1.36	0.01
MMP7	NM_002423.3	matrix metallopeptidase 7	1.37	0.00
PDLIM5	NM_006457.2	PDZ and LIM domain 5	1.37	0.01
SECISBP2L	NM_014701.2	SECIS binding protein 2-like	1.37	0.00
CXCL8	#N/A	chemokine (C-X-C motif) ligand 8	1.38	0.01
ZMAT3	NM_152240.1	zinc finger, matrin-type 3	1.38	0.04
RERE	NM_001042682.1	arginine-glutamic acid dipeptide (RE) repeats	1.38	0.00
SPEN	NM_015001.2	spen family transcriptional repressor	1.38	0.00
MYADM	NM_001020821.1	myeloid-associated differentiation marker	1.38	0.01
TCAF1	#N/A	TRPM8 channel-associated factor 1	1.38	0.01
WSB1	NM_134265.2	WD repeat and SOCS box containing 1	1.39	0.01
PNPT1	NM_033109.2	polyribonucleotide nucleotidyltransferase 1	1.39	0.03
COL16A1	NM_001856.3	collagen, type XVI, alpha 1	1.40	0.01
POLR2A	NM_000937.2	polymerase (RNA) II (DNA directed) polypeptide A, 220kDa	1.40	0.00
ZNF394	NM_032164.2	zinc finger protein 394	1.40	0.04
ZNF652	NM_014897.1	zinc finger protein 652	1.40	0.02
ATP9A	NM_006045.1	ATPase, class II, type 9A	1.41	0.00
OCIAD1	NM_017830.1	OCIA domain containing 1	1.41	0.05
NFIB	NM_005596.2	nuclear factor I/B	1.41	0.00
PDCD7	NM_005707.1	programmed cell death 7	1.41	0.00
LILRB3	NM_006864.2	leukocyte immunoglobulin-like receptor, subfamily B (with TM and ITIM domains), member 3	1.41	0.02
SLC7A2	NM_003046.4	solute carrier family 7 (cationic amino acid transporter, y+ system), member 2	1.41	0.01
COL4A2	NM_001846.2	collagen, type IV, alpha 2	1.41	0.00
LOC441087	NM_001013716.1	uncharacterized LOC441087	1.41	0.00
C21orf58	NM_058180.3	chromosome 21 open reading frame 58	1.41	0.02
SIX4	NM_017420.3	SIX homeobox 4	1.41	0.00
SLC25A51	#N/A	solute carrier family 25, member 51	1.42	0.04
TNC	NM_002160.2	tenascin C	1.42	0.02
C2orf69	NM_153689.5	chromosome 2 open reading frame 69	1.42	0.02
IRF1	NM_002198.1	interferon regulatory factor 1	1.42	0.00
PIK3CA	NM_006218.2	phosphatidylinositol-4,5-bisphosphate 3-kinase, catalytic subunit alpha	1.43	0.00

DUSP19	NM_080876.2	dual specificity phosphatase 19	1.43	0.05
POSTN	NM_006475.1	periostin, osteoblast specific factor	1.43	0.01
CBLB	NM_170662.3	Cbl proto-oncogene B, E3 ubiquitin protein ligase	1.43	0.03
HIATL2	NR_002894.1	hippocampus abundant transcript-like 2	1.44	0.03
MIR221	NR_029635.1	microRNA 221	1.44	0.00
LAMA2	NM_001079823.1	laminin, alpha 2	1.44	0.00
ZMAT3	NM_152240.1	zinc finger, matrin-type 3	1.44	0.02
SPP1	NM_000582.2	secreted phosphoprotein 1	1.44	0.00
DSP	NM_001008844.1	Desmoplakin	1.44	0.01
CCL2	NM_002982.3	chemokine (C-C motif) ligand 2	1.45	0.00
MAPK7	NM_139032.1	mitogen-activated protein kinase 7	1.45	0.00
DYNC1H1	NM_001376.2	dynein, cytoplasmic 1, heavy chain 1	1.46	0.00
EID2B	NM_152361.1	EP300 interacting inhibitor of differentiation 2B	1.46	0.04
IRF3	NM_001571.2	interferon regulatory factor 3	1.46	0.00
SNX4	NM_003794.2	sorting nexin 4	1.46	0.00
HIPK2	NM_022740.2	homeodomain interacting protein kinase 2	1.46	0.00
ANXA7	NM_004034.1	annexin A7	1.46	0.00
CUX1	NM_181552.2	cut-like homeobox 1	1.46	0.00
FNDC3B	NM_001135095.1	fibronectin type III domain containing 3B	1.47	0.00
L3MBTL3	NM_032438.1	l(3)mbt-like 3 (Drosophila)	1.47	0.00
TNFSF10	NM_003810.2	tumor necrosis factor (ligand) superfamily, member 10	1.48	0.00
TROVE2	NM_004600.4	TROVE domain family, member 2	1.48	0.00
ITGA11	NM_001004439.1	integrin, alpha 11	1.48	0.00
NEK6	NM_014397.3	NIMA-related kinase 6	1.48	0.00
MGP	NM_000900.2	matrix Gla protein	1.49	0.02
FBXO22	NM_147188.1	F-box protein 22	1.49	0.00
FBLN5	NM_006329.2	fibulin 5	1.49	0.02
RGS2	NM_002923.1	regulator of G-protein signaling 2	1.50	0.04
SOCS4	NM_199421.1	suppressor of cytokine signaling 4	1.50	0.00
P3H2	#N/A	prolyl 3-hydroxylase 2	1.50	0.00
MAP4K4	NM_145686.2	mitogen-activated protein kinase kinase kinase kinase 4	1.50	0.00
IFNAR1	NM_000629.2	interferon (alpha, beta and omega) receptor 1	1.50	0.00
ZNF430	NM_025189.2	zinc finger protein 430	1.50	0.02
THBS2	NM_003247.2	thrombospondin 2	1.51	0.04
SPTAN1	NM_003127.1	spectrin, alpha, non-erythrocytic 1	1.51	0.00
BMPR2	NM_001204.5	bone morphogenetic protein receptor, type II (serine/threonine kinase)	1.51	0.00

SERTAD2	NM_014755.1	SERTA domain containing 2	1.62	0.00
INIP	#N/A	INTS3 and NABP interacting protein	1.62	0.03
MTMR3	NM_021090.3	myotubularin related protein 3	1.62	0.00
CASK	NM_003688.1	calcium/calmodulin-dependent serine protein kinase (MAGUK family)	1.64	0.00
POSTN	NM_006475.1	periostin, osteoblast specific factor	1.64	0.02
SHISA2	NM_001007538.1	shisa family member 2	1.65	0.00
MAP4K4	NM_145686.2	mitogen-activated protein kinase kinase kinase kinase 4	1.65	0.00
SDC1	NM_002997.4	syndecan 1	1.65	0.00
ZNF608	NM_020747.2	zinc finger protein 608	1.65	0.00
DOCK10	NM_014689.2	dedicator of cytokinesis 10	1.66	0.00
BLZF1	NM_003666.2	basic leucine zipper nuclear factor 1	1.66	0.01
LOC728903	XM_001128866.2	uncharacterized LOC728903	1.66	0.00
RERG	NM_032918.1	RAS-like, estrogen-regulated, growth inhibitor	1.66	0.00
FLNB	NM_001457.1	filamin B, beta	1.67	0.00
SLC7A1	NM_003045.3	solute carrier family 7 (cationic amino acid transporter, y+ system), member 1	1.67	0.01
KCNH6	NM_173092.1	potassium channel, voltage gated eag related subfamily H, member 6	1.67	0.03
MED1	NM_004774.3	mediator complex subunit 1	1.68	0.00
VGLL3	NM_016206.2	vestigial-like family member 3	1.68	0.01
DUXAP3	NR_002220.1	double homeobox A pseudogene 3	1.68	0.02
FAT1	NM_005245.3	FAT atypical cadherin 1	1.68	0.00
RAPH1	NM_203365.2	Ras association (RalGDS/AF-6) and pleckstrin homology domains 1	1.69	0.01
DMC1	NM_007068.2	DNA meiotic recombinase 1	1.69	0.02
COL4A1	NM_001845.4	collagen, type IV, alpha 1	1.69	0.00
BDNF	NM_170734.2	brain-derived neurotrophic factor	1.69	0.01
PTGDS	NM_000954.5	prostaglandin D2 synthase 21kDa (brain)	1.69	0.00
MIR100HG	#N/A	mir-100-let-7a-2 cluster host gene	1.69	0.00
LOC642947	NM_001039895.2	uncharacterized LOC642947	1.70	0.00
PTPRE	NM_130435.2	protein tyrosine phosphatase, receptor type, E	1.71	0.00
IGFBP5	NM_000599.2	insulin-like growth factor binding protein 5	1.71	0.00
COBLL1	NM_014900.3	cordon-bleu WH2 repeat protein-like 1	1.72	0.00
NACC1	NM_052876.2	nucleus accumbens associated 1, BEN and BTB (POZ) domain containing	1.73	0.00
MTMR3	NM_021090.3	myotubularin related protein 3	1.73	0.00
SPINT2	NM_021102.2	serine peptidase inhibitor, Kunitz type, 2	1.74	0.00
ERRFI1	NM_018948.2	ERBB receptor feedback inhibitor 1	1.74	0.01
PRRC2C	#N/A	proline-rich coiled-coil 2C	1.74	0.00
MMP7	NM_002423.3	matrix metallopeptidase 7	1.75	0.00

SPAG9	NM_003971.3	sperm associated antigen 9	1.52	0.00
SLC16A12	NM_213606.1	solute carrier family 16, member 12	1.52	0.02
DOCK11	NM_144658.3	dedicator of cytokinesis 11	1.52	0.00
MAPK11	NM_002751.5	mitogen-activated protein kinase 11	1.52	0.00
RB1CC1	NM_001083617.1	RB1-inducible coiled-coil 1	1.52	0.00
MCM8	NM_182802.1	minichromosome maintenance 8 homologous recombination repair factor	1.52	0.02
KLF4	NM_004235.3	Kruppel-like factor 4 (gut)	1.52	0.00
FNDC3B	NM_001135095.1	fibronectin type III domain containing 3B	1.52	0.00
ITPK1-AS1	#N/A	ITPK1 antisense RNA 1	1.52	0.03
CAMK2D	NM_001221.2	calcium/calmodulin-dependent protein kinase II delta	1.53	0.00
FAM46A	NM_017633.2	family with sequence similarity 46, member A	1.53	0.00
WISP1	NM_003882.2	WNT1 inducible signaling pathway protein 1	1.54	0.04
GJC1	NM_001080383.1	gap junction protein, gamma 1, 45kDa	1.54	0.01
RAB22A	NM_020673.2	RAB22A, member RAS oncogene family	1.54	0.01
LRRC37BP1	#N/A	leucine rich repeat containing 37B pseudogene 1	1.54	0.00
SLC30A7	NM_133496.3	solute carrier family 30 (zinc transporter), member 7	1.55	0.00
DNAJC28	NM_017833.3	DnaJ (Hsp40) homolog, subfamily C, member 28	1.55	0.01
ZMIZ1	NM_020338.2	zinc finger, MIZ-type containing 1	1.56	0.00
BMS1P5	NR_003611.2	BMS1 ribosome biogenesis factor pseudogene 5	1.56	0.03
PTGS2	NM_000963.1	prostaglandin-endoperoxide synthase 2 (prostaglandin G/H synthase and cyclooxygenase)	1.57	0.00
GREM1	NM_013372.5	gremlin 1, DAN family BMP antagonist	1.57	0.02
SLC38A1	NM_030674.3	solute carrier family 38, member 1	1.57	0.00
MCMDC2	#N/A	minichromosome maintenance domain containing 2	1.58	0.04
TMEM183A	NM_138391.4	transmembrane protein 183A	1.59	0.00
IGFBP5	NM_000599.2	insulin-like growth factor binding protein 5	1.59	0.00
DPF2	NM_006268.3	D4, zinc and double PHD fingers family 2	1.59	0.00
TNC	NM_002160.2	tenascin C	1.59	0.02
LOC641737	#N/A	uncharacterized LOC641737	1.60	0.02
LOC729324	XR_041500.1	hCG1986447	1.60	0.00
IRF2	NM_002199.3	interferon regulatory factor 2	1.60	0.00
CDH2	NM_001792.2	cadherin 2, type 1, N-cadherin (neuronal)	1.60	0.03
TRIL	NM_014817.3	TLR4 interactor with leucine-rich repeats	1.60	0.00
GABPB2	NM_144618.1	GA binding protein transcription factor, beta subunit 2	1.61	0.01
MAPK7	NM_139032.1	mitogen-activated protein kinase 7	1.61	0.00
PTEN	NM_000314.4	phosphatase and tensin homolog	1.61	0.00
PTGIS	NM_000961.3	prostaglandin I2 (prostacyclin) synthase	1.61	0.00

RTMR	NM_029004.5	reticulon 4 receptor	1.94	0.00	0.00
PCDB2	NM_033151.3	plexin-A4-like dehydratase/dimerization cofactor of hepatocyte nuclear factor 1 alpha (TCF1) 2	1.94	0.00	0.00
HCHE	NM_052932.2	EF-hand domain family, member D1	1.94	0.01	0.00
LOC389000	NM_001013667.1	uncharacterized LOC389000	1.93	0.00	0.00
EZE	EZE transcription factor 3		1.93	0.00	0.00
PDGFRB	NM_002609.3	platelet-derived growth factor receptor, beta polypeptide	1.93	0.00	0.00
SLC4A2	NM_033148.2	solute carrier family 4 (misgenesium transporter), member 2	1.93	0.00	0.00
GREM1	NM_013372.5	gremlin 1, DAN family BMP antagonist	2.00	0.02	0.00
NCOR2	NM_001012761.1	nuclear receptor corepressor 2	2.01	0.00	0.00
SMAD2	NM_001003652.2	SMAD family member 2	2.02	0.00	0.00
PSD	NM_014338.3	pleckstrin and Sec7 domain containing 4 pseudogene	2.02	0.00	0.00
AOC4P	#N/A	amine oxidase, copper containing 4 pseudogene	2.02	0.00	0.00
ZFP36	NM_003407.2	zinc finger protein 36, C3H type homolog (mouse)	2.02	0.00	0.00
LINC01018	#N/A	long intergenic non-protein coding RNA 1018	2.03	0.03	0.00
DLC1	NM_024767.2	DLC1 Rho GTPase activating protein	2.03	0.03	0.00
TACSTD2	NM_002353.1	tumor-associated calcium signal transducer 2	2.04	0.00	0.00
CREB1	NM_004379.2	cAMP responsive element binding protein 1	2.05	0.00	0.00
PURB	NM_033224.3	purine-rich element binding protein B	2.06	0.00	0.00
HOXA10	NM_018951.3	homeobox A10	2.06	0.00	0.00
NUP50	NM_007172.2	nucleoporin 50kDa	2.06	0.00	0.00
RAMP2-AS1	#N/A	RAMP2 antisense RNA 1	2.07	0.00	0.00
BAZ2B	NM_013450.2	bromodomain adjacent to zinc finger domain, 2B	2.10	0.00	0.00
CDKN2AIPNL	NM_080659.1	CDKN2A interacting protein N-terminal like	2.12	0.00	0.00
COL12A1	NM_080645.2	collagen, type XII, alpha 1	2.12	0.00	0.00
ADGRL1	#N/A	adhesion G protein-coupled receptor L1	2.14	0.00	0.00
LOC728888	NR_002288.1	calcineurin-like EF-hand protein 1 pseudogene	2.15	0.00	0.00
EPAP2	NM_022352.2	endoplasmic reticulum aminopeptidase 2	2.16	0.00	0.00
H19	NR_002196.1	H19, imprinted maternally expressed transcript (non-protein coding)	2.19	0.01	0.00
FBN2	NM_001999.3	fibrillin 2	2.19	0.02	0.00
VCAM1	NM_001078.2	vascular cell adhesion molecule 1	2.20	0.02	0.00
MYH10	NM_005964.1	myosin, heavy chain 10, non-muscle	2.21	0.02	0.00
CEP350	NM_014810.3	centrosomal protein 350kDa	2.22	0.02	0.00
ACTC1	NM_005159.4	actin, alpha, cardiac muscle 1	2.25	0.02	0.00
IL8	NM_000584.2	interleukin 8	2.26	0.02	0.00
TOR1A	NM_000113.2	torsin family 1, member A (torsin A)	2.27	0.02	0.00
ARHGC3	NM_020801.1	arrestin domain containing 3	2.33	0.00	0.00

SLITRK4	NM_173078.2	SLIT and NTRK-like family, member 4	1.76	0.00
IL10	NM_000572.2	interleukin 10	1.77	0.00
CXCL8	#N/A	chemokine (C-X-C motif) ligand 8	1.77	0.02
LCOR	NM_032440.2	ligand dependent nuclear receptor corepressor	1.78	0.00
AAK1	NM_014911.3	AP2 associated kinase 1	1.78	0.00
STRN	NM_003162.2	striatin, calmodulin binding protein	1.79	0.00
LCOR	NM_032440.2	ligand dependent nuclear receptor corepressor	1.79	0.00
LAMA2	NM_001079823.1	laminin, alpha 2	1.80	0.00
AIRE	NM_000658.1	autoimmune regulator	1.80	0.00
PTPRE	NM_130435.2	protein tyrosine phosphatase, receptor type, E	1.80	0.00
LOC613037	NR_002555.2	nuclear pore complex interacting protein pseudogene	1.81	0.00
TIAM1	NM_003253.2	T-cell lymphoma invasion and metastasis 1	1.82	0.00
SH3PXD2A	NM_014631.2	SH3 and PX domains 2A	1.82	0.00
RPRD1A	NM_018170.3	regulation of nuclear pre-mRNA domain containing 1A	1.82	0.00
FAT1	NM_005245.3	FAT atypical cadherin 1	1.82	0.00
ZNF549	NM_153263.1	zinc finger protein 549	1.83	0.03
RHOBTB3	NM_014899.3	Rho-related BTB domain containing 3	1.84	0.01
WAPL	#N/A	WAPL cohesin release factor	1.84	0.00
IPO8	NM_006390.2	importin 8	1.84	0.00
BMPR2	NM_001204.5	bone morphogenetic protein receptor, type II (serine/threonine kinase)	1.84	0.00
SPP1	NM_000582.2	secreted phosphoprotein 1	1.85	0.00
STARD13	NM_178008.1	StAR-related lipid transfer (START) domain containing 13	1.86	0.00
LYSMD3	NM_198273.1	LysM, putative peptidoglycan-binding, domain containing 3	1.86	0.00
TIMP3	NM_000362.4	TIMP metallopeptidase inhibitor 3	1.86	0.05
JARID2	NM_004973.2	jumonji, AT rich interactive domain 2	1.86	0.00
SRRM2	NM_016333.2	serine/arginine repetitive matrix 2	1.89	0.00
MFAP4	NM_002404.1	microfibrillar-associated protein 4	1.89	0.00
AFAP1	NM_198595.2	actin filament associated protein 1	1.90	0.00
FXR2	NM_004860.2	fragile X mental retardation, autosomal homolog 2	1.90	0.00
TYK2	NM_003331.3	tyrosine kinase 2	1.90	0.00
MTF2	NM_007358.2	metal response element binding transcription factor 2	1.90	0.00
STARD13	NM_178008.1	StAR-related lipid transfer (START) domain containing 13	1.90	0.00
ABCC3	NM_003786.2	ATP-binding cassette, sub-family C (CFTR/MRP), member 3	1.92	0.00
IL18	NM_001562.2	interleukin 18	1.92	0.00
ABCA1	NM_005502.2	ATP-binding cassette, sub-family A (ABC1), member 1	1.92	0.00
SVEP1	NM_153366.2	sushi, von Willebrand factor type A, EGF and pentraxin domain containing 1	1.93	0.01

STRN	NM_003162.2	striatin, calmodulin binding protein	2.35	0.00
ITPKC	NM_025194.2	inositol-trisphosphate 3-kinase C	2.36	0.00
FLRT2	NM_013231.4	fibronectin leucine rich transmembrane protein 2	2.37	0.00
PTGS2	NM_000963.1	prostaglandin-endoperoxide synthase 2 (prostaglandin G/H synthase and cyclooxygenase)	2.42	0.00
NACC1	NM_052876.2	nucleus accumbens associated 1, BEN and BTB (POZ) domain containing	2.44	0.00
LUM	NM_002345.3	Lumican	2.46	0.00
PDE4A	NM_006202.1	phosphodiesterase 4A, cAMP-specific	2.48	0.00
NR2C2	NM_003298.3	nuclear receptor subfamily 2, group C, member 2	2.50	0.00
SNX29	NM_001080530.2	sorting nexin 29	2.51	0.00
CCL20	NM_004591.1	chemokine (C-C motif) ligand 20	2.51	0.00
LPP	NM_005578.2	LIM domain containing preferred translocation partner in lipoma	2.51	0.00
NR2C2	NM_003298.3	nuclear receptor subfamily 2, group C, member 2	2.52	0.00
CREBL2	NM_001310.2	cAMP responsive element binding protein-like 2	2.53	0.00
TMEM132B	NM_052907.2	transmembrane protein 132B	2.55	0.00
IFFO2	NM_001136265.1	intermediate filament family orphan 2	2.57	0.00
LRRFIP1	NM_004735.2	leucine rich repeat (in FLII) interacting protein 1	2.58	0.00
SMURF1	NM_020429.1	SMAD specific E3 ubiquitin protein ligase 1	2.60	0.00
ACTA2	NM_001613.1	actin, alpha 2, smooth muscle, aorta	2.60	0.00
BCR	NM_004327.3	breakpoint cluster region	2.64	0.00
ANKFY1	NM_016376.3	ankyrin repeat and FYVE domain containing 1	2.67	0.00
WNK3	NM_020922.2	WNK lysine deficient protein kinase 3	2.69	0.00
IGDCC4	NM_020962.1	immunoglobulin superfamily, DCC subclass, member 4	2.70	0.00
MAPKBP1	NM_014994.1	mitogen-activated protein kinase binding protein 1	2.79	0.00
C7	NM_000587.2	complement component 7	2.87	0.01
SULF1	NM_015170.1	sulfatase 1	3.05	0.00
GLS	NM_014905.2	Glutaminase	3.59	0.00
RNU6-1	NR_004394.1	RNA, U6 small nuclear 1	-2.44	0.04
RNU6-15P	#N/A	RNA, U6 small nuclear 15, pseudogene	-2.40	0.03
TNFAIP3	NM_006290.2	tumor necrosis factor, alpha-induced protein 3	-2.09	0.00
PITX1	NM_002653.3	paired-like homeodomain 1	-2.04	0.05
DLGAP5	NM_014750.3	discs, large (Drosophila) homolog-associated protein 5	-1.65	0.00
DLGAP5	NM_014750.3	discs, large (Drosophila) homolog-associated protein 5	-1.65	0.00
PLAU	NM_002658.2	plasminogen activator, urokinase	-1.61	0.01
ADIRF	#N/A	adipogenesis regulatory factor	-1.57	0.00
GINS2	NM_016095.1	GINS complex subunit 2 (Psf2 homolog)	-1.57	0.00
STRA13	NM_144998.2	stimulated by retinoic acid 13	-1.51	0.00

CENPW	#N/A	centromere protein W	-1.50	0.00
POLE2	NM_002692.2	polymerase (DNA directed), epsilon 2, accessory subunit	-1.42	0.00
MT1IP	NR_003669.1	metallothionein 1I, pseudogene	-1.42	0.00
SERPINB7	NM_003784.2	serpin peptidase inhibitor, clade B (ovalbumin), member 7	-1.41	0.00
TRIP13	NM_004237.2	thyroid hormone receptor interactor 13	-1.39	0.00
AURKA	NM_198436.1	aurora kinase A	-1.39	0.00
PTTG1	NM_004219.2	pituitary tumor-transforming 1	-1.39	0.00
AURKA	NM_198436.1	aurora kinase A	-1.38	0.00
BUB1	NM_004336.2	BUB1 mitotic checkpoint serine/threonine kinase	-1.38	0.00
MT1G	NM_005950.1	metallothionein 1G	-1.37	0.00
HMMR	NM_012485.1	hyaluronan-mediated motility receptor (RHAMM)	-1.36	0.00
TACC3	NM_006342.1	transforming, acidic coiled-coil containing protein 3	-1.34	0.00
FAM64A	NM_019013.1	family with sequence similarity 64, member A	-1.33	0.00
BIRC5	NM_001012271.1	baculoviral IAP repeat containing 5	-1.33	0.00
SNRNP25	NM_024571.3	small nuclear ribonucleoprotein 25kDa (U11/U12)	-1.32	0.00
TMEFF2	NM_016192.2	transmembrane protein with EGF-like and two follistatin-like domains 2	-1.32	0.03
HMMR	NM_012485.1	hyaluronan-mediated motility receptor (RHAMM)	-1.31	0.00
ADM	NM_001124.1	Adrenomedullin	-1.30	0.00
RPS24	NM_033022.2	ribosomal protein S24	-1.30	0.00
STMN2	NM_007029.2	stathmin 2	-1.29	0.02
TUBA1A	NM_006009.2	tubulin, alpha 1a	-1.29	0.00
PTTG1	NM_004219.2	pituitary tumor-transforming 1	-1.28	0.00
KIAA0101	NM_001029989.1	KIAA0101	-1.28	0.00
HSD11B1	NM_005525.2	hydroxysteroid (11-beta) dehydrogenase 1	-1.28	0.00
CLDN11	NM_005602.4	claudin 11	-1.27	0.01
TPX2	NM_012112.4	TPX2, microtubule-associated	-1.27	0.00
PPP1R14B	NM_138689.2	protein phosphatase 1, regulatory (inhibitor) subunit 14B	-1.27	0.00
ADK	NM_006721.2	adenosine kinase	-1.26	0.00
PTTG3P	NR_002734.1	pituitary tumor-transforming 3, pseudogene	-1.25	0.01
MELK	NM_014791.2	maternal embryonic leucine zipper kinase	-1.25	0.00
RNASEH2A	NM_006397.2	ribonuclease H2, subunit A	-1.25	0.00
MELK	NM_014791.2	maternal embryonic leucine zipper kinase	-1.24	0.00
FJX1	NM_014344.2	four jointed box 1	-1.24	0.00
TYMS	NM_001071.1	thymidylate synthetase	-1.24	0.00
KIF20A	NM_005733.1	kinesin family member 20A	-1.23	0.00
STMN2	NM_007029.2	stathmin 2	-1.22	0.01

AURKB	NM_004217.2	aurora kinase B	-1.22	0.00
RFC4	NM_181573.1	replication factor C (activator 1) 4, 37kDa	-1.22	0.00
ITPKA	NM_002220.1	inositol-trisphosphate 3-kinase A	-1.22	0.00
ACYP1	NM_203488.1	acylphosphatase 1, erythrocyte (common) type	-1.21	0.00
HSD17B7P2	NR_003086.1	hydroxysteroid (17-beta) dehydrogenase 7 pseudogene 2	-1.21	0.00
RPL39L	NM_052969.1	ribosomal protein L39-like	-1.20	0.00
MT1P3	#N/A	metallothionein 1 pseudogene 3	-1.20	0.00
SAPCD2	#N/A	suppressor APC domain containing 2	-1.20	0.00
EBP	NM_006579.1	emopamil binding protein (sterol isomerase)	-1.19	0.00
SGOL2	NM_152524.3	shugoshin-like 2 (S. pombe)	-1.18	0.00
POLA2	NM_002689.2	polymerase (DNA directed), alpha 2, accessory subunit	-1.18	0.00
F3	NM_001993.2	coagulation factor III (thromboplastin, tissue factor)	-1.17	0.03
NEK2	NM_002497.2	NIMA-related kinase 2	-1.17	0.00
LRR1	#N/A	leucine rich repeat protein 1	-1.17	0.00
HSD11B1	NM_005525.2	hydroxysteroid (11-beta) dehydrogenase 1	-1.16	0.00
TUBB3	NM_006086.2	tubulin, beta 3 class III	-1.16	0.00
PRC1	NM_199413.1	protein regulator of cytokinesis 1	-1.15	0.00
TTK	NM_003318.3	TTK protein kinase	-1.15	0.01
ACAT2	NM_005891.2	acetyl-CoA acetyltransferase 2	-1.14	0.00
MSRB1	#N/A	methionine sulfoxide reductase B1	-1.13	0.00
MCM7	NM_182776.1	minichromosome maintenance complex component 7	-1.13	0.00
NCAPG	NM_022346.3	non-SMC condensin I complex, subunit G	-1.12	0.00
CSTF3	NM_001033505.1	cleavage stimulation factor, 3' pre-RNA, subunit 3, 77kDa	-1.12	0.03
RGS20	NM_170587.1	regulator of G-protein signaling 20	-1.12	0.00
KIFC1	NM_002263.2	kinesin family member C1	-1.12	0.00
RFC4	NM_181573.1	replication factor C (activator 1) 4, 37kDa	-1.11	0.00
COQ3	NM_017421.3	coenzyme Q3 methyltransferase	-1.11	0.00
PRSS3	NM_002771.2	protease, serine, 3	-1.11	0.00
NME1	NM_198175.1	NME/NM23 nucleoside diphosphate kinase 1	-1.11	0.00
TMSB15B	#N/A	thymosin beta 15B	-1.10	0.01
PARPBP	#N/A	PARP1 binding protein	-1.09	0.00
PRIM1	NM_000946.2	primase, DNA, polypeptide 1 (49kDa)	-1.09	0.00
DNAJC9	NM_015190.3	DnaJ (Hsp40) homolog, subfamily C, member 9	-1.09	0.00
SDHAF3	#N/A	succinate dehydrogenase complex assembly factor 3	-1.09	0.00
HMBS	NM_000190.3	hydroxymethylbilane synthase	-1.09	0.00
PRKCDBP	NM_145040.2	protein kinase C, delta binding protein	-1.09	0.00

RACGAP1	NM_013277.2	Rac GTPase activating protein 1	-1.07	0.00
ABLIM3	NM_014945.2	actin binding LIM protein family, member 3	-1.07	0.00
ITGB3BP	NM_014288.3	integrin beta 3 binding protein (beta3-endonexin)	-1.07	0.00
FANCG	NM_004629.1	Fanconi anemia, complementation group G	-1.07	0.00
PFKFB4	NM_004567.2	6-phosphofructo-2-kinase/fructose-2,6-biphosphatase 4	-1.06	0.01
RPL39L	NM_052969.1	ribosomal protein L39-like	-1.06	0.00
TNFRSF6B	NM_003823.2	tumor necrosis factor receptor superfamily, member 6b, decoy	-1.06	0.00
BCYRN1	NR_001568.1	brain cytoplasmic RNA 1	-1.06	0.00
RPA3	NM_002947.3	replication protein A3, 14kDa	-1.06	0.00
NIF3L1	NM_021824.2	NIF3 NGG1 interacting factor 3-like 1	-1.06	0.00
LRRC20	NM_018239.2	leucine rich repeat containing 20	-1.06	0.00
NUDT1	NM_198954.1	nudix (nucleoside diphosphate linked moiety X)-type motif 1	-1.05	0.00
ZWINT	NM_032997.2	ZW10 interacting kinetochore protein	-1.05	0.00
TPI1	NM_000365.4	triosephosphate isomerase 1	-1.05	0.00
RPA2	NM_002946.3	replication protein A2, 32kDa	-1.05	0.00
SEMA3A	NM_006080.2	sema domain, immunoglobulin domain (Ig), short basic domain, secreted, (semaphorin) 3A	-1.04	0.00
MRPL24	NM_145729.1	mitochondrial ribosomal protein L24	-1.04	0.00
MRPL24	NM_145729.1	mitochondrial ribosomal protein L24	-1.04	0.00
CCDC34	NM_030771.1	coiled-coil domain containing 34	-1.04	0.04
ARHGAP22	NM_021226.2	Rho GTPase activating protein 22	-1.04	0.04
DEF8	NM_017702.2	differentially expressed in FDCP 8 homolog (mouse)	-1.03	0.00
ADORA2B	NM_000676.2	adenosine A2b receptor	-1.03	0.00
NME1	NM_198175.1	NME/NM23 nucleoside diphosphate kinase 1	-1.03	0.00
TMSB15B	#N/A	thymosin beta 15B	-1.03	0.01
DEF8	NM_017702.2	differentially expressed in FDCP 8 homolog (mouse)	-1.03	0.00
PIN1	NM_006221.2	peptidylprolyl cis/trans isomerase, NIMA-interacting 1	-1.02	0.00
EGFLAM	NM_182801.1	EGF-like, fibronectin type III and laminin G domains	-1.02	0.00
BOLA3	NM_001035505.1	bolA family member 3	-1.02	0.00
MT2A	NM_005953.2	metallothionein 2A	-1.02	0.01
TSPAN13	NM_014399.3	tetraspanin 13	-1.01	0.02
FAM216A	#N/A	family with sequence similarity 216, member A	-1.01	0.00
IDH1	NM_005896.2	isocitrate dehydrogenase 1 (NADP+), soluble	-1.01	0.02
SAC3D1	NM_013299.3	SAC3 domain containing 1	-1.01	0.00
MT1E	NM_175617.2	metallothionein 1E	-1.01	0.00
MRPL22	NM_014180.2	mitochondrial ribosomal protein L22	-1.00	0.00
KIF22	NM_007317.1	kinesin family member 22	-1.00	0.00

AURKAIP1	NM_017900.1	aurora kinase A interacting protein 1	-0.94	0.00
SAP30	NM_003864.3	Sin3A-associated protein, 30kDa	-0.94	0.00
STUB1	NM_005861.2	STIP1 homology and U-box containing protein 1, E3 ubiquitin protein ligase	-0.94	0.00
UBE2E3	XM_944994.1	ubiquitin-conjugating enzyme E2E 3	-0.94	0.04
NSL1	NM_001042549.1	NSL1, MIS12 kinetochore complex component	-0.93	0.00
MRPS28	NM_014018.2	mitochondrial ribosomal protein S28	-0.93	0.00
PDXP	NM_020315.4	pyridoxal (pyridoxine, vitamin B6) phosphatase	-0.93	0.00
TSSC1	NM_003310.1	tumor suppressing subtransferable candidate 1	-0.93	0.00
BOLA3	NM_001035505.1	bolA family member 3	-0.93	0.00
MGST1	NM_145764.1	microsomal glutathione S-transferase 1	-0.93	0.00
TUBG1	XM_944510.1	tubulin, gamma 1	-0.93	0.00
MCM5	NM_006739.3	minichromosome maintenance complex component 5	-0.92	0.00
HIST2H2AC	NM_003517.2	histone cluster 2, H2ac	-0.92	0.01
NUSAP1	NM_018454.5	nucleolar and spindle associated protein 1	-0.92	0.00
GGH	NM_003878.1	gamma-glutamyl hydrolase (conjugase, folylpolygammaglutamyl hydrolase)	-0.91	0.02
MVD	NM_002461.1	mevalonate (diphospho) decarboxylase	-0.91	0.00
EXOSC9	NM_001034194.1	exosome component 9	-0.91	0.00
CD69	NM_001781.1	CD69 molecule	-0.91	0.05
HDDC3	NM_198527.2	HD domain containing 3	-0.91	0.00
ERH	NM_004450.1	enhancer of rudimentary homolog (Drosophila)	-0.91	0.00
MRPL15	NM_014175.2	mitochondrial ribosomal protein L15	-0.91	0.00
C19orf60	NM_001100419.1	chromosome 19 open reading frame 60	-0.91	0.00
NHP2	NM_001034833.1	NHP2 ribonucleoprotein	-0.91	0.00
SIVA1	NM_006427.3	SIVA1, apoptosis-inducing factor	-0.91	0.00
S100A13	NM_001024210.1	S100 calcium binding protein A13	-0.90	0.00
H2AFX	NM_002105.2	H2A histone family, member X	-0.90	0.00
ACYP1	NM_203488.1	acylphosphatase 1, erythrocyte (common) type	-0.90	0.00
TUBB4B	#N/A	tubulin, beta 4B class IVb	-0.90	0.01
NRIP3	NM_020645.1	nuclear receptor interacting protein 3	-0.90	0.00
FARS2	NM_006567.3	phenylalanyl-tRNA synthetase 2, mitochondrial	-0.90	0.00
SPA17	NM_017425.2	sperm autoantigenic protein 17	-0.90	0.01
TUBG1	XM_944510.1	tubulin, gamma 1	-0.90	0.00
CMC1	NM_182523.1	C-x(9)-C motif containing 1	-0.90	0.00
COA1	#N/A	cytochrome c oxidase assembly factor 1 homolog	-0.89	0.00
ICT1	NM_001545.1	immature colon carcinoma transcript 1	-0.89	0.00
EXOSC9	NM_001034194.1	exosome component 9	-0.89	0.00

SNRNP25	NM_024571.3	small nuclear ribonucleoprotein 25kDa (U11/U12)	-1.00	0.00
COL13A1	NM_080815.2	collagen, type XIII, alpha 1	-1.00	0.01
LSM2	NM_021177.3	LSM2 homolog, U6 small nuclear RNA and mRNA degradation associated	-1.00	0.02
NUP37	NM_024057.2	nucleoporin 37kDa	-1.00	0.00
POP5	NM_198202.1	POP5 homolog, ribonuclease P/MRP subunit	-0.98	0.00
SUV39H1	NM_003173.2	suppressor of variegation 3-9 homolog 1 (Drosophila)	-0.98	0.00
NSMCE4A	NM_017615.1	NSE4 homolog A, SMC5-SMC6 complex component	-0.98	0.00
NUDT2	NM_147173.1	nudix (nucleoside diphosphate linked moiety X)-type motif 2	-0.98	0.00
GSTO1	NM_004832.1	glutathione S-transferase omega 1	-0.98	0.00
MCM4	NM_005914.2	minichromosome maintenance complex component 4	-0.98	0.00
DDX39A	#N/A	DEAD (Asp-Glu-Ala-Asp) box polypeptide 39A	-0.98	0.00
MPP4	NM_033066.1	membrane protein, palmitoylated 4 (MAGUK p55 subfamily member 4)	-0.97	0.00
RBMX	NM_002139.2	RNA binding motif protein, X-linked	-0.97	0.00
MED31	NM_016060.2	mediator complex subunit 31	-0.97	0.00
MRPL22	NM_014180.2	mitochondrial ribosomal protein L22	-0.97	0.00
MRPL35	NM_016622.2	mitochondrial ribosomal protein L35	-0.97	0.00
GPSM2	NM_013296.3	G-protein signaling modulator 2	-0.97	0.01
NFU1	NM_001002755.1	NFU1 iron-sulfur cluster scaffold	-0.96	0.00
SERPINB7	NM_003784.2	serpin peptidase inhibitor, clade B (ovalbumin), member 7	-0.96	0.00
TFB1M	NM_016020.1	transcription factor B1, mitochondrial	-0.96	0.02
C19orf48	NM_199249.1	chromosome 19 open reading frame 48	-0.96	0.01
MRPS15	NM_031280.2	mitochondrial ribosomal protein S15	-0.96	0.00
STEAP1	XM_940149.1	six transmembrane epithelial antigen of the prostate 1	-0.96	0.00
PAGR1	#N/A	PAXIP1 associated glutamate-rich protein 1	-0.96	0.00
IDH1	NM_005896.2	isocitrate dehydrogenase 1 (NADP+), soluble	-0.96	0.03
CLIC1	NM_001288.4	chloride intracellular channel 1	-0.96	0.00
BEX1	NM_018476.3	brain expressed, X-linked 1	-0.95	0.02
CCDC167	#N/A	coiled-coil domain containing 167	-0.95	0.00
INSIG1	NM_198336.1	insulin induced gene 1	-0.95	0.01
LIPG	NM_006033.2	lipase, endothelial	-0.95	0.02
SDF2L1	NM_022044.2	stromal cell-derived factor 2-like 1	-0.95	0.00
PRIM1	NM_000946.2	primase, DNA, polypeptide 1 (49kDa)	-0.95	0.00
FEN1	NM_004111.4	flap structure-specific endonuclease 1	-0.95	0.00
LPIN1	NM_145693.1	lipin 1	-0.95	0.00
RANBP1	NM_002882.2	RAN binding protein 1	-0.94	0.00
NUSAP1	NM_018454.5	nucleolar and spindle associated protein 1	-0.94	0.01

EBNA1BP2	NM_006824.1	EBNA1 binding protein 2	-0.86	0.01
EIF5A	NM_001970.3	eukaryotic translation initiation factor 5A	-0.86	0.00
LSM4	NM_012321.2	LSM4 homolog, U6 small nuclear RNA and mRNA degradation associated	-0.86	0.04
RPS19BP1	NM_194326.2	ribosomal protein S19 binding protein 1	-0.86	0.00
LPXN	NM_004811.1	Leupaxin	-0.86	0.00
ACOT7	NM_181864.2	acyl-CoA thioesterase 7	-0.86	0.00
SMIM4	#N/A	small integral membrane protein 4	-0.86	0.00
RPL34	NM_000995.2	ribosomal protein L34	-0.86	0.00
DANCR	#N/A	differentiation antagonizing non-protein coding RNA	-0.86	0.02
NT5DC2	NM_022908.1	5'-nucleotidase domain containing 2	-0.85	0.00
HOXA9	NM_152739.3	homeobox A9	-0.85	0.04
HJURP	NM_018410.3	Holliday junction recognition protein	-0.85	0.01
TIMM21	#N/A	translocase of inner mitochondrial membrane 21 homolog (yeast)	-0.85	0.01
HSPB11	#N/A	heat shock protein family B (small), member 11	-0.85	0.00
MICB	NM_005931.2	MHC class I polypeptide-related sequence B	-0.85	0.01
TYSND1	NM_001040273.1	trypsin domain containing 1	-0.85	0.01
EIF2B3	NM_020365.2	eukaryotic translation initiation factor 2B, subunit 3 gamma, 58kDa	-0.85	0.00
SPC25	NM_020675.3	SPC25, NDC80 kinetochore complex component	-0.85	0.00
FSD1	XM_001130761.1	fibronectin type III and SPRY domain containing 1	-0.85	0.00
EIF6	NM_181466.1	eukaryotic translation initiation factor 6	-0.84	0.00
TOMM22	NM_020243.4	translocase of outer mitochondrial membrane 22 homolog (yeast)	-0.84	0.00
GRK5	NM_005308.2	G protein-coupled receptor kinase 5	-0.84	0.02
TUBB	NM_178014.2	tubulin, beta class I	-0.84	0.00
TSPAN4	NM_001025235.1	tetraspanin 4	-0.84	0.00
LMNB1	NM_005573.2	lamin B1	-0.84	0.00
RPLP0	NM_001002.3	ribosomal protein, large, P0	-0.84	0.00
MRPL12	NM_002949.2	mitochondrial ribosomal protein L12	-0.84	0.00
NDUFAF2	NM_174889.3	NADH dehydrogenase (ubiquinone) complex I, assembly factor 2	-0.84	0.00
GSTO1	NM_004832.1	glutathione S-transferase omega 1	-0.84	0.00
PSMA6	NM_002791.1	proteasome subunit alpha 6	-0.84	0.00
TNFRSF6B	NM_003823.2	tumor necrosis factor receptor superfamily, member 6b, decoy	-0.84	0.00
PSRC1	NM_001032290.1	proline/serine-rich coiled-coil 1	-0.84	0.00
NUF2	NM_031423.3	NUF2, NDC80 kinetochore complex component	-0.84	0.00
H2AFZ	NM_002106.3	H2A histone family, member Z	-0.84	0.00
PPIH	NM_006347.3	peptidylprolyl isomerase H (cyclophilin H)	-0.83	0.00
MRPL39	NM_017446.3	mitochondrial ribosomal protein L39	-0.83	0.00

PRMT1	NM_198319.2	protein arginine methyltransferase 1	-0.83	0.00
SMAD6	NM_005585.3	SMAD family member 6	-0.83	0.00
DRAP1	NM_006442.2	DR1-associated protein 1 (negative cofactor 2 alpha)	-0.83	0.00
TWF2	NM_007284.3	twinfilin actin binding protein 2	-0.83	0.00
TRAP1	NM_016292.1	TNF receptor-associated protein 1	-0.83	0.00
PRMT1	NM_198319.2	protein arginine methyltransferase 1	-0.83	0.00
MRPL52	NM_180981.1	mitochondrial ribosomal protein L52	-0.83	0.00
MRPL54	NM_172251.1	mitochondrial ribosomal protein L54	-0.83	0.00
RNF181	NM_016494.3	ring finger protein 181	-0.83	0.00
PHF19	NM_015651.1	PHD finger protein 19	-0.83	0.00
VPS29	NM_016226.3	VPS29 retromer complex component	-0.82	0.00
C4orf27	NM_017897.1	chromosome 4 open reading frame 27	-0.82	0.00
CSTF2	NM_001325.2	cleavage stimulation factor, 3' pre-RNA, subunit 2, 64kDa	-0.82	0.00
HINT1	NM_005340.3	histidine triad nucleotide binding protein 1	-0.82	0.01
NHP2	NM_001034833.1	NHP2 ribonucleoprotein	-0.82	0.00
KIF2C	NM_006845.2	kinesin family member 2C	-0.82	0.01
SERP2	NM_001010897.1	stress-associated endoplasmic reticulum protein family member 2	-0.82	0.01
DUT	NM_001025248.1	deoxyuridine triphosphatase	-0.82	0.00
NUDT2	NM_147173.1	nudix (nucleoside diphosphate linked moiety X)-type motif 2	-0.82	0.00
MRPL23	NM_021134.2	mitochondrial ribosomal protein L23	-0.82	0.01
CTSZ	NM_001336.2	cathepsin Z	-0.82	0.00
TPI1	NM_000365.4	triosephosphate isomerase 1	-0.82	0.00
C14orf2	NM_004894.1	chromosome 14 open reading frame 2	-0.82	0.00
MRPS11	NM_176805.1	mitochondrial ribosomal protein S11	-0.82	0.01
EEF1D	NM_032378.2	eukaryotic translation elongation factor 1 delta (guanine nucleotide exchange protein)	-0.82	0.01
LRIR1	#N/A	leucine rich repeat protein 1	-0.82	0.00
PSMD10	NM_002814.2	proteasome 26S subunit, non-ATPase 10	-0.81	0.00
RPL34	NM_000995.2	ribosomal protein L34	-0.81	0.00
LSM10	NM_032661.1	LSM10, U7 small nuclear RNA associated	-0.81	0.02
BOLA2	NM_001031827.1	bolA family member 2	-0.81	0.00
RPL6	NM_001024662.1	ribosomal protein L6	-0.81	0.01
DEPDC1	NM_017779.3	DEP domain containing 1	-0.81	0.00
PSMG4	NM_001128591.1	proteasome (prosome, macropain) assembly chaperone 4	-0.81	0.00
GPX1	NM_201397.1	glutathione peroxidase 1	-0.81	0.00
AP1S1	NM_057089.2	adaptor-related protein complex 1, sigma 1 subunit	-0.81	0.01
RANBP1	NM_002882.2	RAN binding protein 1	-0.81	0.00

RPS21	NM_001024.3	ribosomal protein S21	-0.81	0.00
NHP2	NM_001034833.1	NHP2 ribonucleoprotein	-0.81	0.00
TRAPPC5	NM_001042452.1	trafficking protein particle complex 5	-0.81	0.00
OMSS1	#N/A	oms1 ribosomal small subunit homolog (yeast)	-0.80	0.00
CSE1L	NM_001316.2	CSE1 chromosome segregation 1-like (yeast)	-0.80	0.00
MRPL1	NM_020236.2	mitochondrial ribosomal protein L1	-0.80	0.00
CSE1L	NM_001316.2	CSE1 chromosome segregation 1-like (yeast)	-0.80	0.00
GCSH	NM_004483.3	glycine cleavage system protein H (aminomethyl carrier)	-0.80	0.00
FAM96A	NM_032231.4	family with sequence similarity 96, member A	-0.80	0.00
PTGES2	NM_198938.1	prostaglandin E synthase 2	-0.80	0.00
HMBS	NM_000190.3	hydroxymethylbilane synthase	-0.80	0.00
TSPO	NM_000714.4	translocator protein (18kDa)	-0.80	0.00
MCM2	NM_004526.2	minichromosome maintenance complex component 2	-0.80	0.01
BANF1	NM_003860.2	barrier to autointegration factor 1	-0.80	0.00
KIF23	NM_138555.1	kinesin family member 23	-0.80	0.00
SNRNP40	NM_004814.2	small nuclear ribonucleoprotein 40kDa (U5)	-0.80	0.00
ZWILCH	NM_017975.3	zwilch kinetochore protein	-0.80	0.00
GLE1	NM_001003722.1	GLE1 RNA export mediator	-0.80	0.01
DNLZ	NM_001080449.1	DNL-type zinc finger	-0.80	0.00
ATP5G1	NM_001002027.1	ATP synthase, H+ transporting, mitochondrial Fo complex, subunit C1 (subunit 9)	-0.80	0.00
PAQR4	NM_152341.2	progestin and adipoQ receptor family member IV	-0.80	0.04
ATL3	NM_015459.3	atlastin GTPase 3	-0.80	0.00
PSMG1	NM_203433.1	proteasome (prosome, macropain) assembly chaperone 1	-0.79	0.00
DPH5	NM_001077394.1	diphthamide biosynthesis 5	-0.79	0.00
RPS7	NM_001011.3	ribosomal protein S7	-0.79	0.00
NTHL1	NM_002528.4	nth-like DNA glycosylase 1	-0.79	0.01
S100A13	NM_001024210.1	S100 calcium binding protein A13	-0.79	0.00
GATB	#N/A	glutamyl-tRNA(Gln) amidotransferase, subunit B	-0.79	0.01
SNRPC	NM_003093.1	small nuclear ribonucleoprotein polypeptide C	-0.79	0.00
RUVBL2	NM_006666.1	RuvB-like AAA ATPase 2	-0.79	0.00
TSPAN4	NM_001025235.1	tetraspanin 4	-0.79	0.00
PLK1	NM_005030.3	polo-like kinase 1	-0.79	0.02
PSMB7	NM_002799.2	proteasome subunit beta 7	-0.79	0.00
DGCR6	NM_005675.2	DiGeorge syndrome critical region gene 6	-0.79	0.00
COPS6	NM_006833.4	COP9 signalosome subunit 6	-0.79	0.00
RAC2	NM_002872.3	ras-related C3 botulinum toxin substrate 2 (rho family, small GTP binding protein Rac2)	-0.79	0.03

RPLP0	NM_001002.3	ribosomal protein, large, P0	-0.79	0.00
HMGB2	NM_002129.2	high mobility group box 2	-0.79	0.01
NSDHL	NM_015922.1	NAD(P) dependent steroid dehydrogenase-like	-0.79	0.01
FBXO5	NM_012177.2	F-box protein 5	-0.79	0.02
DGCR6	NM_005675.2	DiGeorge syndrome critical region gene 6	-0.79	0.00
NDN	NM_002487.2	necdin, melanoma antigen (MAGE) family member	-0.79	0.00
LAYN	NM_178834.3	Layilin	-0.79	0.00
MASTL	NM_032844.1	microtubule associated serine/threonine kinase-like	-0.79	0.00
DNTTIP1	NM_052951.2	deoxynucleotidyltransferase, terminal, interacting protein 1	-0.79	0.00
AKIP1	#N/A	A kinase (PRKA) interacting protein 1	-0.79	0.02
MRPL27	NM_148571.1	mitochondrial ribosomal protein L27	-0.79	0.00
MRPL11	NM_170739.1	mitochondrial ribosomal protein L11	-0.79	0.00
SAAL1	NM_138421.2	serum amyloid A-like 1	-0.79	0.00
NDP	NM_000266.1	Norrie disease (pseudoglioma)	-0.78	0.01
COMMD8	NM_017845.3	COMM domain containing 8	-0.78	0.00
BOP1	NM_015201.3	block of proliferation 1	-0.78	0.01
TRAPPC2L	NM_016209.2	trafficking protein particle complex 2-like	-0.78	0.01
MRPS33	NM_016071.2	mitochondrial ribosomal protein S33	-0.78	0.00
DCXR	NM_016286.2	dicarbonyl/L-xylulose reductase	-0.78	0.05
RPUSD3	NM_173659.2	RNA pseudouridylate synthase domain containing 3	-0.78	0.00
PMM1	NM_002676.1	phosphomannomutase 1	-0.77	0.00
SPC24	NM_182513.1	SPC24, NDC80 kinetochore complex component	-0.77	0.00
COMMD10	NM_016144.2	COMM domain containing 10	-0.77	0.00
RPL36	NM_033643.2	ribosomal protein L36	-0.77	0.00
ABCA13	NM_152701.2	ATP-binding cassette, sub-family A (ABC1), member 13	-0.77	0.00
CLPP	NM_006012.2	caseinolytic mitochondrial matrix peptidase proteolytic subunit	-0.77	0.01
ACTL6A	NM_177989.2	actin-like 6A	-0.77	0.00
PLAC8	NM_016619.1	placenta-specific 8	-0.77	0.00
BCL2L12	NM_001040698.1	BCL2-like 12 (proline rich)	-0.77	0.00
GSDMD	NM_024736.5	gasdermin D	-0.77	0.00
GUK1	NM_000858.4	guanylate kinase 1	-0.77	0.00
POLR3K	NM_016310.2	polymerase (RNA) III (DNA directed) polypeptide K, 12.3 kDa	-0.77	0.00
RABEPK	NM_005833.2	Rab9 effector protein with kelch motifs	-0.77	0.00
PRMT5	NM_006109.3	protein arginine methyltransferase 5	-0.77	0.00
PRELID1	NM_013237.2	PRELI domain containing 1	-0.77	0.01
BCS1L	NM_001079866.1	BC1 (ubiquinol-cytochrome c reductase) synthesis-like	-0.77	0.00

NDUFB6	NM_002493.3	NADH dehydrogenase (ubiquinone) 1 beta subcomplex, 6, 17kDa	-0.77	0.00
ADSL	NM_000026.1	adenylosuccinate lyase	-0.77	0.00
DPH5	NM_001077394.1	diphthamide biosynthesis 5	-0.77	0.00
RPS7	NM_001011.3	ribosomal protein S7	-0.77	0.01
NOL12	NM_024313.2	nucleolar protein 12	-0.77	0.00
RSFA	#N/A	ribosome binding factor A (putative)	-0.77	0.00
SLC2A4RG	NM_020062.3	SLC2A4 regulator	-0.77	0.00
SPC25	NM_020675.3	SPC25, NDC80 kinetochore complex component	-0.76	0.00
FAM96A	NM_032231.4	family with sequence similarity 96, member A	-0.76	0.00
RQCD1	NM_005444.1	RCD1 required for cell differentiation 1 homolog (S. pombe)	-0.76	0.00
PROCR	NM_006404.3	protein C receptor, endothelial	-0.76	0.01
BNIP3	NM_004052.2	BCL2/adenovirus E1B 19kDa interacting protein 3	-0.76	0.01
ACTR1B	NM_005735.2	ARP1 actin-related protein 1 homolog B, centractin beta (yeast)	-0.76	0.00
BCL7C	XM_940124.1	B-cell CLL/lymphoma 7C	-0.76	0.00
MIF	NM_002415.1	macrophage migration inhibitory factor (glycosylation-inhibiting factor)	-0.76	0.00
GTF3A	NM_002097.1	general transcription factor IIIA	-0.76	0.00
ABHD12	NM_015600.3	abhydrolase domain containing 12	-0.76	0.00
FAM162B	NM_001085480.1	family with sequence similarity 162, member B	-0.76	0.03
SHMT1	NM_004169.3	serine hydroxymethyltransferase 1 (soluble)	-0.76	0.00
MRPL53	NM_053050.2	mitochondrial ribosomal protein L53	-0.76	0.00
MND1	NM_032117.2	meiotic nuclear divisions 1	-0.76	0.01
HMGB1P1	#N/A	high mobility group box 1 pseudogene 1	-0.76	0.00
STUB1	NM_005861.2	STIP1 homology and U-box containing protein 1, E3 ubiquitin protein ligase	-0.76	0.00
FOXRED1	NM_017547.2	FAD-dependent oxidoreductase domain containing 1	-0.76	0.00
GTPBP6	NM_012227.1	GTP binding protein 6 (putative)	-0.76	0.01
GLRX3	NM_006541.3	glutaredoxin 3	-0.76	0.00
MKKS	NM_018848.2	McKusick-Kaufman syndrome	-0.76	0.00
COMMD10	NM_016144.2	COMM domain containing 10	-0.76	0.00
POLD2	NM_001127218.1	polymerase (DNA directed), delta 2, accessory subunit	-0.76	0.00
TRIOBP	NM_001039141.1	TRIO and F-actin binding protein	-0.76	0.00
SIVA1	NM_006427.3	SIVA1, apoptosis-inducing factor	-0.76	0.00
DTD1	NM_080820.4	D-tyrosyl-tRNA deacylase 1	-0.76	0.00
B9D2	NM_030578.2	B9 protein domain 2	-0.76	0.00
FDPS	NM_002004.2	farnesyl diphosphate synthase	-0.75	0.01
BAD	NM_032989.1	BCL2-associated agonist of cell death	-0.75	0.00
TP53I3	NM_004881.2	tumor protein p53 inducible protein 3	-0.75	0.00

STOML2	NM_013442.1	stomatin (EPB72)-like 2	-0.75	0.00
ACOT7	NM_181864.2	acyl-CoA thioesterase 7	-0.75	0.00
MND1	NM_032117.2	meiotic nuclear divisions 1	-0.75	0.00
RAD54B	NM_012415.2	RAD54 homolog B (S. cerevisiae)	-0.75	0.00
MRPS12	NM_033362.2	mitochondrial ribosomal protein S12	-0.75	0.00
EMG1	NM_006331.5	EMG1 N1-specific pseudouridine methyltransferase	-0.75	0.02
MRPL33	NM_145330.2	mitochondrial ribosomal protein L33	-0.75	0.00
GALE	NM_001008216.1	UDP-galactose-4-epimerase	-0.75	0.00
AP1S1	NM_057089.2	adaptor-related protein complex 1, sigma 1 subunit	-0.75	0.02
MRPS23	NM_016070.2	mitochondrial ribosomal protein S23	-0.75	0.00
YEATS4	NM_006530.2	YEATS domain containing 4	-0.75	0.00
KYNU	NM_001032998.1	Kynureninase	-0.75	0.00
RBX1	NM_014248.2	ring-box 1, E3 ubiquitin protein ligase	-0.74	0.00
PSMB3	NM_002795.2	proteasome subunit beta 3	-0.74	0.00
MRPL40	NM_003776.2	mitochondrial ribosomal protein L40	-0.74	0.00
ANKRD9	NM_152326.2	ankyrin repeat domain 9	-0.74	0.04
NOSIP	NM_015953.3	nitric oxide synthase interacting protein	-0.74	0.00
EIF6	NM_181466.1	eukaryotic translation initiation factor 6	-0.74	0.00
C19orf70	NM_205767.1	chromosome 19 open reading frame 70	-0.74	0.00
MRPL13	NM_014078.4	mitochondrial ribosomal protein L13	-0.74	0.00
TROAP	NM_005480.2	trophinin associated protein	-0.74	0.01
NUP88	NM_002532.3	nucleoporin 88 kDa	-0.74	0.00
TXNDC17	NM_032731.3	thioredoxin domain containing 17	-0.74	0.00
ZWINT	NM_032997.2	ZW10 interacting kinetochore protein	-0.74	0.00
TRIAP1	NM_016399.2	TP53 regulated inhibitor of apoptosis 1	-0.74	0.00
PDSS1	NM_014317.3	prenyl (decaprenyl) diphosphate synthase, subunit 1	-0.74	0.02
RPPH1	NR_002312.1	ribonuclease P RNA component H1	-0.74	0.04
SLC25A42	NM_178526.2	solute carrier family 25, member 42	-0.74	0.00
MTCP1	NM_014221.3	mature T-cell proliferation 1	-0.74	0.00
SLC25A11	NM_003562.3	solute carrier family 25 (mitochondrial carrier; oxoglutarate carrier), member 11	-0.74	0.00
RAD51C	NM_002876.2	RAD51 paralog C	-0.73	0.00
FLOT1	NM_005803.2	flotillin 1	-0.73	0.03
CYC1	NM_001916.3	cytochrome c-1	-0.73	0.00
TUFM	NM_003321.3	Tu translation elongation factor, mitochondrial	-0.73	0.00
FANCE	NM_021922.2	Fanconi anemia, complementation group E	-0.73	0.02
DRG1	NM_004147.3	developmentally regulated GTP binding protein 1	-0.73	0.00

C7orf55	NM_197994.2	chromosome 7 open reading frame 55	-0.73	0.01
PHF19	NM_015651.1	PHD finger protein 19	-0.73	0.01
HRAS	NM_176795.2	Harvey rat sarcoma viral oncogene homolog	-0.73	0.04
BCL2L12	NM_001040698.1	BCL2-like 12 (proline rich)	-0.73	0.00
ROMO1	NM_080748.2	reactive oxygen species modulator 1	-0.73	0.00
MRPL55	NM_181462.1	mitochondrial ribosomal protein L55	-0.73	0.00
IFI27L1	NM_145249.2	interferon, alpha-inducible protein 27-like 1	-0.73	0.00
COX7B	NM_001866.2	cytochrome c oxidase subunit VIIb	-0.73	0.00
VRK1	NM_003384.2	vaccinia related kinase 1	-0.73	0.00
MRPS7	NM_015971.2	mitochondrial ribosomal protein S7	-0.73	0.00
PLK4	NM_014264.3	polo-like kinase 4	-0.73	0.00
RAN	NM_006325.2	RAN, member RAS oncogene family	-0.72	0.00
PUDP	#N/A	pseudouridine 5'-phosphatase	-0.72	0.00
ABHD8	NM_024527.4	abhydrolase domain containing 8	-0.72	0.00
COPE	NM_199442.1	coatomer protein complex, subunit epsilon	-0.72	0.00
NUP85	NM_024844.3	nucleoporin 85kDa	-0.72	0.01
PSME2	NM_002818.2	proteasome activator subunit 2	-0.72	0.01
MRPL41	NM_032477.1	mitochondrial ribosomal protein L41	-0.72	0.00
MIPOL1	NM_138731.3	mirror-image polydactyly 1	-0.72	0.00
ENKD1	#N/A	enkurin domain containing 1	-0.72	0.01
MRPL18	NM_014181.2	mitochondrial ribosomal protein L18	-0.72	0.00
AP1S1	NM_057089.2	adaptor-related protein complex 1, sigma 1 subunit	-0.72	0.02
PRDX4	NM_006406.1	peroxiredoxin 4	-0.72	0.00
TUBA4A	NM_006000.1	tubulin, alpha 4a	-0.72	0.01
MRPL38	NM_032478.2	mitochondrial ribosomal protein L38	-0.72	0.00
ECT2	NM_018098.4	epithelial cell transforming 2	-0.72	0.00
SSNA1	NM_003731.1	Sjogren syndrome nuclear autoantigen 1	-0.72	0.01
ISOC2	NM_024710.1	isochorismatase domain containing 2	-0.72	0.00
MID1IP1	NM_021242.4	MID1 interacting protein 1	-0.71	0.00
PSMC3	NM_002804.4	proteasome 26S subunit, ATPase 3	-0.71	0.00
ATAD3A	NM_018188.2	ATPase family, AAA domain containing 3A	-0.71	0.00
C5orf46	NM_206966.2	chromosome 5 open reading frame 46	-0.71	0.00
RPL26P30	#N/A	ribosomal protein L26 pseudogene 30	-0.71	0.00
PPA2	NM_176866.2	pyrophosphatase (inorganic) 2	-0.71	0.03
NPRL2	#N/A	NPR2-like, GATOR1 complex subunit	-0.71	0.00
COPS5	NM_006837.2	COP9 signalosome subunit 5	-0.71	0.00

SMIM3	#N/A	small integral membrane protein 3	-0.89	0.02
MZT1	#N/A	mitotic spindle organizing protein 1	-0.89	0.00
SUCLG1	NM_003849.2	succinate-CoA ligase, alpha subunit	-0.89	0.00
LSS	NM_002340.3	lanosterol synthase (2,3-oxidosqualene-lanosterol cyclase)	-0.89	0.00
BOLA2	NM_001031827.1	bolA family member 2	-0.89	0.00
ICAM3	NM_002162.2	intercellular adhesion molecule 3	-0.89	0.00
FAM83D	NM_030919.2	family with sequence similarity 83, member D	-0.89	0.02
RRP7A	NM_015703.3	ribosomal RNA processing 7 homolog A	-0.89	0.04
GEMIN6	NM_024775.9	gem (nuclear organelle) associated protein 6	-0.89	0.00
C19orf60	NM_001100419.1	chromosome 19 open reading frame 60	-0.89	0.00
PRADC1	#N/A	proteasome-associated domain containing 1	-0.89	0.00
MT1A	NM_005946.2	metallothionein 1A	-0.89	0.01
MRPL34	NM_023937.2	mitochondrial ribosomal protein L34	-0.89	0.00
SIVA1	NM_006427.3	SIVA1, apoptosis-inducing factor	-0.89	0.00
PLGRKT	#N/A	plasminogen receptor, C-terminal lysine transmembrane protein	-0.89	0.00
LAMTOR4	#N/A	late endosomal/lysosomal adaptor, MAPK and MTOR activator 4	-0.89	0.01
GDF5	NM_000557.2	growth differentiation factor 5	-0.89	0.04
C1orf112	NM_018186.2	chromosome 1 open reading frame 112	-0.89	0.00
NDUFB6	NM_002493.3	NADH dehydrogenase (ubiquinone) 1 beta subcomplex, 6, 17kDa	-0.89	0.00
RPS6KB2	NM_003952.2	ribosomal protein S6 kinase, 70kDa, polypeptide 2	-0.89	0.00
NHP2	NM_001034833.1	NHP2 ribonucleoprotein	-0.89	0.00
NDC80	NM_006101.1	NDC80 kinetochore complex component	-0.87	0.00
UQCC2	#N/A	ubiquinol-cytochrome c reductase complex assembly factor 2	-0.87	0.00
BUB3	NM_004725.2	BUB3 mitotic checkpoint protein	-0.87	0.00
PSMG1	NM_203403.1	proteasome (prosome, macropain) assembly chaperone 1	-0.87	0.00
RAD51AP1	NM_006479.3	RAD51 associated protein 1	-0.87	0.00
RFC5	NM_007370.3	replication factor C (activator 1) 5, 36.5kDa	-0.87	0.00
COL13A1	NM_080815.2	collagen, type XIII, alpha 1	-0.87	0.01
HMGB1P1	#N/A	high mobility group box 1 pseudogene 1	-0.87	0.00
COQ2	NM_015697.6	coenzyme Q2 4-hydroxybenzoate polyprenyltransferase	-0.87	0.00
EXOSC8	NM_181503.1	exosome component 8	-0.87	0.01
C7orf50	NM_032350.4	chromosome 7 open reading frame 50	-0.87	0.00
MRPL17	NM_022061.2	mitochondrial ribosomal protein L17	-0.87	0.00
TMEM256	#N/A	transmembrane protein 256	-0.87	0.02
FAM105A	NM_019018.1	family with sequence similarity 105, member A	-0.87	0.01
HEBP2	NM_014320.2	heme binding protein 2	-0.86	0.02

F3	NM_001993.2	coagulation factor III (thromboplastin, tissue factor)	-0.71	0.01
NDUFB7	NM_004146.4	NADH dehydrogenase (ubiquinone) 1 beta subcomplex, 7, 18kDa	-0.71	0.00
BOLA2	NM_001031827.1	bolA family member 2	-0.71	0.00
TUBB7P	#N/A	tubulin, beta 7, pseudogene	-0.71	0.02
ELP6	#N/A	elongator acetyltransferase complex subunit 6	-0.71	0.01
MMP1	NM_002421.2	matrix metallopeptidase 1	-0.71	0.02
TTC1	NM_003314.1	tetratricopeptide repeat domain 1	-0.71	0.00
FIBP	NM_004214.4	fibroblast growth factor (acidic) intracellular binding protein	-0.71	0.00
C16orf13	NM_001040162.1	chromosome 16 open reading frame 13	-0.71	0.00
GINS4	NM_032336.1	GINS complex subunit 4 (Sld5 homolog)	-0.70	0.01
TOMM6	NM_001134493.1	translocase of outer mitochondrial membrane 6 homolog (yeast)	-0.70	0.00
NAA38	#N/A	N(alpha)-acetyltransferase 38, NatC auxiliary subunit	-0.70	0.04
AKIP1	#N/A	A kinase (PRKA) interacting protein 1	-0.70	0.01
SNRPG	NM_003096.2	small nuclear ribonucleoprotein polypeptide G	-0.70	0.00
PMVK	NM_006556.3	phosphomevalonate kinase	-0.70	0.00
KNSTRN	#N/A	kinetochore-localized astrin/SPAG5 binding protein	-0.70	0.00
NT5C3B	#N/A	5'-nucleotidase, cytosolic IIIB	-0.70	0.00
RHOC	NM_001042678.1	ras homolog family member C	-0.70	0.00

Table 11 GO biological process term and p-value in network from up-regulated miRNA

ID	Gene ontology	p-value	adj. p-value (Bonferroni)
GO:0045595	regulation of cell differentiation	1.634E-10	1.050E-6
GO:0010628	positive regulation of gene expression	1.469E-9	2.360E-6
GO:0009891	positive regulation of biosynthetic process	1.914E-9	2.360E-6
GO:1902680	positive regulation of RNA biosynthetic process	2.308E-9	2.360E-6

Table 12 GO biological process term and p-value in network from down-regulated miRNA

ID	Gene ontology	p-value	adj. p-value (Bonferroni)
GO:0045944	positive regulation of transcription from RNA polymerase II promoter	6.891E-8	2.641E-4
GO:0010628	positive regulation of gene expression	2.568E-7	4.921E-4
GO:0045893	positive regulation of transcription, DNA-templated	2.213E-6	1.901E-3
GO:1903508	positive regulation of nucleic acid-templated transcription	2.213E-6	1.901E-3

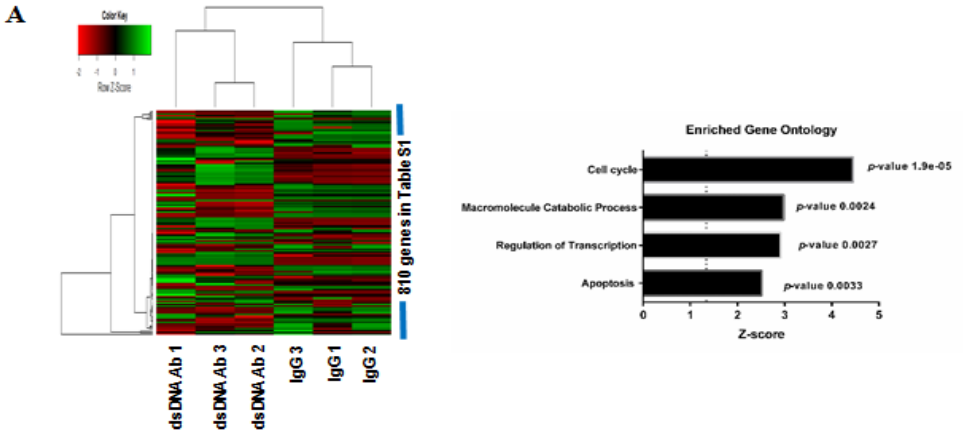

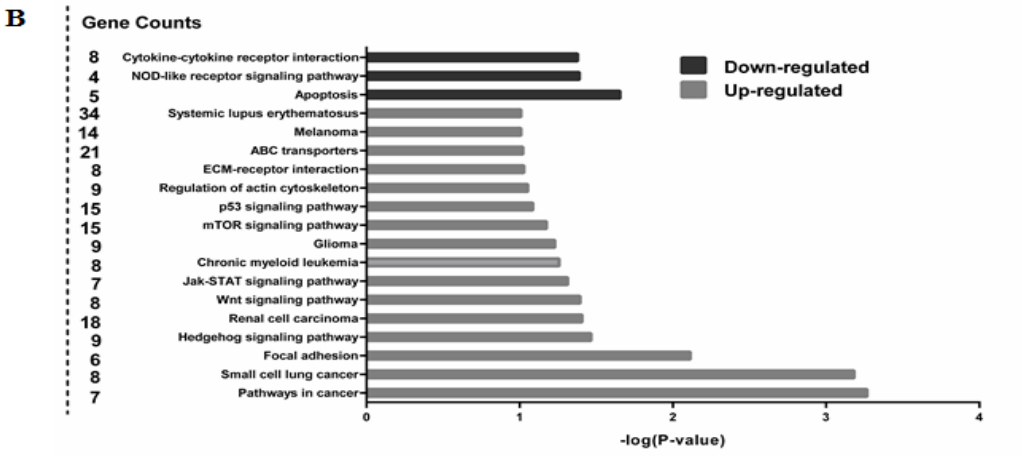

C

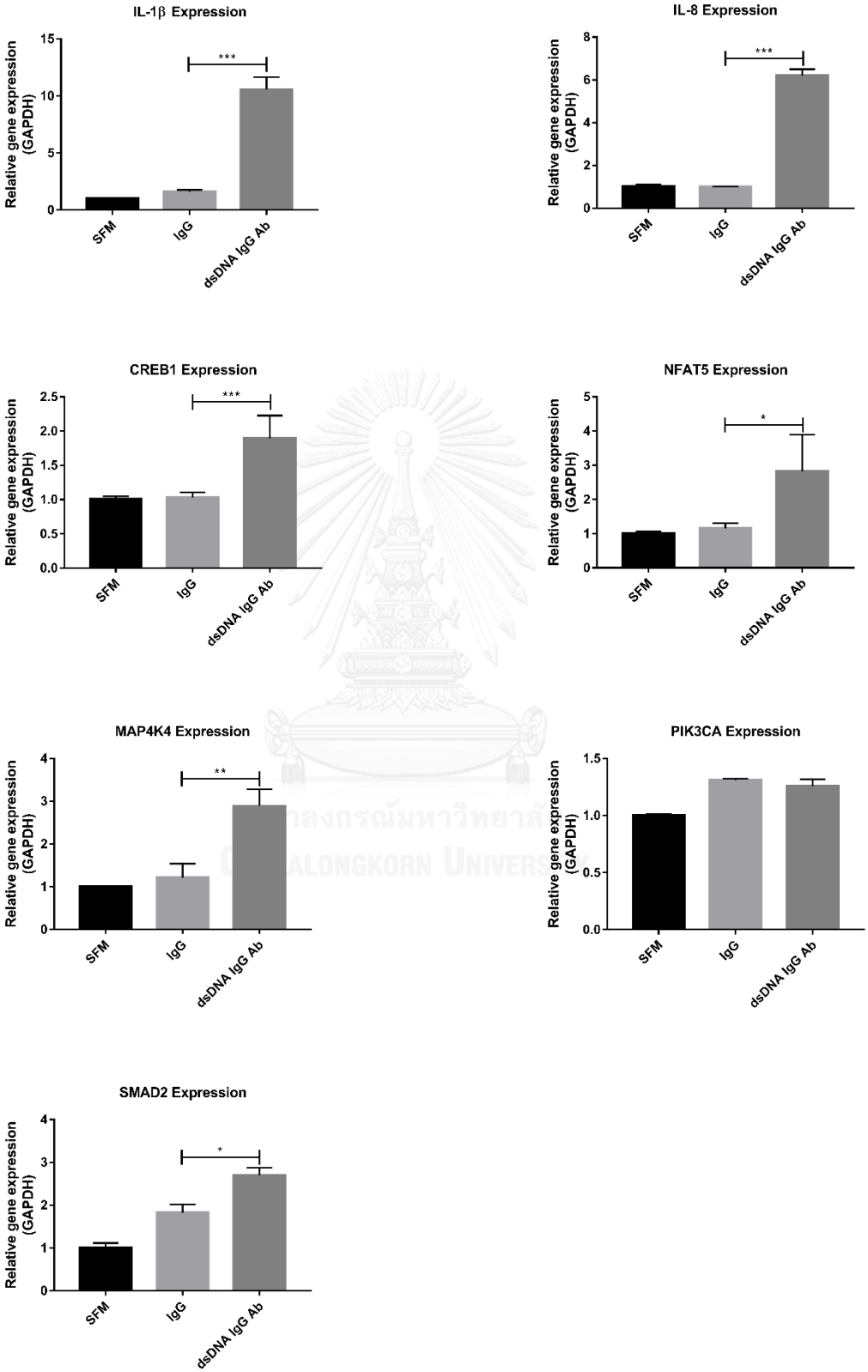
IL-1β Expression
Relative gene expression (GAPDH)
15
10
5
0
***
SFM
IgG
dsDNA IgG Ab
IL-8 Expression
Relative gene expression (GAPDH)
8
6
4
2
0
***
SFM
IgG
dsDNA IgG Ab
CREB1 Expression
Relative gene expression (GAPDH)
2.5
2.0
1.5
1.0
0.5
0.0
***
SFM
IgG
dsDNA IgG Ab
NFAT5 Expression
Relative gene expression (GAPDH)
5
4
3
2
1
0
*
SFM
IgG
dsDNA IgG Ab
MAP4K4 Expression
Relative gene expression (GAPDH)
4
3
2
1
0
**
SFM
IgG
dsDNA IgG Ab
PIK3CA Expression
Relative gene expression (GAPDH)
1.5
1.0
0.5
0.0
SFM
IgG
dsDNA IgG Ab
SMAD2 Expression
Relative gene expression (GAPDH)
4
3
2
1
0
*
SFM
IgG
dsDNA IgG Ab

D

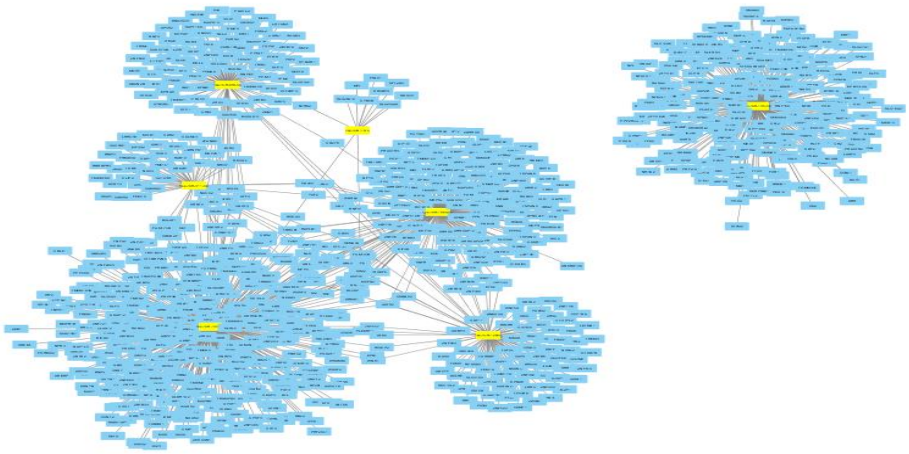

Figure 14 Transcriptomics analysis of anti-dsDNA IgG antibodies stimulated HMC in the early response (3 hours)

A. (Left) Heat-map show correlation of significant different mRNA expression in anti-dsDNA IgG antibodies and non-specific IgG controls. Green represent up-regulation and red represent down-regulation. (Right) Bar graph show the functional annotation clustering and enrichment score with p-value by DAVID analysis (https://david.ncifcrf.gov/tools.jsp). **B.** The KEGG-pathways from up-regulated or down-regulated genes during anti-dsDNA IgG antibodies stimulation compared to non-specific IgG controls. Data represent three biological replicates. Multiple corrections were done by FDR correction. P-value which is less than 0.05 was considered as significantly change. **C.** Real-time PCR validation from cDNA microarray. The graphs represent relative gene expression compared to house-keeping gene (GAPDH). Fold-change were calculated using methods explained in the part of *material and method.* **D.** Network analysis between high abundance miRNA and their mRNA predicted targets using ingenuity pathway analysis. For up-regulated miRNAs, there are including miR-1260b, miR-130a, miR-151b, miR-199b, miR-411 and miR-654. For down-regulated miRNA, there is only miR-145. The graph was plot using Cytoscape version 3.4.0 (http://www.cytoscape.org/).

Study the functional role of miR-10a by transciently knock down miR-10a or over expressed miR-10a in the HMCs.

As previous showed that miR-10a were specifically down-regulated in anti-dsDNA IgG antibodies activated HMCs, the miR-10a targets from mRNA profiling were obtained from previous integrated data (table 13). Functional annotation and clustering of those 81 predicted target genes highlighted the WNT-signalling pathways as a major target pathway for miR-10a after anti-dsDNA IgG antibodies activation. Since previous reports showed that the WNT signalling pathways usually associated with cell proliferation and differentiation (25) and HMCs expansion is major characteristic in lupus nephritis histology, down-regulated miR-10a might be a potential candidate miRNA which regulate HMCs proliferation. To examine functional role of miR-10a, the miR-10a inhibitor and miR-10a mimic were transfected into HMCs to knock down miRNA and over-express miRNA expression, respectively. Cell proliferation were determined by MTS assay at 24, 48 and 72 hours. The transfection efficiency was highly effective after 24-hour transfection and continue decrease after time (figure 15A). Interestingly, the miR-10a knock-down could slightly increase HMCs cell proliferation when compared to scramble controls, meanwhile over expression could result in the reduction of cells proliferation.

To identify a mechanism which miR-10a control cells proliferation, miR-10a target genes including known validated target genes and some predicted target genes were selected. The target genes were detected in both miR-10a knock down and miR-10a over-expression in HMCs from 24 to 48 hours. For known validated targets genes, we selected *HOXA1* (26), *KLF4* (27) and *MAP3K7* (28) to ensure our transfection systems. Surprisingly, the *HOXA1* was gradually up-regulated at 24 hours and highly up-regulated at 48 hours after miR-10a inhibitor were transfected, while the *KLF4* and *MAP3K7* were significantly up-regulated at 30 hours after miR-10a inhibitor transfection. In contrast, the miR-10 over-expression could down-regulated *HOXA1* expression with similar pattern as miR-10a knock down, whereas *KLF4* and *MAP3K7* were down-regulated at 24-hour after transfection (figure 15). Noticeably, time-point could affect microRNA function as well as different target genes might result in the different magnitude of responding. For predicted target, potential target genes with their relative function to drive cells proliferation or apoptosis were examined (table 14).

There were including *CREB1, NFAT5, MAP4K4, PIK3CA*, and *SMAD2*. These genes were bearing the miR-10a binding region at their UTR according to the bioinformatics prediction. From results, it showed that only *NFAT5* were up-regulated in miR-10a knock down at 24 hours, but *CREB1, MAP4K4, PIK3CA* and *SMAD2* were not significantly changed. In contrast, miR-10a mimic transfection led to the down-regulation of *NFAT5*, however, it was not statistical significance. Moreover, the miR-10a over-expression resulted in the significant down-regulation of *CREB1*, *MAP4K4* and *PIK3CA* at 24-hour, while only SMAD2 were significantly down-regulated at 48 hour (figure 16). Since *NFAT5* (nuclear factor of activated T cells), a well-known osmo-protective transcription factor, has been reported to control several pro-inflammatory cytokines such as IL-6, IL-1β and TNF-α expression in the isotonic condition (29). We hypothesized that miR-10a might indirectly regulate pro-inflammatory cytokines expression. The proinflammatory cytokine expression were determined in the same system. It showed that the miR-10a knock down for 30-hour promoted the TNF-α expression significantly. On the other hand, it did not up-regulate IL-6 and IL-1β expression (figure 16). Since IL-6 was marked as stimulation marker in the early experiment, it was unexpected that miR-10a could not up-regulate IL-6 expression. This might be because anti-dsDNA IgG antibodies might affect other miRNA which is responsible to control IL-6 expression, but it was not miR-10a. However, it is found that miR-10a mimic transfection resulted in the down-regulation of IL-6 expression at 48 hours.

From the discrepancy results between miRNA inhibitor transfection and mimic transfection, this can be suggested that the miRNA over-expression showed enhanced effects more than the miRNA knock down. Interestingly, previous experiments showed that miR-10a knock out mice did not result in any abnormality (97). However, the administration of carcinogen could stimulate the cancer development in female miR-10a knock-out mice which involved in WNT-signalling pathways. In addition, the inhibition of miR-10a might resulted in up-regulation of other miRNA which involved in the same pathways while miR-10a over expression might be more efficient way to directly determine the effects of miR-10a in our system. However, from our results, it therefore concluded that miR-10a might directly control *NFAT5* which associated with *TNF-α* expression. The up-regulation of *NFAT5* might be important in HMCs

proliferation in miR-10a knock down HMCs. The CREB1, PIK3CA, MAP4K4 and SMAD2 might need more concise experiment to identify as miR-10a target genes.

Table 13 The list of upregulated transcripts in anti-dsDNA IgG antibodies stimulation which contain miR-10a binding site at their 3' untranslated regions predicted by ingenuity pathway analysis (IPA) with high confidence

ID	RefSeq_mRNA	Gene Name
AAK1	NM_014911	AP2 associated kinase 1
ABCC3	NM_001144070	ATP-binding cassette, sub-family C (CFTR/MRP), member 3
BCL6	NM_001706	B-cell CLL/lymphoma 6
DPF2	NM_006268	D4, zinc and double PHD fingers family 2
E2F3	NM_001949	E2F transcription factor 3
EFHC1	NM_018100	EF-hand domain (C-terminal) containing 1
EPHA10	NM_173641	EPH receptor A10
EPHA2	NM_004431	EPH receptor A2
EDEM1	NM_014674	ER degradation enhancer, mannosidase alpha-like 1
FBXO22	NM_147188	FBXO22 opposite strand (non-protein coding); F-box protein 22
INO80D	NM_017759	INO80 complex subunit D
LYSMD3	NM_198273	LysM, putative peptidoglycan-binding, domain containing 3
NEK6	NM_001145001	NIMA (never in mitosis gene a)-related kinase 6
RB1CC1	NM_014781	RB1-inducible coiled-coil 1
RBMS3	NM_001003793	RNA binding motif, single stranded interacting protein
SIX4	NM_017420	SIX homeobox 4
SMAD2	NM_005901	SMAD family member 2
SMURF1	NM_181349	SMAD specific E3 ubiquitin protein ligase 1
STARD13	NM_178006	StAR-related lipid transfer (START) domain containing 13
TIAM1	NM_003253	T-cell lymphoma invasion and metastasis 1
WNK3	NM_001002838	WNK lysine deficient protein kinase 3
ANK3	NM_020987	ankyrin 3, node of Ranvier (ankyrin G)
ANKFY1	NM_016376	ankyrin repeat and FYVE domain containing 1
ANXA7	NM_001156	annexin A7
ARRDC3	NM_020801	arrestin domain containing 3
BCR	NM_004327	breakpoint cluster region
BAZ2B	NM_013450	bromodomain adjacent to zinc finger domain, 2B
CREB1	NM_004379	cAMP responsive element binding protein 1

ID	RefSeq_mRNA	Gene Name
CREBL2	NM_001310	cAMP responsive element binding protein-like 2
CAMK2G	NM_001222	calcium/calmodulin-dependent protein kinase II gamma
CASK	NM_003688	calcium/calmodulin-dependent serine protein kinase (MAGUK family)
CEP350	NM_014810	centrosomal protein 350kDa
DOCK11	NM_144658	dedicator of cytokinesis 11
DVL3	NM_004423	dishevelled, dsh homolog 3 (Drosophila)
FLRT2	NM_013231	fibronectin leucine rich transmembrane protein 2
FXR2	NM_004860	fragile X mental retardation, autosomal homolog 2
GLS	NM_014905	Glutaminase
IGDCC4	NM_020962	immunoglobulin superfamily, DCC subclass, member 4
IPO8	NM_006390	importin 8
ITPKC	NM_025194	inositol 1,4,5-trisphosphate 3-kinase C
IFFO2	NM_001136265	intermediate filament family orphan 2
JARID2	NM_004973	jumonji, AT rich interactive domain 2
L3MBTL3	NM_001007102	l(3)mbt-like 3 (Drosophila)
LPHN1	NM_014921	latrophilin 1
LRRFIP1	NM_001137550	leucine rich repeat (in FLII) interacting protein 1
LCOR	NM_001170765	ligand dependent nuclear receptor corepressor
MED1	NM_004774	mediator complex subunit 1
MTF2	NM_007358	metal response element binding transcription factor 2
MAPKBP1	NM_014994	mitogen-activated protein kinase binding protein 1
MAP4K4	NM_145687	mitogen-activated protein kinase kinase kinase kinase 4
MTMR3	NM_021090	myotubularin related protein 3
NONO	NM_007363	non-POU domain containing, octamer-binding
NFIX	NM_002501	nuclear factor I/X (CCAAT-binding transcription factor)
NFAT5	NM_006599	nuclear factor of activated T-cells 5, tonicity-responsive
NCOR2	NM_006312	nuclear receptor co-repressor 2
NCOA6	NM_001318240	nuclear receptor coactivator 6
NR2C2	NM_001291694	nuclear receptor subfamily 2, group C, member 2
NUP50	NM_007172	nucleoporin 50kDa
NACC1	NM_052876	nucleus accumbens associated 1, BEN and BTB (POZ) domain containing
PISD	NM_178022	phosphatidylserine decarboxylase
PDE4A	NM_001243121	phosphodiesterase 4A, cAMP-specific (phosphodiesterase E2 dunce homolog, Drosophila)
PIK3CA	NM_006218	phosphoinositide-3-kinase, catalytic, alpha polypeptide
PCBD2	NM_032151	pterin-4 alpha-carbinolamine dehydratase/dimerization cofactor of hepatocyte nuclear factor 1 alpha (TCF1) 2
PURB	NM_033224	purine-rich element binding protein B
RPRD1A	NM_001303412	regulation of nuclear pre-mRNA domain containing 1A

ID	RefSeq_mRNA	Gene Name
RTN4R	NM_023004	reticulon 4 receptor
SCARB2	NM_005506	scavenger receptor class B, member 2
SERPINE1	NM_000602	serpin peptidase inhibitor, clade E (nexin, plasminogen activator inhibitor type 1), member 1
SLC41A2	NM_032148	solute carrier family 41, member 2
SNX29	NM_032167	sorting nexin 29
SNX4	NM_003794	sorting nexin 4
SPAG9	NM_001130528	sperm associated antigen 9
STRN	NM_003162	striatin, calmodulin binding protein
SDC1	NM_002997	syndecan 1
TMEM132B	NM_052907	transmembrane protein 132B; hypothetical LOC121296
TMEM183A	NM_138391	transmembrane protein 183A
TMEM183B	NM_052907	transmembrane protein 183B
UBE2I	NM_194260	ubiquitin-conjugating enzyme E2I (UBC9 homolog, yeast)
WAPAL	NM_015045	wings apart-like homolog (Drosophila)
ZNF608	NM_020747	zinc finger protein 608

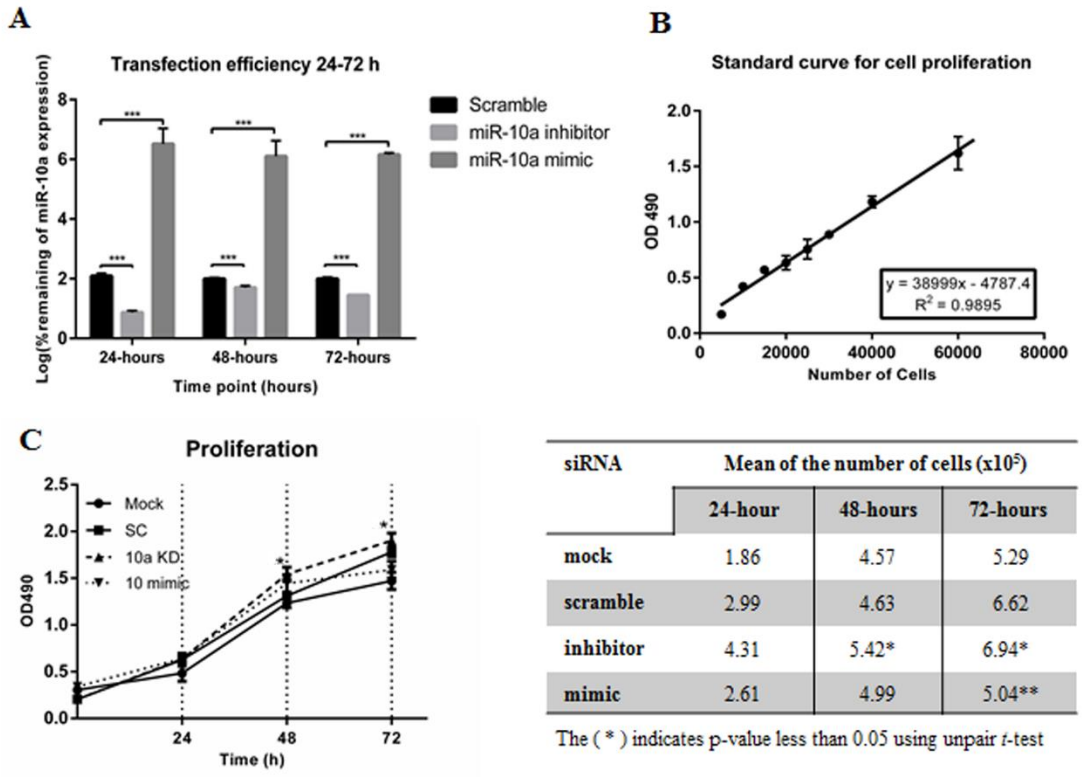

siRNA	Mean of the number of cells (x10^5)		
	24-hour	48-hours	72-hours
mock	1.86	4.57	5.29
scramble	2.99	4.63	6.62
inhibitor	4.31	5.42*	6.94*
mimic	2.61	4.99	5.04**

The (*) indicates p-value less than 0.05 using unpair *t*-test

Figure 15 Transfection efficiency of miR-10a inhibitor and miR-10a mimic transfection and proliferation assay using MTS

A. Transfection efficiency after miR-10a inhibitor and miR-10a mimic transfection for 24, 48 and 72 hours. **B.** Standard curve to determine cell density depending on the absorbance of by-product from MTS for 4 hours (OD 490). **C.** The cell proliferation assay was determined as time dependent manner 0, 24, 48 and 72 hours after transfection. One-way ANOVA were applied to compare the absorbance at different time-point. The (*) or (**) denote significantly different from non-specific IgG controls (p-value < 0.05) or (p < 0.001), respectively.

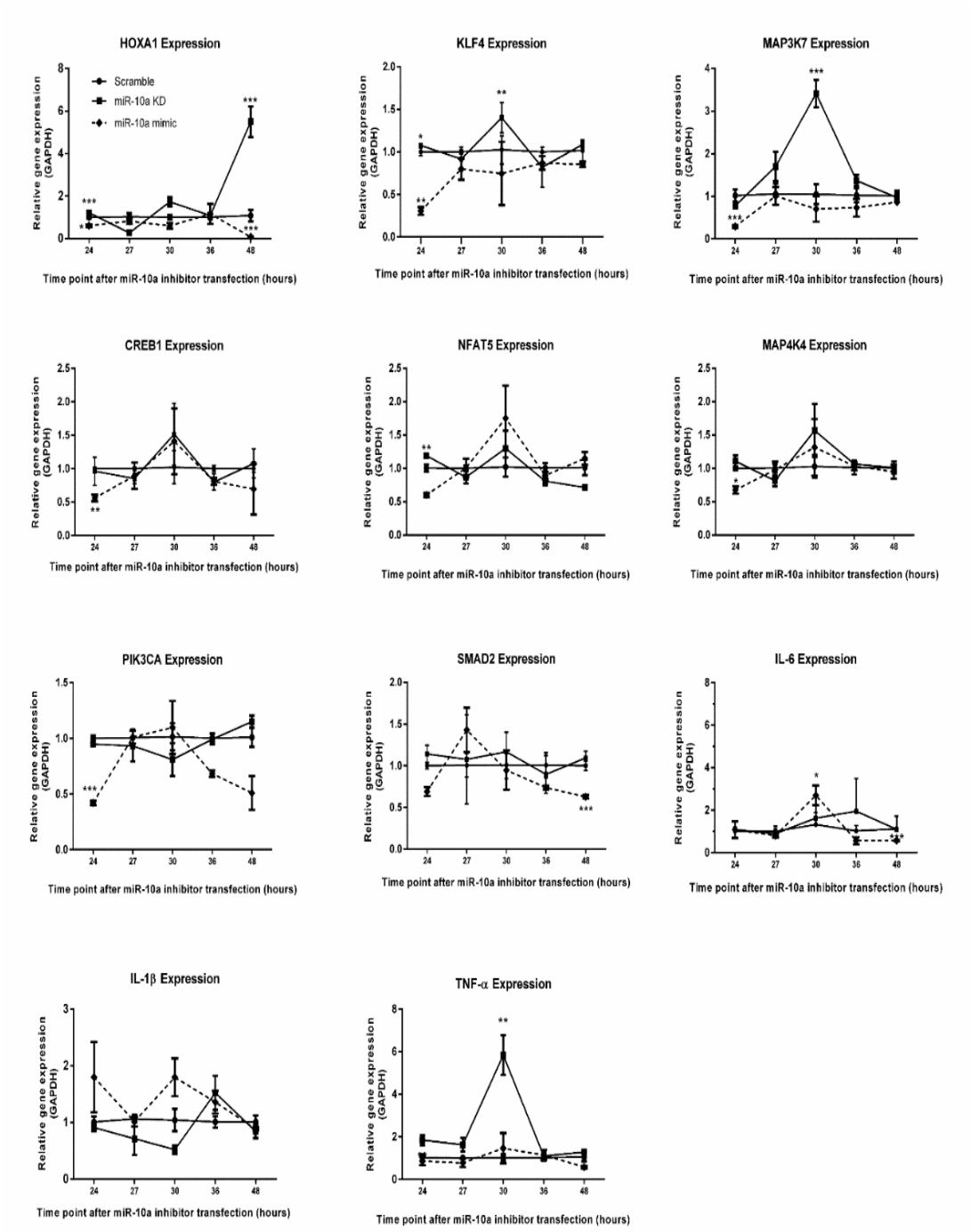

Figure 16 The qPCR results of known validated and predicted miR-10a target genes with related pro-inflammatory cytokine genes from 24 to 48 hour after miR-10a inhibitor and miR-10a mimic transfection

The HMC ($2x10^5$) were culture in serum and antibiotics deficiency medium overnight. The miR-10a inhibitor and miR-10a mimic were transfected into HMC using

Lipofectamine RNAiMAX with recommended protocol. The cells were initially collected at 24, 27, 30, 36 and 48 hours after transfection. The fold change was compared in the group within the same time point. Data shown is the mean ± S.E.M of a minimum of 3 biological replicates. The (*), (**), (***) denotes significantly different from scramble controls (p-value < 0.05), (p-value < 0.01) and (p-value < 0.001), respectively.

Table 14 Predicted target genes and its related function from literature reviews

Gene Symbols	Full name	Function	References
CREB1	Cyclic AMP-responsive element-binding protein 1	Up-regulation of this gene were characterized as an oncogenic transcription factor in renal cell carcinoma	(98)
NFAT5	nuclear factor of activated T-cells 5	Up-regulation of this gene in peritoneal dialysis patients is associated with NF-κB induction, potentially resulting in the recruitment of macrophages	(99)
PIK3CA	phosphatidylinositol-4,5-bisphosphate 3-kinase catalytic subunit alpha	Up-regulation of this gene could induce cell proliferation and considered as oncogenic genes in several cancers	(100)
MAP4K4	mitogen-activated protein kinase kinase kinase kinase 4	Up-regulation of this gene was associated with tumor cell survival	(101)
SMAD2	SMAD family member 2	Up-regulation of this gene enhanced TRAIL-induced apoptosis in activated hepatic stellate cells, which facilitate the resolution of hepatitis fibrosis	(102)

Transcriptomics profiling of miR-10a knock down showed that interleukin-8 were direct target of miR-10a

As it is interesting to examine how miR-10a knock down would affects transcriptomics profiling in HMCs, the total RNA extracted from HMCs were applied for microarray. The differential gene expression analysis revealed 1264 genes altered after miR-10a inhibitor transfection (raw p-value < 0.05), it should be noted that the p-value correction could not yield any significantly alter gene expression. This suggested that transiently miR-10a knock down might have little effects on gene expression. However, among 1264 genes, it was showed that interleukin-8 (IL-8) and matrix metalloproteinase protein 10 (MMP-10) were up-regulated more than 1.5-fold (figure 17A). Using bioinformatics prediction, analysis showed that 3'UTR of IL-8 also contained miR-10a conserved seed regions (mfe = -23.1, mirSVR score = -0.1843, PhastCons score = 0.6004, figure 17B). Although there was no conserved complementary region found in *MMP10* 3'UTR, the low confidences binding region of miR-10a could be detected in *MMP10* 3'UTR. Next, the *IL8* and *MMP10* were chosen for further validation using Real-Time PCR. The results confirmed that only *IL8* were up-regulated significantly in miR-10a KD HMC, while *MMP10* were slightly up-regulated but not statistically significant. In contrast, miR-10a over-expression led to significantly down-regulated of *IL8* after 48 hours (figure 17C). In consistent, the results showed that miR-10a mimic transfection downregulated hIL-8 secretion significantly at 48 and 72 hours, by the way, miR-10a inhibitor transfection was not affected hIL-8 production in HMCs. It is because the less efficiency of siRNA which was responsible for miR-10a inhibition. Confirmation experiments with potential miR-10a inhibitor should be validate for further conclusion. However, according to the miR-10a mimic transfection results, this confirmed that miR-10a might be important in generating hIL-8 in HMCs (figure 18).

As previous showed that *NFAT5* and *IL8* were up-regulated in miR-10a knock down and down-regulated in miR-10a overexpression, we hypothesized that *NFAT5* and *IL8* might be a direct target of miR-10a. Reporter assay were conducted by using pmiR-Glo plasmid that inserted a sequence of 3'UTR of IL-8 or 3'UTR of *NFAT5*. These regions were predicted to contain miR-10a conserved seed region. The plasmids

were co-transfected with miR-10a mimic, miR-10a inhibitor and scramble controls compared to the pmiR-Glo plain plasmid. It was found that luciferase activity was inhibit in plasmid containing IL-8 3'UTR co-transfected with miR-10a mimic (figure 17D). In concurrent, miR-10a inhibitor co-transfected with IL-8 3'UTR increased luciferase activity when compared to plain plasmid. This suggested that IL-8 was a direct target of miR-10a. On the other hand, the luciferase assay for *NFAT5* did not show any activity reduction after miR-10a mimic transfection or supplementary activity in miR-10a inhibitor transfection (figure 17D). This suggested that *NFAT5* might not be miR-10a direct target genes. Even though luciferase assay could not be able to confirm that NFAT5 is a miR-10a target genes, previous evidences were proved that miR-10a might have an indirect effect on *NFAT5* expression. This might need further experiment to confirm using other techniques. In summary, from this result, we firstly identified IL-8 as a novel target for miR-10a which might implicate in LN pathogenesis during anti-dsDNA IgG antibodies induced kidney injury.

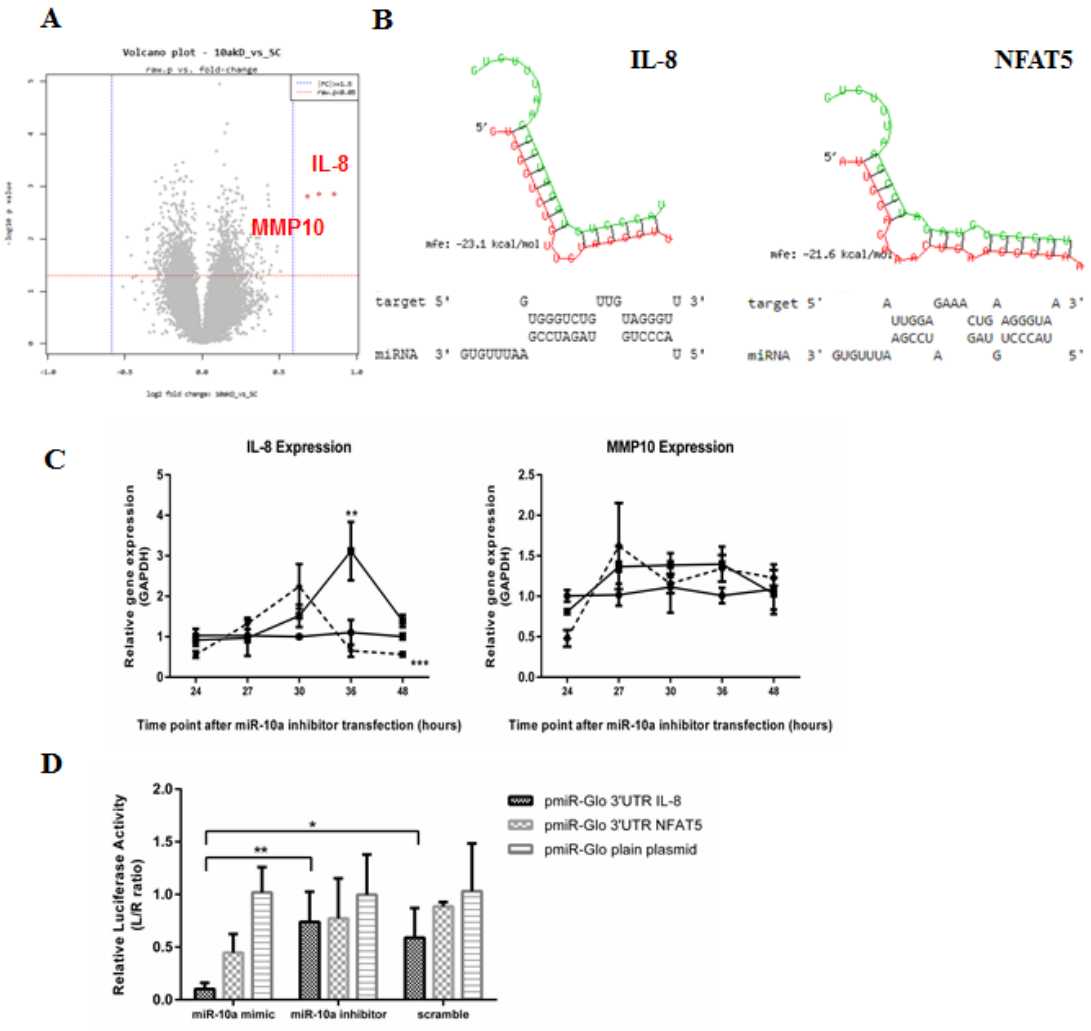

Figure 17 Transcriptomics profiling of miR-10a knock-down HMC and luciferase assay showed interleukin-8 as its direct target.

A. Volcano plot represents fold change expression and *p*-value using un-pair student's *t*-test. **B.** Bioinformatics prediction of 3'UTR binding site in IL-8 and NFAT5 and miR-10a with predictive energy of binding and probability for actual binding. **C.** The graph shows IL-8 and MMP10 expression in different time-point after miR-10a inhibitor and miR-10a mimic transfection. **D.** The graph shows luciferase activity in miR-10a mimic co-transfection with plasmid containing IL-8 3'UTR, NFAT5 3'UTR and negative controls. Data shown are mean ± S.E.M of minimum three replicated experiment. The (*), (**), (***) indicate significantly difference *p*-value < 0.05, *p*-value < 0.01 and *p*-value < 0.001 from scramble group.

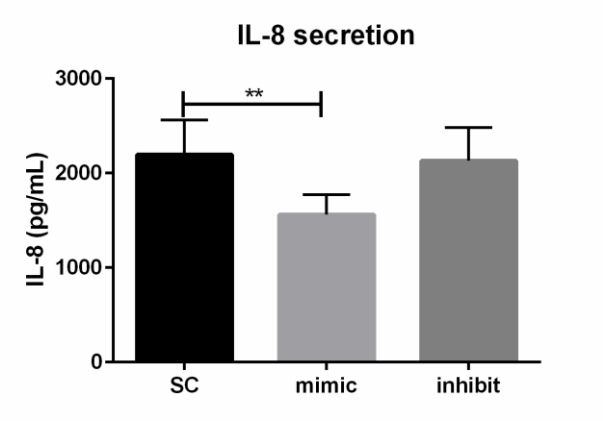

Figure 18 The interleukin-8 secretion in HMCs transfected with miR-10a mimic, miR-10a inhibitor and scramble transfection.

The graph represents results from three biological replicates and three independent experiments. (**) denotes the significant different between group using unpair student's *t*-test, p-value < 0.05.

CHAPTER V

DISCUSSION

Auto-antibodies induced inflammation with mesangial cells expansion is common feature found in LN, especially class I-IV. Here, we reported functional role of auto antibodies mediated mesangial cells microRNA inducing inflammation and cell proliferations. This might help to explain a complex pathogenesis of LN disease. Regarding to the fact that anti-dsDNA antibodies were associated with renal involvement in SLE patients (5), we used anti-dsDNA antibodies as representative autoantibodies mediated molecular reaction in the HMCs. According to the results, we confirmed that anti-dsDNA antibodies enhanced IL6 expression and could directly bind to mesangial cells membrane through their F'(ab) region. The IL6 were highly upregulated after anti-dsDNA antibodies incubate with serum, while heat inactivated serum reduced IL-6 expression. Since heat-inactivated serum destroyed heat-labile proteins (complements systems), this suggested that complement pathways are essential for IL6 induction in HMCs. The complements system is composed of various soluble proteins and is classified in the innate immune responses. It contained more than 30 proteins, presented both in the fluid phase and anchored to cell membranes. To activate complements system, there are three main mechanisms including, the classical, alternative, and lectin pathways. In SLE pathogenesis, the complements systems are strongly related with tissue damage and inflammation, however, the deficiency in early components of complements systems lead to lupus development. In this study, it is supposed that antibody recognition on HMC membrane antigens induced classical complement induction leading to complement fixation. Previous reports demonstrated that a capability of anti-dsDNA IgG antibody to fix complement could determine the nephritogenic activity of antibody (103). This could help to explain that some patients who bear anti-dsDNA antibody in their circulation did not develop lupus nephritis.

Besides IL-6 production, our transcriptome showed that anti-dsDNA IgG antibodies stimulation up-regulated number of genes in cell cycles, WNT-signalling, JAK-STAT signalling, mTOR signalling, p53 signalling and SLE-related genes (*IL8, IL1*). Functional annotation clustering showed that most of elevated genes are involved in cells cycle. Thus, this suggested that anti-dsDNA IgG antibody induction directly

affects cells cycle in HMCs in the early response which might be a consequence from p53 signalling, mTOR and WNT-signalling pathway. In addition, interferon type I signalling which is a well-known pathway found to be up-regulated in SLE patients are upregulated during anti-dsDNA IgG treatment. Accordingly, antibody mediated resident kidney cells could partially amplify inflammatory cascase within kidney. It also confirmed that our *in vitro* model can at least be used to explain the LN pathogenesis in term of auto antibody induction.

For miRNA profiling, we identified number of dysregulated miRNAs in anti-dsDNA IgG antibody induction. These are including miR-181a, miR-125b*, miR-127, miR-411 and miR-10a. However, in the validation step, miR-181a, miR-411, miR-125b* were not significantly altered upon antibody stimulation while miR-127 had increased trend without statistical significant. The miR-146a and miR-411 expression were down-regulated in both IgG and anti-dsDNA IgG Abs stimulation. This might be a non-specific reaction of the cell to stimuli, possibly through Fcγ receptor. The miR-146a was selected as it was previously well characterized in various organ or cells and it was involved in type I IFN signalling pathway. The downregulation of miR-146a was found commonly in SLE patients. Although previous experiment demonstrated that miR-146a was upregulated in glomerular and urine of SLE patients, it was due to the accumulation of lymphocytes within the kidney (104). The miR-146a were associated with several autoimmune disease especially SLE (24). Specific miR-146a knockout mice resulted in autoimmune development with anti-dsDNA antibody production (37). Based on our result, we could hypothesize that non-specific antibody stimulation to HMC could result in downregulation of miR-146a and it might partly result in the stimulation of interferon secretion. Similarly, the miR-411 were downregulated in anti-dsDNA IgG antibody stimulation. The miR-411 was reported to control cell proliferation (93, 105). cell proliferation in HMC. Nevertheless, the validation experiments are needed to elucidate the mechanism of HMC responded to these nonspecific IgG.

Several disturb miRNAs were identified in LN kidney biopsy, urine and serum samples (75, 88, 106). In LN kidney biopsy, the study revealed that miR-26 and miR-30 regulated gene in the type I IFN signalling pathways (25). Study of aberrant miRNA in lupus-prone mice during active stages demonstrated that the let-7a up-regulation in

mesangial cells mediated IL-6 up-regulation (26). While combined IFN-γ and TNF-α stimulation on HMCs induces miR-155 expression through TAB2 and NF-κB. For miRNAs related to fibrosis, study identified miR-150 could promote renal fibrosis by increasing profibrotic molecules through downregulation of SOCS1. The miR-192 was increased in fibrotic kidney and found to regulate ZEB1 and ZEB2 which enhance expression in TGF-β expression (107). For miRNAs related to cell proliferation, previous reports showed that the miR17-92 are involved in enlarge kidney glomeruli, mesangial cells expansion and hyper cellularity and proteinuria (108). The miR-21 was found to regulate mesangial cells proliferation (109). Comparing between previous reports and our miRNA screening results, only a few of miRNA showed similar pattern of miRNA expression. This might be due to the limitation of using only 1 pool sample per group. Moreover, the expression on miRNA in patient's samples were demonstrate a various type of cell miRNA disturbance, while our model is specific miRNA expression in HMCs which stimulated with auto antibody. Although most of the miRNA are not change resembling previous result, some of them showed similar trend of expression. These were including miR-145, miR-30a, miR-20a/b, miR-221, miR-302d, miR-200c. These miRNAs were reported as a biomarker for LN to recognize kidney injuries, cell proliferation and apoptosis pathways (110). For example, the miR-200c were found significantly down-regulated in urine and its expression was correlated with glomerular filtration rate in SLE patients. We notice that the miRNA expression are highly specific, as different classes of LN revealed different pattern of miRNA expression (72). Furthermore, previous reports observed a different pattern of miRNA expression after repeat biopsy in LN patients (77). Since a variety of miRNA expression occur in clinical samples, it might be useful to investigate miRNA expression in specific with specific stimuli. This might help to explain the role of miRNA in the cells.

Regarding to our results, the miR-10a was specifically down-regulated in HMCs stimulated with anti-dsDNA IgG Ab. The miR-10 family was co-evolution with the *Hox* clusters which is a conserved transcription factors correcting anterior-posterior patterning of bilaterian animals (111). In human, the miR-10 family consists of miR-10a and miR-10b, which are encoded upstream of *HOXB4* and *HOXD4* respectively. They found other miRNA which are encoded in the *Hox* clusters including miR-99a/b,

miR-100 and miR-125 (112). Because the same sequence at seed region between miR-10a and miR-10b, they have the overlapping target genes. Deregulation of miR-10 was found in several cancers, and it is important in cell transformation and control cell cycles (113-119). Additionally, study in pig endothelial cells showed upregulation of *MAP3K7* and *βTRC* as a direct target for miR-10a (120). This initially demonstrated the impact of miR-10a during inflammatory process. Down-regulated miR-10a in dendritic cells isolated from inflammatory bowel disease mice led to *IL-12/IL-23p40* upregulation, which determined as miR-10a target gene (121). Although the expression of miR-10a was not specific in kidney cells, the expression of miR-10a was predominately expressed in kidney from both mouse and human (122). Down-regulation of miR-10a was determined as kidney injuries marker in ischemic-reperfusion mouse model (95, 123). From our results, we found that miR-10a was downregulated in kidney biopsy from excessive mesangial cell proliferation LN histology types (class IV). Their expression was correlated with proteinuria, which is the classic biomarker of kidney functional abnormality. This indicated that miR-10a downregulation in HMCs might reflect in proteinuria in LN patients. In consistent, repeated administration of anti-dsDNA IgG antibody in mouse induced proteinuria and organ damage (55). On the other hand, treating with IgM anti-dsDNA could eliminate the pathologic in the (NZB X NZW) F_1 lupus-prone mice. Lower glomerular immune complexes deposition is associated with a reduced inflammatory response and impaired organ damage. The reduced frequency of GN in SLE patients who have IgM anti-dsDNA antibodies may therefore reflect a disease-modifying effect of this class of autoantibodies that has potential therapeutic implications. The accumulating evidences are saying that miR-10a might be important in LN-pathogenesis.

To characterize miR-10a target, the miR-10a inhibitor and miR-10a mimic were transfected into HMCs. We could confirmed that our transfection systems were working properly by amplified previous characterized miR-10a target genes including *HOXA1* (124), *KLF4* (97) and *MAP3K7* (120). These genes were important in cell proliferation, differentiation, and pro-inflammatory cytokine production. Differentially expressed of these genes might display a dispensable of miR-10a expression in term of cell division and cytokine secretion. In concurrent, we were trying to identify novel miR-10a target genes in HMCs. Referring to integrative analysis, we sorted potential

candidate and verified its expression in our transfection systems. Unexpectedly, we could not detect a huge different between miR-10a inhibitor transfection compared to scramble control, whereas miR-10a mimic transfection impact most of target genes including *CREB1, PIK3CA, MAP4K4, SMAD2* and *IL6.* In our opinion, the discrepancy results between miR-10a inhibitor and miR-10a mimic transfection were a consequence from redundancy of miRNA function. As the miRNAs could affects several genes at the same time, thus, miRNA knockdown might not be able to upregulate several target genes. In contrast, miR-10a overexpression downregulate several gene expression since those genes contain miR-10a binding region.

In miR-10a inhibitor transfection, *NFAT5* was the only gene which slightly upregulated. The *NFAT5* has been reported to control IL-6, IL-1 beta and TNF-alpha expression in isotonic condition (125). Additionally, IL6 was our stimulation marker as we mention above. We therefore study the pro-inflammatory cytokine production in this system. Surprisingly, the result showed that *TNF-α* was up-regulated significantly in miR-10a knock-down HMCs but had no effect on *IL-6* and *IL-1β* expression (data not shown). Since anti-dsDNA antibodies stimulated HMC resulted in increased IL-6 expression, however, miR-10a knockdown did not show IL-6 up-regulation. We hypothesized that miR-10a might not be the important regulator for IL-6 expression. Other miRNAs might be responsible for directing control IL-6 expression. Recent evidence in rheumatoid arthritis reported that TNF-α and IL-1β stimulation to fibroblast-like synoviocytes (FLSs) resulted in miR-10a downregulation through NF-κB dependent manner inducing YY1 transcription factor (126). It is also possible that miR-10a could be further down-regulated by these pro-inflammatory cytokines; however, we did not investigate this point in our study.

Surprisingly, transient knockdown miR-10a in HMC showed only two genes which up-regulated more than 1.5-fold. These results were similarly with previous reports in mouse model (97). The miR-10a knockout mice did not show any abnormality in cell development or increase the expression of HOXB4 which located downstream from miR-10a and has been purposed as miR-10a target genes. Nevertheless, oncogenic injury induction in miR-10a knockout mice promote intestinal tumorigenesis in female adenomatous polyposis coli knock out mice. In agreement, there was no significant enrichment of expression of miR-21 target genes in the miR-

21 knockout mice, while unilateral ureteral obstruction induced a set of miR-21 target genes after 7 days (127). From these result, we suggested that specific inductions are necessary to investigate miRNA target genes. Nonetheless, human aortic endothelial cell lines transfected with miR-10a inhibitor for 48 hours was found several genes differentially changed. This might due to different cell types with different transfection method. In our opinion, since miRNA is transiently expressed under a specific condition, it is, therefore, important to investigate miRNA target genes under stimulated condition. There is various technique to confirm miRNA target genes. For instant, protein detection could help to investigate miRNA target as well as AGO-protein immunoprecipitation incorporated with small RNA sequencing.

We identified *IL8* as a novel target of miR-10a using transcriptomic profiling of transient miR-10a inhibitor transfection. This is consistent with cDNA microarray results in which *IL8* was upregulated in anti-dsDNA IgG antibodies stimulation. This draw our attention to IL-8 which was previously characterized in urine from LN patients, however, it was not correlated with disease activity (128). Previously, the miR-10a down-regulation showed indirectly control IL-8 expression through MAP3K7 and βTCR. Here, we found that promoted MAP3K7 expression was found in miR-10a knockdown mesangial cells. Regarding to evidences, we therefore concluded that miR-10a might be a key controller for *IL8* expression and production via direct and indirect mechanisms.

The IL-8 polymorphism was associated with severe LN in African American (129). However, the report in Asian ethic found that IL8 polymorphism were not correlated with LN development. The contradiction might be because of the samples size and disease stages. However, study of LN kidney biopsy found increase amount of IL-8 in LN compared to healthy controls as well as increase of IL-8 in urine from LN patients (130). As IL-8 is known as phagocytic cell recruiting factor, it is possible that IL8 might be important during early phase of auto antibodies mediated LN development. Moreover, the IL8 could enhance adhesion molecule expression in neighbouring cells such as endothelial cells and glomerular basement membrane (131). Accordingly, up-regulation of IL-8 in HMC could attracted phagocytic cells into inflammatory site. Neutrophils, a major component of phagocytic cells in circulation, were a sources of renal endogenous nucleosome-induced immune complexes formation

(132, 133), The neutrophil undergoes “NETosis” cell death programming, which enhances chromatin accumulation in glomerulus (134, 135). Obviously, *in vivo* experiment confirmed that neutrophils producing IL-8 autocrine are essential for immune complexes deposition inducing inflammation (136). However, in our experimental model was an *in vitro* system, it is necessary to confirm the results in the spontaneous developed LN mice.

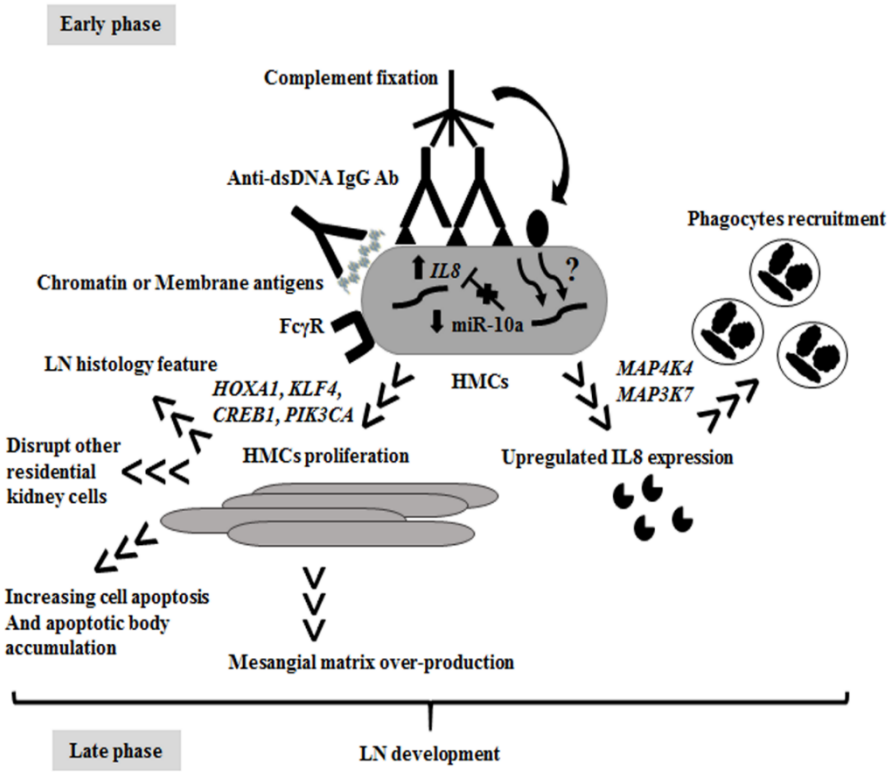

Figure 19 Putative mechanism of auto antibody mediated human mesangial cell induced inflammation and aberrant miRNA downstream regulation.

In the early phase, auto antibodies (Ab) attach to chromatin structure or membrane antigens on human mesangial cell (HMC) membranes inducing complement fixation. miR-10a is downregulated and enhances cell proliferation or apoptosis through *HOXA1, KLF4, CREB1* and *PIK3CA*. *IL8* or *CXCL8* are putative direct targets of miR-10a. The IL-8 attracts phagocytes into the kidney. HMCs interact with endothelial cells and the glomerular basement membrane, and abnormal functions of HMCs might disturb other

resident kidney cell functions. The increase in HMC number might increase mesangial matrixes resulting in chromatin or apoptotic body accumulation. In summary, these processes might drive the progression of lupus nephritis (LN) disease and provide insights into LN pathogenesis.

Since HMCs are specific cell found in kidney, the advantage of this study is abnormal miRNA expression in HMCs might be able to represent LN disease stage or pathology. This could further determine as biomarker to evaluate the LN prognosis and diagnosis. Besides, the previous studies in HMC were mainly focus in the late phase response of inflammation especially in extracellular matrix production and kidney fibrosis (77, 127, 137, 138). Our study is a first report of miRNA profile that control acute inflammation responses in HMC stimulated with auto antibody. In conclusion, our experiments confirmed the pathogenic effect of anti-dsDNA IgG antibodies on HMCs. This lead to deregulation of miRNA system, which subsequently interrupt gene expression related to abnormal cellular phenotype. The antibody recognizes HMCs membrane antigens and mediated complement fixation. The miR-10a was found to be downregulated in auto anti-dsDNA IgG antibodies stimulation induced IL-8 expression that determined as miR-10a novel target genes. The IL8 increasing shed some light to focus on innate immune systems which might important during early auto antibody mediate inflammation in autoimmune disease (figure 19).

REFERENCES

1. Weening JJ. The Classification of Glomerulonephritis in Systemic Lupus Erythematosus Revisited. Journal of the American Society of Nephrology. 2004;15(2):241-50.
2. Chan TM. Treatment of severe lupus nephritis: the new horizon. Nat Rev Nephrol. 2015;11(1):46-61.
3. Hahn BH. Antibodies to DNA. N Engl J Med. 1998;338(19):1359-68.
4. Olson SW, Lee JJ, Prince LK, Baker TP, Papadopoulos P, Edison J, et al. Elevated subclinical double-stranded DNA antibodies and future proliferative lupus nephritis. Clin J Am Soc Nephrol. 2013;8(10):1702-8.
5. Conti F, Ceccarelli F, Perricone C, Massaro L, Marocchi E, Miranda F, et al. Systemic Lupus Erythematosus with and without Anti-dsDNA Antibodies: Analysis from a Large Monocentric Cohort. Mediators Inflamm. 2015;2015:328078.
6. Yung S, Chan TM. Anti-DNA antibodies in the pathogenesis of lupus nephritis — The emerging mechanisms. Autoimmunity Reviews. 2008;7(4):317-21.
7. Lech M, Anders HJ. The pathogenesis of lupus nephritis. J Am Soc Nephrol. 2013;24(9):1357-66.
8. Couser WG, Salant DJ. In situ immune complex formation and glomerular injury. Kidney Int. 1980;17(1):1-13.
9. Fenton KA, Tommeras B, Marion TN, Rekvig OP. Pure anti-dsDNA mAbs need chromatin structures to promote glomerular mesangial deposits in BALB/c mice. Autoimmunity. 2010;43(2):179-88.
10. Deocharan B, Qing X, Lichauco J, Putterman C. Alpha-actinin is a cross-reactive renal target for pathogenic anti-DNA antibodies. J Immunol. 2002;168(6):3072-8.
11. Du H, Chen M, Zhang Y, Zhao M-h, Wang H-Y. Cross-reaction of anti-DNA autoantibodies with membrane proteins of human glomerular mesangial cells in sera from patients with lupus nephritis. Clinical and Experimental Immunology. 2006;145(1):21-7.
12. Zhang H, Zhao C, Wang S, Huang Y, Wang H, Zhao J, et al. Anti-dsDNA antibodies induce inflammation via endoplasmic reticulum stress in human mesangial cells. J Transl Med. 2015;13:178.
13. Kurihara H, Sakai T. Cell biology of mesangial cells: the third cell that maintains the glomerular capillary. Anatomical science international. 2016.
14. Davies M. The mesangial cell: a tissue culture view. Kidney Int. 1994;45(2):320-7.
15. Schlondorff D, Banas B. The mesangial cell revisited: no cell is an island. J Am Soc Nephrol. 2009;20(6):1179-87.
16. Dey N, Ghosh-Choudhury N, Kasinath BS, Choudhury GG. TGFbeta-stimulated microRNA-21 utilizes PTEN to orchestrate AKT/mTORC1 signaling for mesangial cell hypertrophy and matrix expansion. PLoS One. 2012;7(8):e42316.
17. Yung S, Cheung KF, Zhang Q, Chan TM. Anti-dsDNA Antibodies Bind to Mesangial Annexin II in Lupus Nephritis. Journal of the American Society of Nephrology. 2010;21(11):1912-27.
18. Zhang Y, Yang J, Jiang S, Fang C, Xiong L, Cheng H, et al. The Lupus-derived Anti-double-stranded DNA IgG Contributes to Myofibroblast-like Phenotype in Mesangial Cells. Journal of Clinical Immunology. 2012.

19. Qing X, Zavadil J, Crosby MB, Hogarth MP, Hahn BH, Mohan C, et al. Nephritogenic anti-DNA antibodies regulate gene expression in MRL/lpr mouse glomerular mesangial cells. Arthritis Rheum. 2006;54(7):2198-210.
20. Bartel DP. MicroRNAs: genomics, biogenesis, mechanism, and function. Cell. 2004;116(2):281-97.
21. Etheridge A, Lee I, Hood L, Galas D, Wang K. Extracellular microRNA: a new source of biomarkers. Mutation research. 2011;717(1-2):85-90.
22. Janssen HL, Reesink HW, Lawitz EJ, Zeuzem S, Rodriguez-Torres M, Patel K, et al. Treatment of HCV infection by targeting microRNA. N Engl J Med. 2013;368(18):1685-94.
23. O'Connell RM, Rao DS, Baltimore D. microRNA regulation of inflammatory responses. Annu Rev Immunol. 2012;30:295-312.
24. Shen N, Liang D, Tang Y, de Vries N, Tak PP. MicroRNAs-novel regulators of systemic lupus erythematosus pathogenesis. Nat Rev Rheumatol. 2012;8(12):701-9.
25. Costa-Reis P, Russo PA, Zhang Z, Colonna L, Maurer K, Gallucci S, et al. The Role of MicroRNAs and Human Epidermal Growth Factor Receptor 2 in Proliferative Lupus Nephritis. Arthritis Rheumatol. 2015;67(9):2415-26.
26. Chafin CB, Regna NL, Dai R, Caudell DL, Reilly CM. MicroRNA-let-7a expression is increased in the mesangial cells of NZB/W mice and increases IL-6 production in vitro. Autoimmunity. 2013;46(6):351-62.
27. Costa Reis AP, Russo P, Gallucci S, Sullivan KE. A150: Control of Cell Proliferation in Lupus Nephritis: The Role of miRNAs and HER2. Arthritis & Rheumatology. 2014;66:S194-S.
28. Chen K, Rajewsky N. The evolution of gene regulation by transcription factors and microRNAs. Nat Rev Genet. 2007;8(2):93-103.
29. He L, Hannon GJ. MicroRNAs: small RNAs with a big role in gene regulation. Nat Rev Genet. 2004;5(7):522-31.
30. Ma X, Liu Q. MicroRNAs in the pathogenesis of systemic lupus erythematosus. Int J Rheum Dis. 2013;16(2):115-21.
31. Eulalio A, Huntzinger E, Izaurralde E. Getting to the root of miRNA-mediated gene silencing. Cell. 2008;132(1):9-14.
32. Lindsay MA. microRNAs and the immune response. Trends Immunol. 2008;29(7):343-51.
33. Kato M, Park JT, Natarajan R. MicroRNAs and the glomerulus. Exp Cell Res. 2012;318(9):993-1000.
34. Bartel DP. MicroRNAs: target recognition and regulatory functions. Cell. 2009;136(2):215-33.
35. Ventura A, Young AG, Winslow MM, Lintault L, Meissner A, Erkeland SJ, et al. Targeted deletion reveals essential and overlapping functions of the miR-17 through 92 family of miRNA clusters. Cell. 2008;132(5):875-86.
36. Chen CZ, Li L, Lodish HF, Bartel DP. MicroRNAs modulate hematopoietic lineage differentiation. Science. 2004;303(5654):83-6.
37. Boldin MP, Taganov KD, Rao DS, Yang L, Zhao JL, Kalwani M, et al. miR-146a is a significant brake on autoimmunity, myeloproliferation, and cancer in mice. J Exp Med. 2011;208(6):1189-201.

38. Johnnidis JB, Harris MH, Wheeler RT, Stehling-Sun S, Lam MH, Kirak O, et al. Regulation of progenitor cell proliferation and granulocyte function by microRNA-223. Nature. 2008;451(7182):1125-9.
39. Zan H, Tat C, Casali P. MicroRNAs in lupus. Autoimmunity. 2014;47(4):272-85.
40. Kasitanon N, Louthrenoo W, Sukitawut W, Vichainun R. Causes of death and prognostic factors in Thai patients with systemic lupus erythematosus. Asian Pac J Allergy Immunol. 2002;20(2):85-91.
41. Saxena R, Mahajan T, Mohan C. Lupus nephritis: current update. Arthritis Res Ther. 2011;13(5):240.
42. Borchers AT, Naguwa SM, Shoenfeld Y, Gershwin ME. The geoepidemiology of systemic lupus erythematosus. Autoimmunity Reviews. 2010;9(5):A277-A87.
43. Danchenko N, Satia JA, Anthony MS. Epidemiology of systemic lupus erythematosus: a comparison of worldwide disease burden. Lupus. 2006;15(5):308-18.
44. Sprangers B, Monahan M, Appel GB. Diagnosis and treatment of lupus nephritis flares--an update. Nat Rev Nephrol. 2012;8(12):709-17.
45. Hahn BH, McMahon MA, Wilkinson A, Wallace WD, Daikh DI, Fitzgerald JD, et al. American College of Rheumatology guidelines for screening, treatment, and management of lupus nephritis. Arthritis Care Res (Hoboken). 2012;64(6):797-808.
46. Tsokos GC. Systemic lupus erythematosus. N Engl J Med. 2011;365(22):2110-21.
47. Yang W, Shen N, Ye DQ, Liu Q, Zhang Y, Qian XX, et al. Genome-wide association study in Asian populations identifies variants in ETS1 and WDFY4 associated with systemic lupus erythematosus. PLoS Genet. 2010;6(2):e1000841.
48. Zhao M, Liu S, Luo S, Wu H, Tang M, Cheng W, et al. DNA methylation and mRNA and microRNA expression of SLE CD4+ T cells correlate with disease phenotype. J Autoimmun. 2014;54:127-36.
49. Nowling TK, Gilkeson GS. Mechanisms of tissue injury in lupus nephritis. Arthritis Res Ther. 2011;13(6):250.
50. Pons-Estel GJ, Serrano R, Plasín MA, Espinosa G, Cervera R. Epidemiology and management of refractory lupus nephritis. Autoimmunity Reviews. 2011;10(11):655-63.
51. Appel GB, Contreras G, Dooley MA, Ginzler EM, Isenberg D, Jayne D, et al. Mycophenolate mofetil versus cyclophosphamide for induction treatment of lupus nephritis. J Am Soc Nephrol. 2009;20(5):1103-12.
52. Tesar V, Hruskova Z. Limitations of standard immunosuppressive treatment in ANCA-associated vasculitis and lupus nephritis. Nephron Clin Pract. 2014;128(3-4):205-15.
53. Goilav B, Putterman C. The Role of Anti-DNA Antibodies in the Development of Lupus Nephritis: A Complementary, or Alternative, Viewpoint? Semin Nephrol. 2015;35(5):439-43.
54. Rekvig OP. The anti-DNA antibody: origin and impact, dogmas and controversies. Nat Rev Rheumatol. 2015;11(9):530-40.
55. Fenton K, Fismen S, Hedberg A, Seredkina N, Fenton C, Mortensen ES, et al. Anti-dsDNA antibodies promote initiation, and acquired loss of renal Dnase1 promotes progression of lupus nephritis in autoimmune (NZBxNZW)F1 mice. PLoS One. 2009;4(12):e8474.

56. Rekvig OP. Anti-dsDNA antibodies as a classification criterion and a diagnostic marker for systemic lupus erythematosus: critical remarks. Clin Exp Immunol. 2015;179(1):5-10.
57. Couser WG. Basic and translational concepts of immune-mediated glomerular diseases. J Am Soc Nephrol. 2012;23(3):381-99.
58. Yung S, Chan TM. Autoantibodies and Resident Renal Cells in the Pathogenesis of Lupus Nephritis : Getting to Know the Unknown. Clinical and Developmental Immunology. 2012;2012:1-13.
59. Sun KH, Liu WT, Tsai CY, Tang SJ, Han SH, Yu CL. Anti-dsDNA antibodies cross-react with ribosomal P proteins expressed on the surface of glomerular mesangial cells to exert a cytostatic effect. Immunology. 1995;85(2):262-9.
60. Im SR, Im SW, Chung HY, Pravinsagar P, Jang YJ. Cell- and nuclear-penetrating anti-dsDNA autoantibodies have multiple arginines in CDR3 of VH and increase cellular level of pERK and Bcl-2 in mesangial cells. Mol Immunol. 2015;67(2 Pt B):377-87.
61. Seret G, Le Meur Y, Renaudineau Y, Youinou P. Mesangial Cell-Specific Antibodies Are Central to the Pathogenesis of Lupus Nephritis. Clinical and Developmental Immunology. 2012;2012:1-8.
62. Wilson HM, Stewart KN. Glomerular Epithelial and Mesangial Cell Culture and Characterization. 2012;806:187-201.
63. Abe T, Fleming PA, Masuya M, Minamiguchi H, Ebihara Y, Drake CJ, et al. Granulocyte/macrophage origin of glomerular mesangial cells. International journal of hematology. 2005;82(2):115-8.
64. Masuya M, Drake CJ, Fleming PA, Reilly CM, Zeng H, Hill WD, et al. Hematopoietic origin of glomerular mesangial cells. Blood. 2003;101(6):2215-8.
65. Wong CY, Tan EL, Cheong SK. In vitro differentiation of mesenchymal stem cells into mesangial cells when co-cultured with injured mesangial cells. Cell biology international. 2014;38(4):497-501.
66. Wong CY, Cheong SK, Mok PL, Leong CF. Differentiation of human mesenchymal stem cells into mesangial cells in post-glomerular injury murine model. Pathology. 2008;40(1):52-7.
67. Yung S, Chan TM. Mechanisms of Kidney Injury in Lupus Nephritis - the Role of Anti-dsDNA Antibodies. Front Immunol. 2015;6:475.
68. Tsai CY, Wu TH, Sun KH, Liao TS, Lin WM, Yu CL. Polyclonal IgG anti-dsDNA antibodies exert cytotoxic effect on cultured rat mesangial cells by binding to cell membrane and augmenting apoptosis. Scand J Rheumatol. 1993;22(4):162-71.
69. Yu CL, Sun KH, Tsai CY, Hsieh SC, Yu HS. Anti-dsDNA antibody up-regulates interleukin 6, but not cyclo-oxygenase, gene expression in glomerular mesangial cells: a marker of immune-mediated renal damage? Inflamm Res. 2001;50(1):12-8.
70. Yung S, Zhang Q, Zhang CZ, Chan KW, Lui SL, Chan TM. Anti-DNA antibody induction of protein kinase C phosphorylation and fibronectin synthesis in human and murine lupus and the effect of mycophenolic acid. Arthritis & Rheumatism. 2009;60(7):2071-82.
71. Yung S, Tsang RCW, Leung JKH, Chan TM. Increased mesangial cell hyaluronan expression in lupus nephritis is mediated by anti-DNA antibody-induced IL-1β. Kidney International. 2006;69(2):272-80.

72. Dai Y, Sui W, Lan H, Yan Q, Huang H, Huang Y. Comprehensive analysis of microRNA expression patterns in renal biopsies of lupus nephritis patients. Rheumatol Int. 2009;29(7):749-54.
73. Te JL, Dozmorov IM, Guthridge JM, Nguyen KL, Cavett JW, Kelly JA, et al. Identification of unique microRNA signature associated with lupus nephritis. PLoS One. 2010;5(5):e10344.
74. Stagakis E, Bertsias G, Verginis P, Nakou M, Hatziapostolou M, Kritikos H, et al. Identification of novel microRNA signatures linked to human lupus disease activity and pathogenesis: miR-21 regulates aberrant T cell responses through regulation of PDCD4 expression. Ann Rheum Dis. 2011;70(8):1496-506.
75. Wang G, Tam LS, Li EK, Kwan BC, Chow KM, Luk CC, et al. Serum and urinary cell-free MiR-146a and MiR-155 in patients with systemic lupus erythematosus. J Rheumatol. 2010;37(12):2516-22.
76. Hashad DI, Abdelmagid MH, Elsherif SH. microRNA146a expression in lupus patients with and without renal complications. J Clin Lab Anal. 2012;26(1):35-40.
77. Zhou H, Hasni SA, Perez P, Tandon M, Jang SI, Zheng C, et al. miR-150 promotes renal fibrosis in lupus nephritis by downregulating SOCS1. J Am Soc Nephrol. 2013;24(7):1073-87.
78. Luo X, Zhang L, Li M, Zhang W, Leng X, Zhang F, et al. The role of miR-125b in T lymphocytes in the pathogenesis of systemic lupus erythematosus. Clinical and experimental rheumatology. 2013;31(2):263-71.
79. Liu Y, Dong J, Mu R, Gao Y, Tan X, Li Y, et al. MicroRNA-30a promotes B cell hyperactivity in patients with systemic lupus erythematosus by direct interaction with Lyn. Arthritis Rheum. 2013;65(6):1603-11.
80. Chafin CB, Reilly CM. MicroRNAs implicated in the immunopathogenesis of lupus nephritis. Clin Dev Immunol. 2013;2013:430239.
81. Satoh M, Vazquez-Del Mercado M, Chan EK. Clinical interpretation of antinuclear antibody tests in systemic rheumatic diseases. Mod Rheumatol. 2009;19(3):219-28.
82. Schmittgen TD, Livak KJ. Analyzing real-time PCR data by the comparative C(T) method. Nat Protoc. 2008;3(6):1101-8.
83. Friedlander MR, Mackowiak SD, Li N, Chen W, Rajewsky N. miRDeep2 accurately identifies known and hundreds of novel microRNA genes in seven animal clades. Nucleic Acids Res. 2012;40(1):37-52.
84. Rueda A, Barturen G, Lebron R, Gomez-Martin C, Alganza A, Oliver JL, et al. sRNAtoolbox: an integrated collection of small RNA research tools. Nucleic Acids Res. 2015;43(W1):W467-73.
85. Agarwal V, Bell GW, Nam JW, Bartel DP. Predicting effective microRNA target sites in mammalian mRNAs. eLife. 2015;4.
86. Kruger J, Rehmsmeier M. RNAhybrid: microRNA target prediction easy, fast and flexible. Nucleic Acids Res. 2006;34(Web Server issue):W451-4.
87. Guillermo Barturen AR, Maarten Hamberg, Angel Alganza, Ricardo Lebron, Michalis Kotsyfakis, Bu-Jun Shi, Danijela Koppers-Lalic, Michael Hackenberg. sRNAbench: profiling of small RNAs and its sequence variants in single or multi-species high-throughput experiments. Methods in Next Generation Sequencing. 2014;1(1).

88. Lu J, Kwan BC, Lai FM, Tam LS, Li EK, Chow KM, et al. Glomerular and tubulointerstitial miR-638, miR-198 and miR-146a expression in lupus nephritis. Nephrology (Carlton). 2012;17(4):346-51.
89. Carlsen AL, Schetter AJ, Nielsen CT, Lood C, Knudsen S, Voss A, et al. Circulating microRNA expression profiles associated with systemic lupus erythematosus. Arthritis Rheum. 2013;65(5):1324-34.
90. Brockhausen J, Tay SS, Grzelak CA, Bertolino P, Bowen DG, d'Avigdor WM, et al. miR-181a mediates TGF-beta-induced hepatocyte EMT and is dysregulated in cirrhosis and hepatocellular cancer. Liver international : official journal of the International Association for the Study of the Liver. 2015;35(1):240-53.
91. Dai R, Zhang Y, Khan D, Heid B, Caudell D, Crasta O, et al. Identification of a common lupus disease-associated microRNA expression pattern in three different murine models of lupus. PLoS One. 2010;5(12):e14302.
92. Qu B, Cao J, Zhang F, Cui H, Teng J, Li J, et al. Type I Interferon Inhibition of MicroRNA-146a Maturation Through Up-Regulation of Monocyte Chemotactic Protein-Induced Protein 1 in Systemic Lupus Erythematosus. Arthritis Rheumatol. 2015;67(12):3209-18.
93. Zhao Z, Qin L, Li S. miR-411 contributes the cell proliferation of lung cancer by targeting FOXO1. Tumour biology : the journal of the International Society for Oncodevelopmental Biology and Medicine. 2016;37(4):5551-60.
94. Xia K, Zhang Y, Cao S, Wu Y, Guo W, Yuan W, et al. miR-411 regulated ITCH expression and promoted cell proliferation in human hepatocellular carcinoma cells. Biomedicine & pharmacotherapy = Biomedecine & pharmacotherapie. 2015;70:158-63.
95. Wang N, Zhou Y, Jiang L, Li D, Yang J, Zhang CY, et al. Urinary microRNA-10a and microRNA-30d serve as novel, sensitive and specific biomarkers for kidney injury. PLoS One. 2012;7(12):e51140.
96. Martinez-Ramos R, Garcia-Lozano JR, Lucena JM, Castillo-Palma MJ, Garcia-Hernandez F, Rodriguez MC, et al. Differential expression pattern of microRNAs in CD4+ and CD19+ cells from asymptomatic patients with systemic lupus erythematosus. Lupus. 2014;23(4):353-9.
97. Stadthagen G, Tehler D, Hoyland-Kroghsbo NM, Wen J, Krogh A, Jensen KT, et al. Loss of miR-10a activates lpo and collaborates with activated Wnt signaling in inducing intestinal neoplasia in female mice. PLoS Genet. 2013;9(10):e1003913.
98. Li Y, Chen D, Li Y, Jin L, Liu J, Su Z, et al. Oncogenic cAMP responsive element binding protein 1 is overexpressed upon loss of tumor suppressive miR-10b-5p and miR-363-3p in renal cancer. Oncology reports. 2016;35(4):1967-78.
99. Kitterer D, Latus J, Ulmer C, Fritz P, Biegger D, Ott G, et al. Activation of nuclear factor of activated T cells 5 in the peritoneal membrane of uremic patients. Am J Physiol Renal Physiol. 2015;308(11):F1247-58.
100. Wang L, Wang C, Jia Y, Liu Z, Shu X, Liu K. Resveratrol Increases Anti-Proliferative Activity of Bestatin Through Downregulating P-Glycoprotein Expression Via Inhibiting PI3K/Akt/mTOR Pathway in K562/ADR Cells. Journal of cellular biochemistry. 2016;117(5):1233-9.

101. Chen S, Li X, Lu D, Xu Y, Mou W, Wang L, et al. SOX2 regulates apoptosis through MAP4K4-survivin signaling pathway in human lung cancer cells. Carcinogenesis. 2014;35(3):613-23.
102. Xu F, Zhou D, Meng X, Wang X, Liu C, Huang C, et al. Smad2 increases the apoptosis of activated human hepatic stellate cells induced by TRAIL. International immunopharmacology. 2016;32:76-86.
103. Giles BM, Boackle SA. Linking complement and anti-dsDNA antibodies in the pathogenesis of systemic lupus erythematosus. Immunol Res. 2013;55(1-3):10-21.
104. Zhi YJ, Zhi F, Wang R, Xue L, Gu WY, Wang B, et al. [MicroRNA-10a expression in FAB different subtype of acute myeloid leukemia and its relationship with drug resistance]. Zhongguo shi yan xue ye xue za zhi / Zhongguo bing li sheng li xue hui = Journal of experimental hematology / Chinese Association of Pathophysiology. 2015;23(1):29-33.
105. Zhang Y, Xu G, Liu G, Ye Y, Zhang C, Fan C, et al. miR-411-5p inhibits proliferation and metastasis of breast cancer cell via targeting GRB2. Biochem Biophys Res Commun. 2016;476(4):607-13.
106. Wang W, Mou S, Wang L, Zhang M, Shao X, Fang W, et al. Up-regulation of Serum MiR-130b-3p Level is Associated with Renal Damage in Early Lupus Nephritis. Sci Rep. 2015;5:12644.
107. Wang B, Herman-Edelstein M, Koh P, Burns W, Jandeleit-Dahm K, Watson A, et al. E-cadherin expression is regulated by miR-192/215 by a mechanism that is independent of the profibrotic effects of transforming growth factor-beta. Diabetes. 2010;59(7):1794-802.
108. Xiao C, Srinivasan L, Calado DP, Patterson HC, Zhang B, Wang J, et al. Lymphoproliferative disease and autoimmunity in mice with increased miR-17-92 expression in lymphocytes. Nat Immunol. 2008;9(4):405-14.
109. Denby L, Ramdas V, McBride MW, Wang J, Robinson H, McClure J, et al. miR-21 and miR-214 are consistently modulated during renal injury in rodent models. Am J Pathol. 2011;179(2):661-72.
110. Dolezalova D, Mraz M, Barta T, Plevova K, Vinarsky V, Holubcova Z, et al. MicroRNAs regulate p21(Waf1/Cip1) protein expression and the DNA damage response in human embryonic stem cells. Stem cells. 2012;30(7):1362-72.
111. Lund AH. miR-10 in development and cancer. Cell Death Differ. 2010;17(2):209-14.
112. Tehler D, Hoyland-Kroghsbo NM, Lund AH. The miR-10 microRNA precursor family. RNA Biol. 2011;8(5):728-34.
113. Jia H, Zhang Z, Zou D, Wang B, Yan Y, Luo M, et al. MicroRNA-10a is down-regulated by DNA methylation and functions as a tumor suppressor in gastric cancer cells. PLoS One. 2014;9(1):e88057.
114. Parikh A, Lee C, Joseph P, Marchini S, Baccarini A, Kolev V, et al. microRNA-181a has a critical role in ovarian cancer progression through the regulation of the epithelial-mesenchymal transition. Nat Commun. 2014;5:2977.
115. Sun W, Ma Y, Chen P, Wang D. MicroRNA-10a silencing reverses cisplatin resistance in the A549/cisplatin human lung cancer cell line via the transforming growth factor-beta/Smad2/STAT3/STAT5 pathway. Molecular medicine reports. 2015;11(5):3854-9.
116. Chen X, Ba Y, Ma L, Cai X, Yin Y, Wang K, et al. Characterization of microRNAs in serum: a novel class of biomarkers for diagnosis of cancer and other diseases. Cell Res. 2008;18(10):997-1006.

117. Long MJ, Wu FX, Li P, Liu M, Li X, Tang H. MicroRNA-10a targets CHL1 and promotes cell growth, migration and invasion in human cervical cancer cells. Cancer letters. 2012;324(2):186-96.
118. Khan S, Wall D, Curran C, Newell J, Kerin MJ, Dwyer RM. MicroRNA-10a is reduced in breast cancer and regulated in part through retinoic acid. BMC cancer. 2015;15:345.
119. Ohuchida K, Mizumoto K, Lin C, Yamaguchi H, Ohtsuka T, Sato N, et al. MicroRNA-10a is overexpressed in human pancreatic cancer and involved in its invasiveness partially via suppression of the HOXA1 gene. Annals of surgical oncology. 2012;19(7):2394-402.
120. Fang Y, Shi C, Manduchi E, Civelek M, Davies PF. MicroRNA-10a regulation of proinflammatory phenotype in athero-susceptible endothelium in vivo and in vitro. Proc Natl Acad Sci U S A. 2010;107(30):13450-5.
121. Xue X, Feng T, Yao S, Wolf KJ, Liu CG, Liu X, et al. Microbiota downregulates dendritic cell expression of miR-10a, which targets IL-12/IL-23p40. J Immunol. 2011;187(11):5879-86.
122. Landgraf P, Rusu M, Sheridan R, Sewer A, Iovino N, Aravin A, et al. A mammalian microRNA expression atlas based on small RNA library sequencing. Cell. 2007;129(7):1401-14.
123. Aguado-Fraile E, Ramos E, Conde E, Rodriguez M, Martin-Gomez L, Lietor A, et al. A Pilot Study Identifying a Set of microRNAs As Precise Diagnostic Biomarkers of Acute Kidney Injury. PLoS One. 2015;10(6):e0127175.
124. Zarif MN, Soleimani M, Abolghasemi H, Amirizade N, Arefian E, Rahimian A. Megakaryocytic differentiation of CD133+ hematopoietic stem cells by down-regulation of microRNA-10a. Hematology. 2013;18(2):93-100.
125. Neuhofer W. Role of NFAT5 in inflammatory disorders associated with osmotic stress. Current genomics. 2010;11(8):584-90.
126. Mu N, Gu J, Huang T, Zhang C, Shu Z, Li M, et al. A novel NF-kappaB/YY1/microRNA-10a regulatory circuit in fibroblast-like synoviocytes regulates inflammation in rheumatoid arthritis. Scientific reports. 2016;6:20059.
127. Chau BN, Xin C, Hartner J, Ren S, Castano AP, Linn G, et al. MicroRNA-21 promotes fibrosis of the kidney by silencing metabolic pathways. Science translational medicine. 2012;4(121):121ra18.
128. Rovin BH, Song H, Birmingham DJ, Hebert LA, Yu CY, Nagaraja HN. Urine chemokines as biomarkers of human systemic lupus erythematosus activity. J Am Soc Nephrol. 2005;16(2):467-73.
129. Rovin BH, Lu L, Zhang X. A novel interleukin-8 polymorphism is associated with severe systemic lupus erythematosus nephritis. Kidney Int. 2002;62(1):261-5.
130. Wada T, Yokoyama H, Tomosugi N, Hisada Y, Ohta S, Naito T, et al. Detection of urinary interleukin-8 in glomerular diseases. Kidney Int. 1994;46(2):455-60.
131. Li A, Dubey S, Varney ML, Dave BJ, Singh RK. IL-8 directly enhanced endothelial cell survival, proliferation, and matrix metalloproteinases production and regulated angiogenesis. J Immunol. 2003;170(6):3369-76.

132. Hakkim A, Furnrohr BG, Amann K, Laube B, Abed UA, Brinkmann V, et al. Impairment of neutrophil extracellular trap degradation is associated with lupus nephritis. Proc Natl Acad Sci U S A. 2010;107(21):9813-8.
133. Villanueva E, Yalavarthi S, Berthier CC, Hodgin JB, Khandpur R, Lin AM, et al. Netting neutrophils induce endothelial damage, infiltrate tissues, and expose immunostimulatory molecules in systemic lupus erythematosus. J Immunol. 2011;187(1):538-52.
134. Lande R, Ganguly D, Facchinetti V, Frasca L, Conrad C, Gregorio J, et al. Neutrophils activate plasmacytoid dendritic cells by releasing self-DNA-peptide complexes in systemic lupus erythematosus. Science translational medicine. 2011;3(73):73ra19.
135. Garcia-Romo GS, Caielli S, Vega B, Connolly J, Allantaz F, Xu Z, et al. Netting neutrophils are major inducers of type I IFN production in pediatric systemic lupus erythematosus. Science translational medicine. 2011;3(73):73ra20.
136. Li JL, Lim CH, Tay FW, Goh CC, Devi S, Malleret B, et al. Neutrophils Self-Regulate Immune Complex-Mediated Cutaneous Inflammation through CXCL2. J Invest Dermatol. 2016;136(2):416-24.
137. Liu Y. Renal fibrosis: new insights into the pathogenesis and therapeutics. Kidney Int. 2006;69(2):213-7.
138. Wang B, Komers R, Carew R, Winbanks CE, Xu B, Herman-Edelstein M, et al. Suppression of microRNA-29 expression by TGF-beta1 promotes collagen expression and renal fibrosis. J Am Soc Nephrol. 2012;23(2):252-65.
139. Mene P, Stoppacciaro A. Isolation and propagation of glomerular mesangial cells. Methods Mol Biol. 2009;466:3-17.

APPENDIX

Primary mesangial cell isolation

We also develop the method to isolate mesangial cells from human kidney. We used nephrectomies kidney from unsatisfied donor (HIV-infected donor, Syphilis-infected donor, Chronic kidney disease donor, Kidney injured donor and HLA-incompatible donor). The kidneys were processed using previous described protocol (139). Briefly, juxtamedulla-cortex was minced and passed through the standard filter size 250 µM, 200 µM, 150 µM and 70 µM to gradually separate debris. The glomeruli were retained on 70 µM filter, and washed with RPMI-1640. The glomerulus was checked under light microscope, then it was digested with collagenase IV enzymes for 15-30 minutes at 37^{o} C. The cells were subsequently isolated into single cells by using 21-guange needle. In the following, the cells were seeded in RPMI-1640 containing 20% FBS, 100 mM Penicillin-Streptomycin, 1x HEPES and 1xGlutamaMax. The human mesangial cells were characterized by immunohistochemistry using alpha-actinin, PDGFR-beta (figure 18).

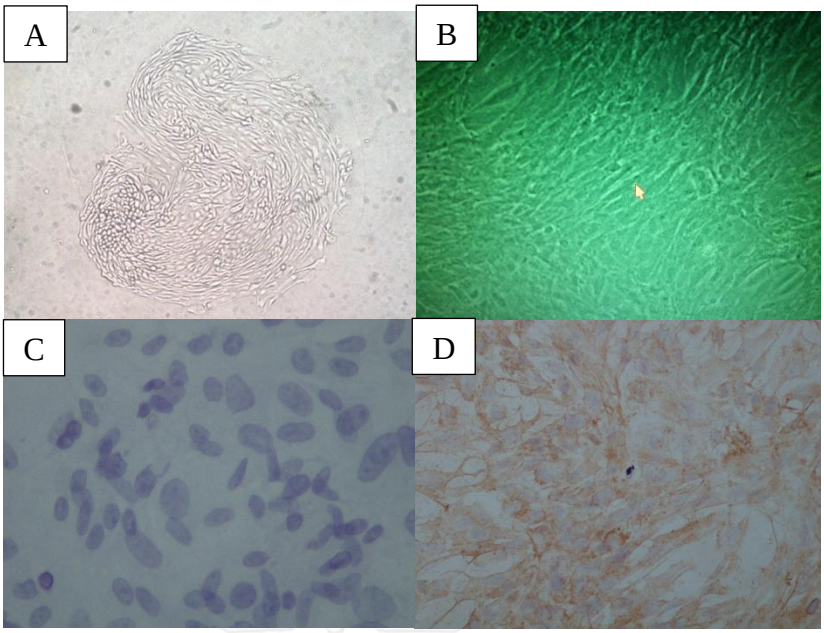

Figure 20 The primary mesangial cells isolation according to standard sieving methods

A) shows glomerulus after washing in RPMI-1640 which retained on 70 µM filter

B) shows human mesangial cells growth after culture for 4 weeks

C) shows negative control for immunohistochemistry

D) shows primary human mesangial cells staining with either PDGFR-beta and alpha actinin (antibodies dilution 1:50 and 1:100).

VITA

Ms. Pattarin Tangtanatakul was born on April, 19th, 1988 in Bangkok, Thailand. She graduated with the Bachelor of Science degree in Medical Technology with second class Honor from Chulalongkorn University in 2009. She got a Royal Golden Jubilee (RGJ) Ph.D. Scholarship from the Thailand Research Fund (TRF) and participated in Medical Microbiology Interdisciplinary Program, Graduate School, Chulalongkorn University for philosophy degree in 2010.